School of Doctoral Studies in Biological Sciences
University of South Bohemia in České Budějovice
Faculty of Science

Pathological mechanisms of polyglutamine disorder in *Drosophila* model of Huntington disease

Ph.D. Thesis

MSc. Yu-Hsien Lin

Supervisor: Prof. RNDr. Michal Žurovec, CSc.

Faculty of Science, University of South Bohemia
Biology Centre of the Czech Academy of Sciences, Institute of Entomology

České Budějovice 2020

This thesis should be cited as:

Lin, YH., 2017: Pathological mechanisms of polyglutamine disorder in *Drosophila* model of Huntington disease

Ph.D. Thesis. University of South Bohemia, Faculty of Science, School of Doctoral Studies in Biological Sciences, České Budějovice, Czech Republic, 110 pp.

Annotation

The first publication in my thesis surveyed the impacts of adenosine homeostasis and its underlying mechanisms in Huntington disease (HD) pathogenesis using a *Drosophila* model. In the second publication, we have extended the use of HD model flies to monitor mHTT effects on innate immune response.

Declaration

I hereby declare that my Ph.D. thesis is my work alone and that I have used only those sources and literature detailed in the list of references.

Further, I declare that, in accordance with Article 47b of Act No. 111/1998 Coll. in the valid wording, I agree to the publication of my Ph.D. thesis in electronic form in a publically accessible part of the STAG database operated by the University of South Bohemia in České Budějovice on its webpage, with the preservation of my rights of authorship to the submitted text of this thesis. Further, I agree to the publication, via the same electronic portal, in accordance with the detailed regulations of Act 111/1998 Coll., of the reviews of the supervisor and opponents of the thesis as well as the record of proceedings and result of the defence of the thesis. I also agree to the comparison of the text of my thesis with the Theses.cz database operated by the National Registry of Theses and the Plagiarism Tracing System.

Place and Date:

Student's signature:

This thesis originated from a partnership of Faculty of Science, University of South Bohemia, and the Institute of Entomology, Biology Centre of the CAS, both supporting doctoral studies in the Physiology and Developmental Biology study programme.

Přírodovědecká fakulta
Faculty of Science

Jihočeská univerzita v Českých Budějovicích
University of South Bohemia in České Budějovice

Financial support

This work was supported by grant agency of the University of South Bohemia (065/2017/P), junior grant project GACR (19-13784Y), The Grant Interreg Bayern - Tschechische Republik Ziel ETZ (2014-2020 No. 123), European Community's Programme Interreg Östereich-Tschechische Republik (REGGEN/ATCZ207).

Acknowledgements

I would like to thank my supervisor, Michal, for guidance and encouragement throughout my Ph.D. study. He has inspired me to become an independent student, and my achievement would not be nearly as good without his help. I would also like to thank all my lab colleagues for helping my experiments and providing me a friendly research environment.

I also appreciate my parents and siblings, they always care about my life, my work and my health. They never stop encourage and support me with their love and patience despite the long distance between us. I would also like to thank all my friends who I met in Taiwan, in Czech Republic and anywhere in the world for enriching my life.

In the end, I would like to express my gratitude to my wife, Feng Ying (and my cat YAHOO as well) for accompanying me to Czech Republic and her continued support and encouragement. Feng-Ying has been my best companion, great love helping me get through stressful period in the most positive way.

List of publications and contributions

The thesis is based on the following publications:

Yu-Hsien Lin, Houda Ouns Maaroufi, Lucie Kucerova, Lenka Rouhova, Tomas Filip, Michal Zurovec (2019). Adenosine signaling and its downstream target mod(mdg4) modify the pathogenic effects of polyglutamine in a *Drosophila* model of Huntington's disease. BioRxiv. doi: 10.1101/2019.12.22.886143

Yu-Hsien Lin conceived the project, performed the experiments and prepared the manuscript.

Yu-Hsien Lin, Houda Ouns Maaroufi, Emad Ibrahim, Lucie Kucerova, Michal Zurovec (2019). Expression of human mutant huntingtin protein in *Drosophila* hemocytes impairs immune responses. Frontiers in immunology. doi: 10.3389/fimmu.2019.02405

Yu-Hsien Lin performed the experiments and prepared the manuscript.

Contents

1. Introduction of adenosine metabolism and signaling

1.1. Adenosine production

Adenosine (Ado) is a key metabolite and conserved purinergic signaling molecule in both vertebrates and invertebrates. It is a basal constituent of nucleic acids and ADP, AMP and ATP as well as a precursor of cellular second messenger, cyclic adenosine monophosphate (cAMP). Extracellular Ado also regulates a number of physiological processes via activating adenosine receptors (AdoRs), which belong to G protein-coupled receptors.

The enzymatic activity responsible for Ado formation from AMP is 5'-nucleotidase, which catalyzes the hydrolysis of the phosphoric ester bond of 5'-ribonucleotides to the corresponding ribonucleoside and phosphate (Strater, 2006). We now know that there are two groups of nucleotidases which act on the formation of Ado. The main source of Ado is cytosolic AMP produced by cytosolic 5'-nucleotidase (Figure 1, #5). It is responsible for more than 70 % of Ado production in mammalian heart cells (Darvish et al., 1996). Another glycoprotein, ecto-5'-nucleotidase (Fig. 1, #1) which is found on the plasma membrane of eukaryotic cells has similar function. It increases the extracellular Ado level by hydrolysis of extracellular AMP to Ado close to the cell membrane, which allows Ado rapidly transporting into cells or binding to receptors before getting deaminated. Extracellular ATP serves as one of the resources for the extracellular Ado production (Zimmermann and Braun, 1996). The conversion of ATP to Ado is mediated by a glycoprotein, ecto-nucleoside triphosphate diphosphohydrolase (NTPDase, also called CD39), which is able to hydrolyze the alpha- and beta phosphate residues of extracellular ATP or ADP into AMP (Figure 1, #9). There are various mechanisms for ATP efflux to the extracellular environment. ATP could be released upon cell death via ruptured cell membranes, such ATP release

from apoptotic cells is also recognized as a “find-me signaling” for recruiting immune cells and prompting clearance of the dying cells via phagocytosis (Elliott et al., 2009). The ATP is also released via exocytosis from intracellular vesicles, or from specific channels such as anion, pannexin, and connexin channels (Faas et al., 2017).

In addition, Ado is also produced from S- adenosylhomocysteine (SAH) via SAH-hydrolase (SAHH) (Figure 1, #6), which was firstly described in rat liver (De La Haba and Cantoni, 1959). This mechanism contributes one-third of the total cardiac Ado at normoxic conditions but not under stress conditions (Deussen et al., 1989). The SAHH catalysis is reversible (Figure 2), and the direction of the reaction is dependent on the local concentration of homocysteine and Ado (Loncar et al., 1997).

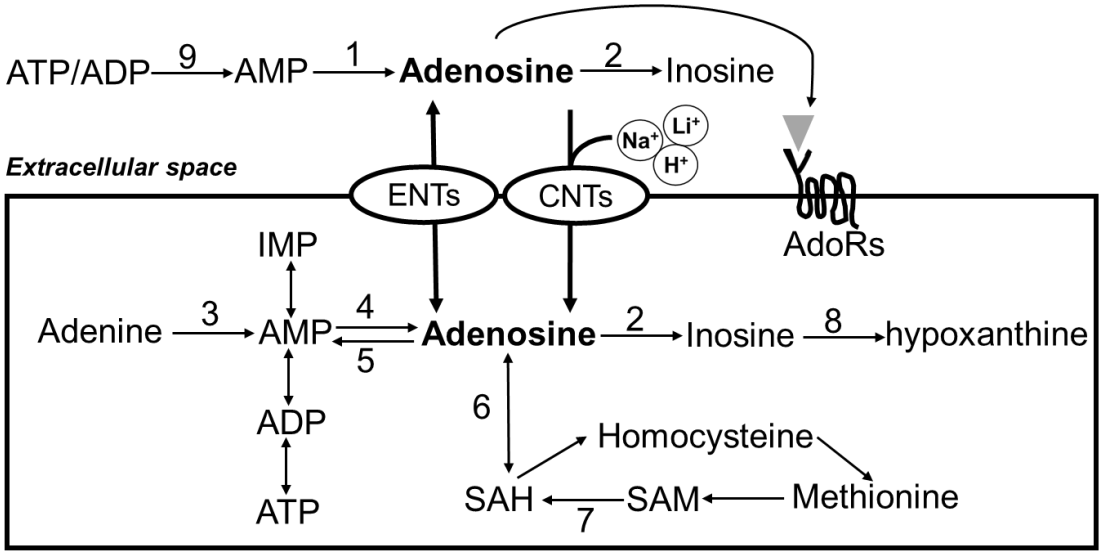

Figure 1. Overview of Ado transport and metabolism. 1, ecto-5′ –nucleotidase (5′-NT, CD73); 2, adenosine deaminase (ADA); 3, adenine phosphoribosyltransferase (APRTase); 4, 5′ -nucleotidase (cN-I); 5, adenosine kinase (ADK); 6, S-adenosylhomocysteine hydrolase; 7, methyltransferases 8, purine nucleoside phosphorylase (PNP). 9. Ecto-nucleoside triphosphate diphosphohydrolase (CD39). AdoRs adenosine receptors, ENTs equilibrative nucleoside transporters, CNTs concentrative nucleoside transporters, SAH S-adenosyll-homocysteine, SAM S -adenosylmethionine. The figure is modified from Masino and Boison (2013).

1.2. Ado metabolism

Since the extracellular Ado could induce its downstream signaling cascades and modulate cellular functions, the level of the Ado needs to be maintained accurately. The enzymes responsible for metabolizing the Ado are adenosine kinase (abbreviation: ADK or AK in mammals, AdenoK in *Drosophila*) and adenosine deaminases (ADAs), which catalyze the phosphorylation and deamination of Ado to AMP and inosine, respectively.

ADAs catalyze the hydrolytic deamination of either Ado or 2'-deoxyadenosine to inosine or 2'- deoxyinosine, respectively (Sideraki et al., 1996). The metabolic product of deamination, inosine or deoxyinosine, are further converted by purine nucleoside phosphorylase (PNP) into hypoxanthine (Figure 1, #8), which is in turn transformed into uric acid by xanthine oxidoreductase. Two types of adenosine deaminases have been identified; a cytosolic adenosine deaminase ADA1 and a secretory adenosine deaminase ADA2 (also named adenosine deaminase-related growth factors, ADGFs in invertebrates). ADA1 is the first Ado degradation enzyme discovered in dog muscle by Schmidt (1928). The interest in ADA1 raised after 1970, when it was realized that the mutation of ADA in human is associated with severe combined immunodeficiency (SCID) (Giblett et al., 1972; Tritsch et al., 1985). ADA1 is localized both intracellularly and on the cell surface complexed with glycoprotein CD26, and it is expressed ubiquitously with highest levels observed in lymphoid tissues, brain and gastrointestinal tract (Kameoka et al., 1993). However, the ADA1 orthologs were not found in plants, fungi or insects (Maier et al., 2005). In contrast, the ADA2-type of enzyme represents a common ADA in most multicellular organisms including invertebrates and vertebrates (Skaldin et al., 2018). Human ADA2 is a homodimer protein containing N-terminal signal peptide, it is mainly secreted by monocytes and

thus is abundant in plasma (Zavialov et al., 2010). The first functionally characterized ADA2-type enzyme was *Drosophila* ADGF-A, and the mutation of the ADGF-A caused larval development and hematopoiesis abnormalities, hyperglycemia, and loss of adipose tissue (Dolezal et al., 2005). Knockout of ADA2 homolog in frogs reduces the body size and causes abnormal body axis in the embryo indicating its important role in the embryogenesis of amphibians (Iijima et al., 2008).

The high K_M of ADA1 (25-150 μM) and ADA2 (2.5 mM) suggest that both ADAs only become important when Ado increases above the K_M value of ADK, which is around 1 μM (De Jong, 1977; Drabikowska et al., 1985; Ford et al., 2000; Singh and Sharma, 2000). ADK is thought to be the major enzyme responsible for Ado metabolism due to its high affinity for Ado, and more than 95% of the Ado is converted to AMP by ADK (Pak et al., 1994) (Figure 1, #5). The ADK also plays an important role for maintaining the energy homeostasis by affecting the cellular AMP, ADP, ATP pools as well as intracellular and extracellular Ado levels.

In addition, as noted above, Ado can be also derived from the hydrolysis of SAH by S-adenosylhomocysteine hydrolase (SAHH). SAHH reaction is reversible and Ado concentration-dependent (Figure 2). Hence SAHH also plays the role, but a minor one, in adjusting the Ado level. The accumulation of Ado and the $_L$-homocysteine will block the conversion of SAH to Ado, and it would further inhibit the transmethylation reactions of S-adenosylmethionine (SAM) to SAH, which finally leads to a decrease of intracellular Ado level (Schutz et al., 1981).

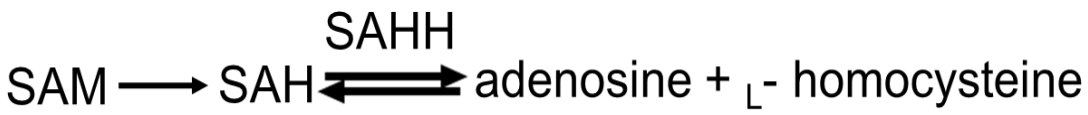

Figure 2. Transmethylation reaction of Ado synthesis

1.3. Ado transport

Ado is an important signaling molecule and the substrate for ATP formation, hence it requires an efficient transportation across the plasma membrane. The transport of Ado, which is quite hydrophilic, needs to be mediated by specialized membrane proteins (Figure 1). There are two protein families involved in the Ado transportation, equilibrative nucleoside transporters (ENTs) and concentrative nucleoside transporters (CNTs), which are encoded by the gene families of solute carrier 29 and 28 (SCL29, SCL28) in mammals, respectively (Molina-Arcas et al., 2009).

In contrast to CNTs, ENTs are ubiquitously expressed in a wide range of tissues (Baldwin et al., 2004). They not only mediate the efflux and influx of Ado, but also may have wider substrate specificity and transport other nucleosides such as uridine or guanosine. There are four ENT proteins in human with different affinity to Ado and other nucleosides. ENT1 and ENT2 have a broad selectivity, transporting most purines and pyrimidines, but ENT3 shows relatively lower affinity for Ado (Crawford et al., 1998; Yao et al., 2002; Baldwin et al., 2005). ENT4 transports Ado as well as monoamine neurotransmitters (such as dopamine and serotonin), but it does not mediate the transport of other nucleosides (Baldwin et al., 2004; Engel et al., 2004). Interestingly, ENT4 shows a higher activity for Ado transport at acidic pH 5.5 and a lower activity at pH 7.5. Consistent with its high abundance in cardiovascular system, it was suggested that this acidic pH preference is associated with its contribution to the regulation of extracellular Ado concentrations during ischemia (Barnes et al., 2006).

CNTs mediate the influx (unidirectional) of nucleosides powered by the transmembrane sodium gradient (Gray et al., 2004). In comparison to ENTs, the CNTs have limited tissue distribution in specialized epithelial cells, such as intestinal epithelia, liver, choroid plexus, as well as in macrophages and leukemic cells (Masino and Boison,

2013). Three CNTs have been reported in human, each having a different nucleosides affinity and conditions for ions co-transportation. Human CNT1 is a pyrimidine-specific transporter, so it cannot transport Ado. The CNT2 is a purine-preferring transporter, although it can also transport uridine. Both CNT1 and CNT2 co-transport a single sodium ion per nucleoside. The CNT3 has relatively wide selectivity for both purine and pyrimidine nucleosides (Ritzel et al., 2001). Unlike CNT1 and CNT2, the CNT3 co-transports two sodium ions per nucleoside. Moreover, the CNT3 displays unique cation interactions with not only Na^+ but also with H^+ and Li^+ that are not shared by CNT1 and CNT2 (Smith et al., 2005).

1.4. Ado receptor

Extracellular Ado is able to activate specific membrane proteins, Ado receptors (AdoRs), to simulate downstream signaling. AdoRs belong to seven-pass transmembrane G-protein-coupled receptors. They are divided into four subtypes in mammals: A1, A2A, A2B and A3 receptors. Each of them has a different tissue distribution and G protein binding preference (Table. 1). The activation of A1 and A3 results in the inhibition of cAMP formation via coupling to Gαi family of G proteins. The activation of A2A and A2B lead to rise the cAMP levels via interacting with Gαs family proteins. Increased cAMP could stimulate cAMP-dependent protein kinase, protein kinase A (PKA), which can directly activate transcription factor cAMP response element-binding protein (CREB) (Antonioli et al., 2015). In addition to the modulation of cAMP secondary messenger system via Gs and Gi, AdoRs can also activate Gq protein (A2B and A3), phospholipase C (A1, A2B, and A3), protein kinase C (A2B and A3), or K_{ATP} channel (A3). Furthermore, all the AdoRs can regulate cell differentiation and proliferation via activating mitogen-activated protein kinase (MAPK) cascades

included extracellular signal-regulated kinase 1 (ERK1), ERK2, Jun-N-terminal kinase (JNK) and p38 (Feoktistov et al., 1999; Schulte and Fredholm, 2003; Trincavelli et al., 2010). These four AdoR subtypes also show different affinity to the Ado. The A1 has the highest affinity to Ado (Ki = 100 nM), and the A3 and A2A have a moderate affinity to Ado (Ki= 290, 310 nM, respectively) whereas A2B shows lowest affinity to Ado (Ki =15000 nM) (Muller and Jacobson, 2011). A recent study generated a mice lacking all four AdoRs [quad knockout (QKO mice)], and the QKO mice showed almost no significant physiological changes compared to wild-type mice under normal (non-stress) conditions. These results demonstrated that AdoRs signaling is not involved in maintaining the physiological homeostasis but is essential for allostatic control (Cunha, 2019; Xiao et al., 2019).

Receptor name	Human gene	Chromosome	G proteins	Localization	Potency of adenosine*
Adenosine A_1 receptor	*ADORA1*	1q32.1	$G_{i,o}$	Broad distribution: high in nerves, heart, kidney and adipose tissue	10^{-8} to 10^{-7}
Adenosine A_{2A} receptor	*ADORA2A*	22q11.23	$G_{s/olf}$	Broad distribution: very high in basal ganglia; high in nerves, blood vessels and immune cells	10^{-8} to 10^{-7}
Adenosine A_{2B} receptor	*ADORA2B*	17p12-p11.2	G_s ($G_{q/11}$; $G_{12/13}$)	Broad distribution, but generally low abundance	3×10^{-7} to 10^{-5}
Adenosine A_3 receptor	*ADORA3*	1p13.2	$G_{i/o}$	Restricted distribution, varying in different species: high in mast cells	10^{-8} to 10^{-7}

Table 1. Different tissue distributions and properties of four AdoR subtypes in human. The table is adapted from Chen et al. (2013).

1.5. Ado signaling in *Drosophila melanogaster*

The study of Ado signaling in *Drosophila* started by the discovery of a new protein family, adenosine deaminase-related growth factors (ADGFs). The first member of this protein family was purified and cloned in 1996 from the culture medium of the flesh fly (*Sarcophaga peregrina*) embryonic cell line. The gene was named insect-derived

growth factor (IDGF) at that time, since it seemed to have a similar function as mammalian growth factors (Homma et al., 1996). Afterwards, six ADGF proteins were described in *Drosophila* including ADGF-A, ADGF-A2, ADGF-B, ADGF-C, ADGF-D, ADGF-E (Zurovec et al., 2002). Sequence similarity searches revealed that ADGFs have similar sequence as mammalian ADA2 and suggested that ADGFs may have ADA activity (Maier et al., 2005). By regulating extracellular Ado metabolism, the high ADA enzymatic activity of ADGF-A plays an important role in mitogenic regulation of the cells *in vitro*. Characterization of growth media of several insect cell lines showed that elevated concentration of Ado blocks cell growth and causes apoptosis due to dysregulation of purine homeostasis (Zurovec et al., 2002). *Drosophila* ADGF-A mutant fly was generated by homologous recombination in 2003 (Dolezal et al., 2003). The ADGF-A mutant has high level of extracellular Ado in the hemolymph, which leads to severe physiological effects including melanotic tumor formation, rise of circulating hemocytes, fat-body disintegration, and lethality in larval stage (Dolezal et al., 2005). This implied that extracellular Ado can regulate multiple physiological processes in *Drosophila* such as hemocyte proliferation and differentiation, metabolic homeostasis, and metamorphosis.

The nucleoside transporters and AdoR have been also identified in *Drosophila*. Three ENTs have been reported by Sankar et al. (2002). Functional characterization of ENTs by RNAi in *Drosophila* Cl.8+ cells indicated that ENT2 is able to transport Ado but not ENT1 or ENT3 (Fleischmannova et al., 2012). Moreover, the Ado transport in Cl.8+ cells is not competed with other purine or pyrimidine nucleosides such as inosine, uridine and guanosine. The expression of *ent2* in the mushroom bodies and antennal lobes of *Drosophila* regulates associative learning and synaptic plasticity via changing the AdoR activity (Knight et al., 2010). Two CNTs have also been identified in

Drosophila and both are able to transport Ado (Fleischmannova et al., 2012), however, their exact physiological functions *in vivo* are still unclarified.

Drosophila AdoR was first described in 2000; it is encoded by the CG9753 gene (Brody and Cravchik, 2000). There is only a single AdoR isoform known in *Drosophila*. It can stimulate the cAMP second messenger system similarly to human A2A and A2B and couple to Gαs of the trimeric G protein (and potentially also Gq) (Dolezelova et al., 2007). AdoR pathway in *Drosophila* has been reported regulating various physiological and pathological processes, including modulation of synaptic plasticity, JNK-mediated stress response, hematopoiesis, and metabolic switching upon immune challenges (Knight et al., 2010; Bajgar et al., 2015; Poernbacher and Vincent, 2018).

2. Introduction of Huntington's disease (HD)

2.1. Pathophysiology of HD

HD is an inherited neurodegenerative disorder caused by an abnormal expansion of CAG trinucleotide in the human Huntingtin (*htt*) gene. Prevalence of HD is 4–10 per 100000 in the Caucasian population, which is much higher than in African or Asian people (Walker, 2007; Ross and Tabrizi, 2011). The onset of symptoms is typically in the middle age between 35-45 years, and the death usually occurs 15-20 years after the onset. Mutant HTT protein (mHTT) contains an extended polyglutamine (polyQ) tract encoded by 40 to over 150 CAG repeats, which causes cytotoxicity and leads to neurodegeneration; this results in involuntary movement, cognitive impairment and psychiatric abnormalities (Vonsattel and DiFiglia, 1998). The major features of HD pathogenesis include abnormal conformations of mHTT aggregates, compromised protein degradation systems, transcriptional disruption and globally metabolic impairment. Apart from protein toxicity, is was also suggested that the mHTT RNA might also contribute to HD pathogenesis. The expansion of CAG-repeat RNA forms a

hairpin structure, which can sequester various protein and compromise their endogenous functions (Nalavade et al., 2013).

The *htt* gene is expressed ubiquitously and involved in fundamental cellular processes, so the expression of mHTT in non-neuronal cells of the brain or in the peripheral tissues may also contribute to the HD symptoms. The peripheral symptoms of HD include weight loss, altered carbohydrate homeostasis, cardiac dysfunction and abnormal immune reactions have been reported. (Sassone et al., 2009; van der Burg et al., 2009).

2.2. *Drosophila* model of HD

Drosophila melanogaster has been earlier established as a HD model. *In vivo* experiments have revealed that the ectopic overexpression of mutant human *htt* (exon 1 with expanded CAG repeats) in the neural tissue of transgenic flies causes neurodegeneration (Steffan et al., 2001; Song et al., 2013). The mechanisms of cellular pathology observed in the HD flies seem similar to those in human patients, including the suppression of mitochondrial function, transcriptional dysregulation and neuronal apoptosis (Taylor et al., 2003; Li et al., 2010). Genetic screening for disease modifiers in HD model flies led to the identification of the effects of sumoylation and HSP70 chaperone machinery on neurodegeneration. The subsequent confirmation that these pathways are involved in the pathology of human patients validates the *Drosophila* model for investigating HD (Warrick et al., 1999; Steffan et al., 2004). Furthermore, since the tissue-specific expression of transgenes in *Drosophila* can be easily controlled using the UAS-Gal4 system, *Drosophila* has also been used to study the effects of HD on non-neuronal cells, including glial cells, photoreceptors, cardiac cells, and salivary glands (Marsh et al., 2000; Tamura et al., 2009; Besson et al., 2010; Weiss et al., 2012;

Melkani et al., 2013).

3. Crosstalk between HD and Ado signaling

The altered Ado homeostasis has been observed in the cerebrospinal fluid of HD patients and mouse HD models (Gianfriddo et al., 2004; Kao et al., 2017). In addition, the upregulation of striatal ENTs, which facilitate Ado transport across the cytoplasmic membrane, disrupts Ado homeostasis in HD mouse and human patients. Such changes were suggested as HD biomarkers for assessing the initial stage of neurodegeneration (Guitart et al., 2016; Kao et al., 2017). However, exact underlying mechanisms of Ado effects and its association with HD pathogenesis are still not clear.

Although mHTT is ubiquitously expressed in the central nervous system (CNS) and peripheral cells in HD patients, it predominantly affects striatal neurons that contain a higher density of A2A and A1 of AdoRs (Blum et al., 2003a). Several studies have demonstrated that the altered AdoR signaling, especially the A2A in the striatum, affect HD pathogenesis (Gomes et al., 2011; Blum et al., 2018). Both the activation and inhibition of A2A by pharmacological treatments have shown benefits in mammalian HD models. In R6/2 mice, the beneficial effect of activating A2A is thought to occur *via* the inhibition of AMPK nuclear translocation, which further decreased neuron death, and mHTT aggregate formation (Ju et al., 2011). The beneficial effects of antagonizing A2A with SCH58261 in R6/2 mice include reduced striatal glutamate and Ado outflow as well as restoring emotional behavior and susceptibility to NMDA toxicity (Gianfriddo et al., 2004; Domenici et al., 2007). The A1 activation has also been shown to have neuroprotective effects; however, the chronic administration of A1 agonists increases neuronal loss whereas the chronic administration of A1 antagonists improves survival and neuronal preservation (Blum et al., 2003b).

4. Aim of my studies

Although it has been known that Ado homeostasis and signaling are abnormal in HD, the underlying mechanisms of Ado effects in HD pathogenesis are still unclear. In my first publication, I used the *Drosophila* HD model to investigate the role of Ado signaling in HD pathogenesis and polyQ aggregate formation.

In addition, it has been suggested that the pathogenic effect of mHTT is not restricted to nervous system, and some aberrant immune responses were observed earlier in the HD mouse models. However, it is still unclear how this immune dysregulation influences the innate immune response against pathogenic infection. Thus in my second publication, I tried to address this question by expressing mHTT in *Drosophila* hemocytes and monitoring its effect on innate immune response.

5. Reference

Antonioli, L., Blandizzi, C., Csoka, B., Pacher, P., and Hasko, G. (2015). Adenosine signalling in diabetes mellitus--pathophysiology and therapeutic considerations. *Nat Rev Endocrinol* 11(4)**,** 228-241. doi: 10.1038/nrendo.2015.10.

Bajgar, A., Kucerova, K., Jonatova, L., Tomcala, A., Schneedorferova, I., Okrouhlik, J., et al. (2015). Extracellular adenosine mediates a systemic metabolic switch during immune response. *PLoS Biol* 13(4)**,** e1002135. doi: 10.1371/journal.pbio.1002135.

Baldwin, S.A., Beal, P.R., Yao, S.Y., King, A.E., Cass, C.E., and Young, J.D. (2004). The equilibrative nucleoside transporter family, SLC29. *Pflugers Arch* 447(5)**,** 735-743. doi: 10.1007/s00424-003-1103-2.

Baldwin, S.A., Yao, S.Y., Hyde, R.J., Ng, A.M., Foppolo, S., Barnes, K., et al. (2005). Functional characterization of novel human and mouse equilibrative nucleoside transporters (hENT3 and mENT3) located in intracellular membranes. *J Biol Chem* 280(16)**,** 15880-15887. doi: 10.1074/jbc.M414337200.

Barnes, K., Dobrzynski, H., Foppolo, S., Beal, P.R., Ismat, F., Scullion, E.R., et al. (2006). Distribution and functional characterization of equilibrative nucleoside transporter-4, a novel cardiac adenosine transporter activated at acidic pH. *Circ Res* 99(5)**,** 510-519. doi: 10.1161/01.RES.0000238359.18495.42.

Besson, M.T., Dupont, P., Fridell, Y.W., and Lievens, J.C. (2010). Increased energy metabolism rescues glia-induced pathology in a Drosophila model of Huntington's disease. *Hum Mol Genet* 19(17)**,** 3372-3382. doi: 10.1093/hmg/ddq249.

Blum, D., Chern, E.C., Domenici, M.R., Buée, L., Lin, C.Y., Ferré, S., et al. (2018). "What Is the Role of Adenosine Tone and Adenosine Receptors in Huntington's Disease?," in *The Adenosine Receptors,* eds. P.A. Borea, K. Varani, S. Gessi, S. Merighi & F. Vincenzi. (Cham: Springer International Publishing), 281-308.

Blum, D., Hourez, R., Galas, M.-C., Popoli, P., and Schiffmann, S.N. (2003a). Adenosine receptors and Huntington's disease: implications for pathogenesis and therapeutics. *The Lancet Neurology* 2(6)**,** 366-374. doi: https://doi.org/10.1016/S1474-4422(03)00411-3.

Blum, D., Hourez, R., Galas, M.C., Popoli, P., and Schiffmann, S.N. (2003b). Adenosine receptors and Huntington's disease: implications for pathogenesis and therapeutics. *Lancet Neurol* 2(6)**,** 366-374. doi: 10.1016/s1474-4422(03)00411-3.

Brody, T., and Cravchik, A. (2000). Drosophila melanogaster G protein-coupled receptors. *J Cell Biol* 150(2)**,** F83-88.

Chen, J.F., Eltzschig, H.K., and Fredholm, B.B. (2013). Adenosine receptors as drug targets - what are the challenges? *Nature Reviews Drug Discovery* 12(4)**,** 265-286. doi: 10.1038/nrd3955.

Crawford, C.R., Patel, D.H., Naeve, C., and Belt, J.A. (1998). Cloning of the human equilibrative, nitrobenzylmercaptopurine riboside (NBMPR)-insensitive nucleoside transporter ei by functional expression in a transport-deficient cell line. *J Biol Chem* 273(9)**,** 5288-5293.

Cunha, R.A. (2019). Signaling by adenosine receptors-Homeostatic or allostatic control? *Plos Biology* 17(4). doi: ARTN e3000213
10.1371/journal.pbio.3000213.

Darvish, A., Pomerantz, R.W., Zografides, P.G., and Metting, P.J. (1996). Contribution of cytosolic and membrane-bound 5'-nucleotidases to cardiac adenosine production. *Am J Physiol* 271(5 Pt 2)**,** H2162-2167.

De Jong, J.W. (1977). Partial purification and properties of rat-heart adenosine kinase. *Arch Int Physiol Biochim* 85(3)**,** 557-569.

De La Haba, G., and Cantoni, G.L. (1959). The enzymatic synthesis of S-adenosyl-L-homocysteine from adenosine and homocysteine. *J Biol Chem* 234(3)**,** 603-608.

Deussen, A., Lloyd, H.G., and Schrader, J. (1989). Contribution of S-adenosylhomocysteine to cardiac adenosine formation. *J Mol Cell Cardiol* 21(8)**,** 773-782.

Dolezal, T., Dolezelova, E., Zurovec, M., and Bryant, P.J. (2005). A role for adenosine deaminase in Drosophila larval development. *PLoS Biol* 3(7)**,** e201. doi: 10.1371/journal.pbio.0030201.

Dolezal, T., Gazi, M., Zurovec, M., and Bryant, P.J. (2003). Genetic analysis of the ADGF multigene family by homologous recombination and gene conversion in Drosophila. *Genetics* 165(2)**,** 653-666.

Dolezelova, E., Nothacker, H.P., Civelli, O., Bryant, P.J., and Zurovec, M. (2007). A Drosophila adenosine receptor activates cAMP and calcium signaling. *Insect Biochem Mol Biol* 37(4)**,** 318-329. doi: 10.1016/j.ibmb.2006.12.003.

Domenici, M.R., Scattoni, M.L., Martire, A., Lastoria, G., Potenza, R.L., Borioni, A., et al. (2007). Behavioral and electrophysiological effects of the adenosine A2A receptor antagonist SCH 58261 in R6/2 Huntington's disease mice. *Neurobiol Dis* 28(2)**,** 197-205. doi: 10.1016/j.nbd.2007.07.009.

Drabikowska, A.K., Halec, L., and Shugar, D. (1985). Purification and properties of adenosine kinase from rat liver: separation from deoxyadenosine kinase activity. *Z Naturforsch C* 40(1-2)**,** 34-41.

Elliott, M.R., Chekeni, F.B., Trampont, P.C., Lazarowski, E.R., Kadl, A., Walk, S.F., et al. (2009). Nucleotides released by apoptotic cells act as a find-me signal to promote phagocytic clearance. *Nature* 461(7261)**,** 282-286. doi: 10.1038/nature08296.

Engel, K., Zhou, M., and Wang, J. (2004). Identification and characterization of a novel monoamine transporter in the human brain. *J Biol Chem* 279(48)**,** 50042-50049. doi: 10.1074/jbc.M407913200.

Faas, M.M., Saez, T., and de Vos, P. (2017). Extracellular ATP and adenosine: The Yin and Yang in immune responses? *Mol Aspects Med* 55**,** 9-19. doi: 10.1016/j.mam.2017.01.002.

Feoktistov, I., Goldstein, A.E., and Biaggioni, I. (1999). Role of p38 mitogen-activated protein kinase and extracellular signal-regulated protein kinase kinase in adenosine A2B receptor-mediated interleukin-8 production in human mast cells. *Mol Pharmacol* 55(4)**,** 726-734.

Fleischmannova, J., Kucerova, L., Sandova, K., Steinbauerova, V., Broz, V., Simek, P., et al. (2012). Differential response of Drosophila cell lines to extracellular adenosine. *Insect Biochem Mol Biol* 42(5)**,** 321-331. doi: 10.1016/j.ibmb.2012.01.002.

Ford, H., Jr., Dai, F., Mu, L., Siddiqui, M.A., Nicklaus, M.C., Anderson, L., et al. (2000). Adenosine

deaminase prefers a distinct sugar ring conformation for binding and catalysis: kinetic and structural studies. *Biochemistry* 39(10)**,** 2581-2592.

Gianfriddo, M., Melani, A., Turchi, D., Giovannini, M.G., and Pedata, F. (2004). Adenosine and glutamate extracellular concentrations and mitogen-activated protein kinases in the striatum of Huntington transgenic mice. Selective antagonism of adenosine A2A receptors reduces transmitter outflow. *Neurobiol Dis* 17(1)**,** 77-88. doi: 10.1016/j.nbd.2004.05.008.

Giblett, E.R., Anderson, J.E., Cohen, F., Pollara, B., and Meuwissen, H.J. (1972). Adenosine-deaminase deficiency in two patients with severely impaired cellular immunity. *Lancet* 2(7786)**,** 1067-1069.

Gomes, C.V., Kaster, M.P., Tome, A.R., Agostinho, P.M., and Cunha, R.A. (2011). Adenosine receptors and brain diseases: Neuroprotection and neurodegeneration. *Biochimica Et Biophysica Acta-Biomembranes* 1808(5)**,** 1380-1399. doi: 10.1016/j.bbamem.2010.12.001.

Gray, J.H., Owen, R.P., and Giacomini, K.M. (2004). The concentrative nucleoside transporter family, SLC28. *Pflugers Arch* 447(5)**,** 728-734. doi: 10.1007/s00424-003-1107-y.

Guitart, X., Bonaventura, J., Rea, W., Orru, M., Cellai, L., Dettori, I., et al. (2016). Equilibrative nucleoside transporter ENT1 as a biomarker of Huntington disease. *Neurobiol Dis* 96**,** 47-53. doi: 10.1016/j.nbd.2016.08.013.

Homma, K., Matsushita, T., and Natori, S. (1996). Purification, characterization, and cDNA cloning of a novel growth factor from the conditioned medium of NIH-Sape-4, an embryonic cell line of Sarcophaga peregrina (flesh fly). *J Biol Chem* 271(23)**,** 13770-13775.

Iijima, R., Kunieda, T., Yamaguchi, S., Kamigaki, H., Fujii-Taira, I., Sekimizu, K., et al. (2008). The extracellular adenosine deaminase growth factor, ADGF/CECR1, plays a role in Xenopus embryogenesis via the adenosine/P1 receptor. *J Biol Chem* 283(4)**,** 2255-2264. doi: 10.1074/jbc.M709279200.

Ju, T.C., Chen, H.M., Lin, J.T., Chang, C.P., Chang, W.C., Kang, J.J., et al. (2011). Nuclear translocation of AMPK-alpha1 potentiates striatal neurodegeneration in Huntington's disease. *J Cell Biol* 194(2)**,** 209-227. doi: 10.1083/jcb.201105010.

Kameoka, J., Tanaka, T., Nojima, Y., Schlossman, S.F., and Morimoto, C. (1993). Direct association of adenosine deaminase with a T cell activation antigen, CD26. *Science* 261(5120)**,** 466-469. doi: 10.1126/science.8101391.

Kao, Y.H., Lin, M.S., Chen, C.M., Wu, Y.R., Chen, H.M., Lai, H.L., et al. (2017). Targeting ENT1 and adenosine tone for the treatment of Huntington's disease. *Hum Mol Genet* 26(3)**,** 467-478. doi: 10.1093/hmg/ddw402.

Knight, D., Harvey, P.J., Iliadi, K.G., Klose, M.K., Iliadi, N., Dolezelova, E., et al. (2010). Equilibrative nucleoside transporter 2 regulates associative learning and synaptic function in Drosophila. *J Neurosci* 30(14)**,** 5047-5057. doi: 10.1523/JNEUROSCI.6241-09.2010.

Li, X.J., Orr, A.L., and Li, S. (2010). Impaired mitochondrial trafficking in Huntington's disease. *Biochim Biophys Acta* 1802(1)**,** 62-65. doi: 10.1016/j.bbadis.2009.06.008.

Loncar, R., Flesche, C.W., and Deussen, A. (1997). Determinants of the S-adenosylhomocysteine

(SAH) technique for the local assessment of cardiac free cytosolic adenosine. *J Mol Cell Cardiol* 29(5), 1289-1305. doi: 10.1006/jmcc.1996.0351.

Maier, S.A., Galellis, J.R., and McDermid, H.E. (2005). Phylogenetic analysis reveals a novel protein family closely related to adenosine deaminase. *J Mol Evol* 61(6), 776-794. doi: 10.1007/s00239-005-0046-y.

Marsh, J.L., Walker, H., Theisen, H., Zhu, Y.Z., Fielder, T., Purcell, J., et al. (2000). Expanded polyglutamine peptides alone are intrinsically cytotoxic and cause neurodegeneration in Drosophila. *Hum Mol Genet* 9(1), 13-25.

Masino, S., and Boison, D. (2013). *Adenosine : a key link between metabolism and brain activity.* New York: Springer.

Melkani, G.C., Trujillo, A.S., Ramos, R., Bodmer, R., Bernstein, S.I., and Ocorr, K. (2013). Huntington's disease induced cardiac amyloidosis is reversed by modulating protein folding and oxidative stress pathways in the Drosophila heart. *PLoS Genet* 9(12), e1004024. doi: 10.1371/journal.pgen.1004024.

Molina-Arcas, M., Casado, F.J., and Pastor-Anglada, M. (2009). Nucleoside transporter proteins. *Curr Vasc Pharmacol* 7(4), 426-434.

Muller, C.E., and Jacobson, K.A. (2011). Recent developments in adenosine receptor ligands and their potential as novel drugs. *Biochimica Et Biophysica Acta-Biomembranes* 1808(5), 1290-1308. doi: 10.1016/j.bbamem.2010.12.017.

Nalavade, R., Griesche, N., Ryan, D.P., Hildebrand, S., and Krauss, S. (2013). Mechanisms of RNA-induced toxicity in CAG repeat disorders. *Cell Death Dis* 4, e752. doi: 10.1038/cddis.2013.276.

Pak, M.A., Haas, H.L., Decking, U.K., and Schrader, J. (1994). Inhibition of adenosine kinase increases endogenous adenosine and depresses neuronal activity in hippocampal slices. *Neuropharmacology* 33(9), 1049-1053.

Poernbacher, I., and Vincent, J.P. (2018). Epithelial cells release adenosine to promote local TNF production in response to polarity disruption. *Nat Commun* 9(1), 4675. doi: 10.1038/s41467-018-07114-z.

Ritzel, M.W., Ng, A.M., Yao, S.Y., Graham, K., Loewen, S.K., Smith, K.M., et al. (2001). Molecular identification and characterization of novel human and mouse concentrative Na+-nucleoside cotransporter proteins (hCNT3 and mCNT3) broadly selective for purine and pyrimidine nucleosides (system cib). *J Biol Chem* 276(4), 2914-2927. doi: 10.1074/jbc.M007746200.

Ross, C.A., and Tabrizi, S.J. (2011). Huntington's disease: from molecular pathogenesis to clinical treatment. *Lancet Neurol* 10(1), 83-98. doi: 10.1016/S1474-4422(10)70245-3.

Sankar, N., Machado, J., Abdulla, P., Hilliker, A.J., and Coe, I.R. (2002). Comparative genomic analysis of equilibrative nucleoside transporters suggests conserved protein structure despite limited sequence identity. *Nucleic Acids Res* 30(20), 4339-4350.

Sassone, J., Colciago, C., Cislaghi, G., Silani, V., and Ciammola, A. (2009). Huntington's disease: the current state of research with peripheral tissues. *Exp Neurol* 219(2), 385-397. doi:

10.1016/j.expneurol.2009.05.012.

Schmidt, G. (1928). Über fermentative Desaminierung im Muskel. *Biological Chemistry* 179(4-6)**,** 243–282.

Schulte, G., and Fredholm, B.B. (2003). Signalling from adenosine receptors to mitogen-activated protein kinases. *Cell Signal* 15(9)**,** 813-827.

Schutz, W., Schrader, J., and Gerlach, E. (1981). Different sites of adenosine formation in the heart. *Am J Physiol* 240(6)**,** H963-970.

Sideraki, V., Wilson, D.K., Kurz, L.C., Quiocho, F.A., and Rudolph, F.B. (1996). Site-directed mutagenesis of histidine 238 in mouse adenosine deaminase: substitution of histidine 238 does not impede hydroxylate formation. *Biochemistry* 35(47)**,** 15019-15028. doi: 10.1021/bi961427e.

Singh, L.S., and Sharma, R. (2000). Purification and characterization of intestinal adenosine deaminase from mice. *Mol Cell Biochem* 204(1-2)**,** 127-134.

Skaldin, M., Tuittila, M., Zavialov, A.V., and Zavialov, A.V. (2018). Secreted Bacterial Adenosine Deaminase Is an Evolutionary Precursor of Adenosine Deaminase Growth Factor. *Mol Biol Evol* 35(12)**,** 2851-2861. doi: 10.1093/molbev/msy193.

Smith, K.M., Slugoski, M.D., Loewen, S.K., Ng, A.M., Yao, S.Y., Chen, X.Z., et al. (2005). The broadly selective human Na+/nucleoside cotransporter (hCNT3) exhibits novel cation-coupled nucleoside transport characteristics. *J Biol Chem* 280(27)**,** 25436-25449. doi: 10.1074/jbc.M409454200.

Song, W., Smith, M.R., Syed, A., Lukacsovich, T., Barbaro, B.A., Purcell, J., et al. (2013). Morphometric analysis of Huntington's disease neurodegeneration in Drosophila. *Methods Mol Biol* 1017**,** 41-57. doi: 10.1007/978-1-62703-438-8_3.

Steffan, J.S., Agrawal, N., Pallos, J., Rockabrand, E., Trotman, L.C., Slepko, N., et al. (2004). SUMO modification of Huntingtin and Huntington's disease pathology. *Science* 304(5667)**,** 100-104. doi: 10.1126/science.1092194.

Steffan, J.S., Bodai, L., Pallos, J., Poelman, M., McCampbell, A., Apostol, B.L., et al. (2001). Histone deacetylase inhibitors arrest polyglutamine-dependent neurodegeneration in Drosophila. *Nature* 413(6857)**,** 739-743. doi: Doi 10.1038/35099568.

Strater, N. (2006). Ecto-5'-nucleotidase: Structure function relationships. *Purinergic Signal* 2(2)**,** 343-350. doi: 10.1007/s11302-006-9000-8.

Tamura, T., Sone, M., Yamashita, M., Wanker, E.E., and Okazawa, H. (2009). Glial cell lineage expression of mutant ataxin-1 and huntingtin induces developmental and late-onset neuronal pathologies in Drosophila models. *PLoS One* 4(1)**,** e4262. doi: 10.1371/journal.pone.0004262.

Taylor, J.P., Taye, A.A., Campbell, C., Kazemi-Esfarjani, P., Fischbeck, K.H., and Min, K.T. (2003). Aberrant histone acetylation, altered transcription, and retinal degeneration in a Drosophila model of polyglutamine disease are rescued by CREB-binding protein. *Genes Dev* 17(12)**,** 1463-1468. doi: 10.1101/gad.1087503.

Trincavelli, M.L., Daniele, S., and Martini, C. (2010). Adenosine receptors: what we know and what

we are learning. *Curr Top Med Chem* 10(9)**,** 860-877.

Tritsch, G.L., Paolini, N.S., and Bielat, K. (1985). Adenosine deaminase activity associated with phagocytic vacuoles. Cytochemical demonstration by electron microscopy. *Histochemistry* 82(3)**,** 281-285.

van der Burg, J.M., Bjorkqvist, M., and Brundin, P. (2009). Beyond the brain: widespread pathology in Huntington's disease. *Lancet Neurol* 8(8)**,** 765-774. doi: 10.1016/S1474-4422(09)70178-4.

Vonsattel, J.P., and DiFiglia, M. (1998). Huntington disease. *J Neuropathol Exp Neurol* 57(5)**,** 369-384. doi: 10.1097/00005072-199805000-00001.

Walker, F.O. (2007). Huntington's disease. *Lancet* 369(9557)**,** 218-228. doi: 10.1016/s0140-6736(07)60111-1.

Warrick, J.M., Chan, H.Y., Gray-Board, G.L., Chai, Y., Paulson, H.L., and Bonini, N.M. (1999). Suppression of polyglutamine-mediated neurodegeneration in Drosophila by the molecular chaperone HSP70. *Nat Genet* 23(4)**,** 425-428. doi: 10.1038/70532.

Weiss, K.R., Kimura, Y., Lee, W.C., and Littleton, J.T. (2012). Huntingtin aggregation kinetics and their pathological role in a Drosophila Huntington's disease model. *Genetics* 190(2)**,** 581-600. doi: 10.1534/genetics.111.133710.

Xiao, C.Y., Liu, N.L., Jacobson, K.A., Gavrilova, O., and Reitman, M.L. (2019). Physiology and effects of nucleosides in mice lacking all four adenosine receptors. *Plos Biology* 17(3). doi: ARTN e3000161

10.1371/journal.pbio.3000161.

Yao, S.Y., Ng, A.M., Vickers, M.F., Sundaram, M., Cass, C.E., Baldwin, S.A., et al. (2002). Functional and molecular characterization of nucleobase transport by recombinant human and rat equilibrative nucleoside transporters 1 and 2. Chimeric constructs reveal a role for the ENT2 helix 5-6 region in nucleobase translocation. *J Biol Chem* 277(28)**,** 24938-24948. doi: 10.1074/jbc.M200966200.

Zavialov, A.V., Yu, X., Spillmann, D., Lauvau, G., and Zavialov, A.V. (2010). Structural basis for the growth factor activity of human adenosine deaminase ADA2. *J Biol Chem* 285(16)**,** 12367-12377. doi: 10.1074/jbc.M109.083527.

Zimmermann, H., and Braun, N. (1996). Extracellular metabolism of nucleotides in the nervous system. *J Auton Pharmacol* 16(6)**,** 397-400. doi: 10.1111/j.1474-8673.1996.tb00062.x.

Zurovec, M., Dolezal, T., Gazi, M., Pavlova, E., and Bryant, P.J. (2002). Adenosine deaminase-related growth factors stimulate cell proliferation in Drosophila by depleting extracellular adenosine. *Proc Natl Acad Sci U S A* 99(7)**,** 4403-4408. doi: 10.1073/pnas.062059699.

6. Publication I

Yu-Hsien Lin, Houda Ouns Maaroufi, Lucie Kucerova, Lenka Rouhova, Tomas Filip, Michal Zurovec (2019). Adenosine signaling and its downstream target mod(mdg4) modify the pathogenic effects of polyglutamine in a *Drosophila* model of Huntington's disease. BioRxiv. doi: 10.1101/2019.12.22.886143

Adenosine signaling and its downstream target mod(mdg4) modify the pathogenic effects of polyglutamine in a *Drosophila* model of Huntington's disease

Yu-Hsien Lin[1,2*], Houda Ouns Maaroufi[1,2], Lucie Kucerova[1], Lenka Rouhova[1,2], Tomas Filip[1,2], Michal Zurovec[1,2*]

[1]Biology Centre of the Czech Academy of Sciences, Institute of Entomology, Ceske Budejovice, Czech Republic, [2]Faculty of Science, University of South Bohemia, Ceske Budejovice, Czech Republic

*Correspondence and requests for materials should be addressed to Y.H.L. (email: r99632012@gmail.com) and M.Z. (email: zurovec@entu.cas.cz).

Abstract

Dysregulation of adenosine (Ado) homeostasis has been observed in both rodent models and human patients of Huntington's disease (HD). However, the underlying mechanisms of Ado signaling in HD pathogenesis are still unclear. In the present study, we used a *Drosophila* HD model to examine the concentration of extracellular Ado (e-Ado) as well as the transcription of genes involved in Ado homeostasis and found similar alterations. Through candidate RNAi screening, we demonstrated that silencing the expression of adenosine receptor (*adoR*) and equilibrative nucleoside transporter 2

(*ent2*) not only significantly increases the survival of HD flies but also suppresses both retinal pigment cell degeneration and the formation of mutant Huntingtin (mHTT) aggregates in the brain. We compared the transcription profiles of *adoR* and *ent2* mutants by microarray analysis and identified a downstream target of AdoR signaling, *mod(mdg4)*, which mediates the effects of AdoR on HD pathology in *Drosophila*. Our findings have important implications for the crosstalk between Ado signaling and the pathogenic effects of HD, as well as other human diseases associated with polyglutamine aggregation.

Introduction

Adenosine (Ado) is one of the most common neuromodulators in the nervous system of vertebrates as well as invertebrates and modulates synaptic transmission (Cunha, 2001; Dunwiddie and Masino, 2001). Under normal conditions, the extracellular Ado (e-Ado) concentration is in the nanomolar range, which is sufficient to modulate the appropriate adenosine receptors (AdoRs) in the brain cells tonically (Fredholm, 2007). However, under pathological circumstances the e-Ado level may increase up to 100-fold. In these conditions, Ado functions as an imperfect neuroprotector; in some cases it may be beneficial and in others may worsen tissue damage (Picano and Abbracchio, 2000). Recent experiments with knockout mice for all four *adoRs* demonstrated that Ado signaling is less involved in baseline physiology and likely more crucial for its roles as a signal of stress, damage, and/or danger (Xiao et al., 2019). It has also been suggested that Ado signaling is mainly engaged when an allostatic response is needed (Cunha, 2019).

Due to its impact on important physiological functions in the brain, e-Ado signaling has attracted attention as a possible *therapeutic* agent in Huntington's disease

(HD)(Lee and Chern, 2014), a dominant hereditary neurodegenerative disorder caused by a mutation in the Huntingtin gene (*htt*). Mutated HTT protein (mHTT) contains an expanded polyglutamine (polyQ) tract encoded by 40 to more than 150 repeats of CAG trinucleotide (Vonsattel and DiFiglia, 1998). Although mHTT is ubiquitously expressed in the central nervous system (CNS) and peripheral cells in HD patients, it predominantly affects striatal neurons that contain a higher density of adenosine receptors A2A ($A_{2A}R$) and A1 (A_1R) (Blum et al., 2003a). Several studies have demonstrated that the abnormality of AdoRs activity, especially $A_{2A}R$ in the striatum, contributes to HD pathogenesis (Gomes et al., 2011; Blum et al., 2018a). In addition, the alteration of adenosine tone and the upregulation of striatal equilibrative nucleoside transporters (ENTs), facilitating *Ado transport* across the cytoplasmic membrane, suggest that e-Ado concentration could serve as a HD biomarker for assessing the initial stages of neurodegeneration (Guitart et al., 2016; Kao et al., 2017a). However, the complexity of the system modulating Ado metabolism and the crosstalk between individual AdoRs, as well as their interactions with purinergic (P2) or dopamine receptors, impedes the characterization of HD pathophysiology and downstream mechanisms of e-Ado signaling (Anderson and Nedergaard, 2006; Tyebji et al., 2015).

Drosophila expressing human mHTT has previously been demonstrated as a suitable model system for studying gene interactions in polyQ pathology, and has been used to elicit a number of modifiers for symptoms of HD (Steffan et al., 2001; Lewis and Smith, 2016). *Drosophila* e-Ado signaling is a relatively simple system compared to mammals; it contains a single AdoR isoform (cAMP simulation) and lacks P2X receptors (Kucerova et al., 2012; Fountain, 2013). Human homologs of the *Drosophila* genes involved in the regulation of Ado homeostasis and AdoR are shown in Fig. S1. The lack of adenosine deaminase 1 (ADA1) in *Drosophila* indicates that adenosine

deaminase-related growth factors (ADGFs, related to ADA2), together with adenosine kinase (AdenoK), are the major metabolic enzymes converting extra- and intra-cellular adenosine to inosine and AMP, respectively (Zurovec et al., 2002; Maier et al., 2005; Stenesen et al., 2013). e-Ado signaling in *Drosophila* is involved in regulating various physiological and pathological processes, including modulation of synaptic plasticity, JNK-mediated stress response, hematopoiesis, and metabolic switching upon immune challenges (Knight et al., 2010; Bajgar et al., 2015; Poernbacher and Vincent, 2018).

In the present study, we performed a candidate RNAi screen examining the role of Ado signaling in a *Drosophila* HD model. We co-expressed exon 1 with a polyglutamine *tract* of normal human *htt* Q20 or pathogenic *mhtt* Q93(Steffan et al., 2001) together with *UAS-RNAi* or *UAS*-overexpression constructs specific for *adoR*, Ado transporters, and Ado metabolic enzymes in *Drosophila*. We demonstrated that the downregulation of *adoR* and *ent2* expression reduces cell death, mortality and the formation of mHTT aggregates. In addition, we identified a number of differentially-expressed genes in response to Ado signaling and showed that *mod(mdg4)* is a downstream target of AdoR that mediates its effect in HD pathogenesis.

Results

Phenotypes of *Drosophila* expressing mHTT

To verify the effect *of mHTT expression* on *D. melanogaster*, we used a *UAS/GAL4* system for targeted gene expression. Flies overexpressing normal exon 1 from human huntingtin (Q20 HTT), or its mutant pathogenic form (Q93 mHTT), were driven by the pan-neuronal driver, *elav-GAL4*. The results showed that expression of mHTT under the *elav-GAL4* driver in the *Drosophila* brain is not lethal during the larval stage (Fig. S2A) but reduces both the adult eclosion rate (Fig. S2B) and adult *lifespan* (Fig. S2C).

These results are consistent with previous observations (Song et al., 2013).

Disturbance of extracellular adenosine (e-Ado) homeostasis in HD larvae

A recent study of human HD patients reported a reduced concentration of e-Ado in the cerebrospinal fluid (Kao et al., 2017b). To determine whether e-Ado levels are also altered in HD *Drosophila*, we compared e-Ado levels in the hemolymph of last-instar larvae ubiquitously expressing Q20 HTT and Q93 mHTT driven by the *daughterless-Gal4* driver (*da-GAL4*). The results showed that the e-Ado concentration in the hemolymph of Q93-expressing larvae was significantly lower compared to larvae expressing Q20 or control *da-GAL4* (Fig. 1A).

Since e-Ado concentration may be associated with the level of extracellular ATP (e-ATP), we also examined its titer in the hemolymph of larvae with the same genotypes as the above experiment. As shown in Fig. 1B, there was no significant difference in e-ATP levels between Q20, Q93, and control *da-GAL4* larvae. We thus postulated that the lower level of e-Ado in Q93 larvae might be affected by changes in proteins involved in Ado metabolism or transportation.

Altered transcriptions of genes involved in Ado homeostasis in HD *Drosophila*

Earlier reports have shown that the expression of several genes involved in Ado homeostasis, including Ado receptor, transporters, and genes involved in Ado metabolism, are abnormal in human HD patients as well as in HD mice (Martinez-Mir et al., 1991; Glass et al., 2000; Mievis et al., 2011). Since homologous proteins have also been shown to control Ado homeostasis in flies (Fig. S1), we compared the expression of three *Drosophila adgf* genes (*adgf-a*, *adgf-c*, *adgf-d*), adenosine kinase (*adenoK*), adenosine transporters (*ent1*, *ent2*, *ent3*, *cnt2*), and adenosine receptor (*adoR*) in the brains of Q93- and Q20-expressing larvae. The results showed that the expression of *adgf-a* and *adgf-d*, as well as transporters *ent1*, *ent2*, and *ent3* in the brain of Q93

larvae were significantly lower than in Q20 larvae (Fig. 1D). The expression of *cnt2* and *adoR* showed no difference between Q93 and Q20 larvae.

In order to assess progressive changes in transcription profiles associated with HD pathogenesis, we further examined the expression of genes involved in Ado homeostasis in the heads of 5- and 15-day-old adults, roughly corresponding to early- and late-stage HD (Fig. S2C). Unlike in the larval stage, the expression of metabolic genes *adgf-c*, *adgf-d*, and *adenoK*, and transporter *ent1*, in five-day-old adults was found to be higher in Q93 flies than Q20 flies (Fig. 1E). In addition, 15-day-old Q93 flies showed higher expression of *adgf-d* and *adenoK* (Fig. 1F). Previous studies in *Drosophila* have shown that the downregulation of the transporter *ents* decreases e-Ado concentration (Bajgar et al., 2015; Poernbacher and Vincent, 2018); hence, the reduced expression of three *ent* genes could explain why the e-Ado level is lower in Q93 larvae. Moreover, it has also been shown that the expression of *adgfs* as well as *adenoK* follows the levels of e-Ado upon stress conditions (Zuberova et al., 2010; Bajgar and Dolezal, 2018), suggesting that the lower expression of *adgfs* in Q93 larvae and the higher expression in Q93 adults might be a consequence of elevated e-Ado concentrations resulting from HD pathogenesis.

Functional characterization of Ado homeostasis and signaling in HD flies

To understand the effects of alterations in Ado homeostasis on polyQ pathology, we used the pan-neuronal driver, *elav-GAL4*, for RNAi-mediated silencing of the genes involved in Ado transport, metabolism, and *adoR* in Q93-expressing flies and assessed their survival and formation of mHTT aggregates. In addition, we also co-expressed Q93 with RNAi transgenes in the eyes by using the *gmr-GAL4*(Mugat et al., 2008; Kuo et al., 2013) driver and compared levels of retinal pigment cell degeneration.

Silencing the transcriptions of Ado metabolic enzymes showed that only the RNAi

of *adgf-D* increased the number of eclosion rate (Fig. 2A). Silencing *adgf-A* and *adenoK*, but not *adgf-D* or *adgf-C* RNAi, extended the adult lifespan of Q93-expressing flies (Fig. 2B). To ensure that the mortality of the HD flies was mainly caused by Q93 expression and not by RNAi constructs, we recorded the survival of flies co-expressing normal *htt* Q20 together with RNAi transgenes until all corresponding experimental flies (expressing Q93 together with RNAi constructs) died (Fig. S3A). However, silencing *adgfs* or *adenoK* only affected survival and did not significantly influence mHTT aggregation (Fig. 2C&D) or retinal pigment cell degeneration (Fig. 2E).

Next, we examined the RNAi silencing of *adoR* and Ado transporters in Q93 and control Q20 flies. The results showed that knocking down the expression of *adoR* as well as two transporters, *ent1* and *ent2*, significantly increased the eclosion rate (Fig. 3A) and adult lifespan (Fig. 3B). The RNAi silencing of *ent2* and *adoR* extended the lifespan of HD flies to 30 and 40 days, respectively, which is about 1.5~2 times longer than that of HD flies. In contrast, knocking down *cnt2* expression did not change the viability of HD flies, and knocking down *ent3* did not influence the eclosion rate, although it increased mortality and shortened the lifespan of adult HD flies. The survival of control flies expressing Q20 with individual RNAi constructs are shown in Fig. S3B. mHTT aggregation was significantly reduced (to 50%) in *adoR* RNAi flies (Fig. 3C&D), and a similar suppression of mHTT aggregate formation was also observed in 20-day-old HD flies (Fig. S4). An examination of eye phenotypes in *ent2* RNAi flies showed a significant reduction in retinal pigment cell death (Fig. 3E), but surprisingly we did not observe a significant rescue of cell death by silencing *adoR* (Fig S5). We therefore postulated that it might be due to insufficient RNAi efficiency for suppressing AdoR signaling in the eye. To test this, we combined Q93 flies with the *adoR* RNAi transgene under a *adoR* heterozygote mutant background ($AdoR^{1}$/+) or with

AdoR^{1} homozygote mutant, and both showed significantly decreased retinal pigment cell degeneration similar to *ent2*–RNAi flies (Fig. 3E).

To further validate the RNAi results, we studied flies simultaneously expressing Q93 and overexpressing *ent2*, *adoR*, *adgf-A*, and *adenoK* in the brain and assessed the adult lifespans. Since silencing these genes extended the lifespan of HD flies (Figs. 2B&3B), we expected the opposite effect upon overexpression. As shown in Fig. S6A, *ent2* overexpression significantly increased the mortality of early-stage HD flies; the survival of 5-day-old flies dropped to 60% for HD flies in contrast to 90% for Q93 control flies, and the lifespan of HD flies was significantly shorter than control flies expressing either Q93 alone or together with *gfp* RNAi. Consistently, we co-expressed strong and weak *adoR* overexpressing transgenes with Q93 and both significantly increased the mortality and shortened the lifespan of Q93 flies. The effects of shortening the lifespan were more severe than with *ent2* overexpression. Nevertheless, the increase in mortality by *adgf-A* and *adenoK* overexpression was not as strong as that caused by *ent2* and *adoR* overexpression, although both still showed a significant difference to either Q93 control or Q93/*gfp* RNAi control by weighted log-rank test (Fig. S6B). Hence, we concluded that overexpressing the examined genes enhances the effect of mHTT, resulting in the increased mortality of HD flies. Our results demonstrate that the overexpression and silencing of *ent2* or *adoR* has a stronger influence over HD pathology than genes involved in Ado metabolism.

Interactions of AdoR with ENT1 and ENT2

In order to investigate whether there is a synergy between the effects of AdoR and ENTs, we co-expressed *adoR* RNAi constructs with *ent1* RNAi or *ent2* RNAi in Q93-expressing flies. As shown in Fig. 4A, the silencing of both *ent2* and *adoR* has the same effect as silencing only *adoR*, indicating that ENT2 and AdoR are in the same

pathway. Interestingly, the double knockdown of *ent1* and *adoR* shows a sum of individual effects on lifespan which is longer than the knockdown of *adoR* alone. There seems to be a synergy between ENT1 and AdoR suggesting that ENT1 may have its own effect, which is partially independent from AdoR signaling.

Next, we investigated our hypothesis that the source of e-Ado, which contributes to AdoR activation in Q93 flies, is mainly intracellular and released out of the cells by ENTs. We conducted an epistasis analysis by combining mHTT with *adoR* overexpression and *ent1* or *ent2* RNAi. The results showed that *adoR* overexpression increased the mortality of Q93 flies while the combination of *adoR* overexpression with either *ent1* or *ent2* RNAi minimized the increased mortality caused by *adoR* overexpression (Fig. 4B). Notably, Q93 flies expressing *ent2* RNAi and overexpressing *adoR* had the longest lifespan in comparison to Q93 control or *ent1* RNAi flies. These results suggest that AdoR signaling needs functional Ado transportation to carry out its effect and thus the Ado efflux from these cells is needed for AdoR activity (Fig. 4C&D). The source of e-Ado, which contributes to AdoR activation causing HD pathogenesis, seems to be intracellular and it is mainly released out of the cells through ENT2.

AMPK is not involved in *Drosophila* HD pathogenesis

AMP-activated protein kinase (*AMPK*) is one of the key enzymes maintaining energy balance within a cell by adjusting anabolic and catabolic pathways (Aymerich et al., 2006); both Ado receptors and transporters have been implicated in its activation (Medina-Pulido et al., 2013; Dolinar et al., 2018; Liu et al., 2018; Ruan et al., 2018). Activation of AMPK is beneficial at early stages in mammalian HD models (Vazquez-Manrique et al., 2016); however, in the late stage of the disease it may worsen neuropathological and behavioral phenotypes (Ju et al., 2011).

To find out whether the above-described effects of e-Ado signaling and transport on

HD flies are mediated by AMPK, we co-expressed *Q93 mHTT* with three different recombinant forms of AMPK α subunit (Johnson et al., 2010; Swick et al., 2013), including wild-type AMPKα [M], a phosphomimetic-activated form of AMPKα [T184D], and dominant negative AMPK [DN], and assessed the survival of HD flies. The results showed that neither the activation nor the inhibition of AMPK signaling influenced the eclosion rate (Fig. S7A) or lifespan (Fig. S7B).

To further confirm the genetic data related to AMPK activation or inhibition, we pharmaceutically inhibited AMPK signaling by feeding the larvae with AMPK inhibitor, dorsomorphin (Compound C) (Braco et al., 2012). The results showed that although dorsomorphin had an effect on the development of larvae expressing normal Q20 HTT, it did not influence the eclosion of Q93-expressing larvae (Fig. S7C). Overall, our results show that, unlike in mammalian HD models, AMPK signaling does not play a significant role in the pathological manifestations of mHTT in *Drosophila*.

Identification of potential downstream targets of the AdoR/ENT2 pathway by microarray analysis

Our above results indicate that ENT2 and AdoR contribute to mHTT pathogenesis in HD *Drosophila* and work in the same pathway. To identify their downstream target genes, we compared the expression profiles of larvae carrying mutations in *adoR* or *ent2* as well as adult *adoR* mutants using microarrays (Affymetrix), shown as a Venn diagram in Fig. 5A and B. The intersection between each mutant contains differentially expressed transcripts in all three data sets, including six upregulated (Fig. 6A) and seven downregulated mRNAs (Fig. 5B). Interestingly, according to Flybase (http://flybase.org), four of these genes were expressed in the nervous system (*ptp99A* was upregulated, while *CG6184*, *cindr*, and *mod(mdg4)* were downregulated) (Fig. 5C). To validate the microarray data, we knocked down *adoR* expression in the brain and

examined the transcription of the four candidate genes expressed in the nervous system by qPCR. The results revealed that *ptp99A* and *mod(mdg4)* had the same expression trends as observed in the microarrays (Fig. 5D). We further examined whether the expression of *ptp99A* and *mod(mdg4)* are influenced by an increase of e-Ado level. As shown in Fig. 6E, Ado microinjection significantly increased *mod(mdg4)* expression and decreased *ptp99A* expression, confirming that *mod(mdg4)* is positively regulated and *ptp99A* is negatively regulated by the AdoR/ENT2 pathway.

Suppression of *mod(mdg4)* decreased mHTT aggregation and increased survival of HD flies

In order to examine the potential roles of *ptp99A*, *CG6184*, *cindr*, and *mod(mdg4)* genes in HD pathogenesis, we used RNAi to silence them in HD flies. The results showed that only the RNAi silencing of *mod(mdg4)* extended their lifespan. As shown in Figure 6A, the survival curve of HD flies with a silenced *mod(mdg4)* gene was almost identical to the curve specific for *adoR* RNAi HD flies; this effect was stronger than in *ent2* RNAi HD flies. In addition, *mod(mdg4)* RNAi significantly decreased the formation of mHTT inclusions (Fig. 6B&C) and suppressed retinal pigment cell degeneration (Fig. 7D). In contrast to *mod(mdg4)*, RNAi silencing of the other three genes did not show any significant effect.

To further confirm that *mod(mdg4)* is downstream target of the AdoR pathway and regulated by e-Ado signaling, we first checked the expression of *mod(mdg4)* in larval brains and adult heads of HD flies using qPCR. In Q93 larvae, we found that both the expression level of *mod(mdg4)* (Fig. 7A) and the e-Ado level was lower than in Q20-expressing controls (Fig. 1A). For the 15-day-old (roughly corresponding to late-stage HD) Q93 adults, there was no difference in *mod(mdg4)* expression compared to Q20 control adults (Fig. 7A). We next examined the epistasis relationship between *ent2*,

adoR, and *mod(mdg4)* by combining overexpression of *ent2* or *adoR mod(mdg4)* RNAi in Q93-expressing flies. The results showed that *mod(mdg4)* RNAi suppressed the lethal effects caused by the overexpression of *ent2* and *adoR* (Fig. 8B). These results indicate that *mod(mdg4)* serves as a downstream target of AdoR signaling involved in the process of mHTT inclusion formation and other pathogenic effects (Fig. 7C).

The *mod(mdg4)* locus of *Drosophila* contains several transcription units encoded on both DNA strands producing 31 splicing isoforms (Yu et al., 2014). As shown in Fig. 5B, two of the *mod(mdg4)*-specific microarray probes which target 11 *mod(mdg4)* splicing isoforms (Tab. S2) were downregulated in all three datasets. We performed splice form-specific qPCR analysis and found that *adoR* RNAi silencing leads to the downregulation of multiple *mod(mdg4)* isoforms (Fig. 7D), suggesting that AdoR signaling regulates multiple isoforms.

Discussion

Considerable dysregulation of Ado homeostasis has been observed in HD human patients and mice, but the mechanisms of such changes related to HD pathogenesis still need to be characterized (Blum et al., 2018b). The present study examined the e-Ado titer in the hemolymph of HD *Drosophila* larvae and found that it is lower in Q93-expressing larvae (Fig. 1). Although we did not measure the e-Ado titer in adult flies (due to a problem in acquiring a sufficient amount of hemolymph), the dynamic changes in expression levels of genes involved in Ado homeostasis (Fig. 1D-E), as well as the AdoR-regulated gene, *mod(mdg4)* (Fig. 8A), indicated that e-Ado titer and AdoR activity are variable in different stages of HD. Such dynamic changes of e-Ado homeostasis have also been observed in rodent HD models, whereby striatal adenosine tone is lower during the early stage of the disease and increased during the

later stages (Gianfriddo et al., 2004; Guitart et al., 2016).

Both the activation and inhibition of $A_{2A}R$ by pharmacological treatments have shown benefits in mammalian HD models. In R6/2 mice, the beneficial effect of activating $A_{2A}R$ is thought to occur *via* the inhibition of AMPK nuclear translocation (which contributes to HD pathogenesis including brain atrophy, neuron death, and increased mHTT aggregates formation) (Ju et al., 2011). Beneficial effects by antagonizing $A_{2A}R$ with SCH58261 in R6/2 mice include reduced striatal glutamate and adenosine outflow as well as restoring emotional behavior and susceptibility to NMDA toxicity (Gianfriddo et al., 2004; Domenici et al., 2007). A_1R activation has also been shown to have neuroprotective effects; however, the chronic administration of A_1R agonists (leading to a desensitisation of A1 receptors) increases neuronal loss whereas the chronic administration of A_1R antagonists (inducing an upregulation of A1 receptors) improves survival and neuronal preservation in the same model (Blum et al., 2003b). Our results show that the genetic depletion of AdoR has beneficial effects on HD flies, while the activation of AdoR contributes to mHTT pathogenesis and aggregates formation.

We observed a non-additive interaction between AdoR and ENT2 characteristic for epistasis relationship (Fig. 4B), indicating that ENT2 is required for the transportation of Ado from the intra- to extracellular environment which activates AdoR and, in turn, enhances the effects of mHTT. Our previous report showed that both ENT2 and AdoR participate in modulating synaptic transmission, and that both *adoR* and *ent2* mutations cause defects in associative learning in *Drosophila* (Knight et al., 2010). Consistently, both the inhibition of Ado release by the knockdown of *ent2* in hemocytes and the mutation of *adoR* suppress metabolic reprogramming and hemocyte differentiation upon immune challenges (Bajgar et al., 2015). Furthermore, another

report showed that the disruption of epithelial integrity by Scribbled (*Scrib*) RNAi stimulates Ado release through ENT2, subsequently activating AdoR that, in turn, upregulates tumor necrosis factor (TNF) production which activates JNK signaling (Poernbacher and Vincent, 2018). Interestingly, while the effects of *ent2* and *adoR* RNAi in HD flies were found to completely overlap, *ent1* RNAi showed a synergistic effect, suggesting potential AdoR-independent mechanisms (Fig. 4A). These results correspond to our previous report showing that *Drosophila* ENT1 has lower specificity for Ado transportation in comparison to ENT2 (Fleischmannova et al., 2012). The altered expression of *ent1*, as well as the RNAi effect in HD flies, might be associated with the disturbance of nucleotide homeostasis, similar to that observed in R6/2 and Hdh^{Q150} mice (Toczek et al., 2016).

We identified a downstream target of the AdoR pathway, mod(mdg4), which contributes to the effects of mHTT in the *Drosophila* HD model. The *mod(mdg4)* gene has previously been implicated in the regulation of position effect variegation, chromatin structure, and neurodevelopment (Dorn and Krauss, 2003). The altered expression of *mod(mdg4)* has also been observed in flies expressing untranslated RNA containing CAG and CUG repeats (Mutsuddi et al., 2004; van Eyk et al., 2011). In addition, *mod(mdg4*) has complex splicing, including *trans*-splicing, producing at least 31 isoforms (Krauss and Dorn, 2004). All isoforms contain a common N-terminal BTB/POZ domain which mediates the formation of homomeric, heteromeric, and oligomeric protein complexes (Bardwell and Treisman, 1994; Albagli et al., 1995; Espinas et al., 1999). Among these isoforms, only two [including *mod(mdg4)*-56.3 (isoform H) and *mod(mdg4)*-67.2 (isoform T)] have been functionally characterized. *Mod(mdg4)*-56.3 is required during meiosis for maintaining the chromosome pairing and segregation in males (Thomas et al., 2005; Soltani-Bejnood et al., 2007).

Mod(mdg4)-67.2 interacts with Suppressor of hairy wing [Su(Hw)] and Centrosomal protein 190 kD (CP190) forming a chromatin insulator complex which inhibits the action of the enhancer on the promoter, and is important for early embryo development and oogenesis (Buchner et al., 2000; Soshnev et al., 2013; Melnikova et al., 2018). Although our results showed that silencing all *mod(mdg4)* isoforms decreases the effects of mHTT (Fig. 6), we could not clarify which of the isoforms is specifically involved in HD pathogenesis because AdoR signaling regulates multiple isoforms (Fig. 7D). Interestingly, an earlier report on protein two-hybrid screening indicated that Mod(mdg4) interacts with six Hsp70 family proteins (Giot et al., 2003; Oughtred et al., 2019), and Hsp70 proteins are known for their contribution to the suppression of polyQ aggregates formation and neurodegeneration (Warrick et al., 1999; Chan et al., 2000). Further study will be needed to identify the specific *mod(mdg4)* isoform involved in HD pathogenesis, and whether a decrease in mHTT aggregates by mod(mdg4) RNAi is connected to Hsp70 interaction.

In summary, we observed an alteration in the e-Ado concentration and expression of genes involved in Ado homeostasis in a *Drosophila* HD model. By candidate RNAi screening, we demonstrated that the silencing of *ent2* and *adoR* increases the survival of HD flies in addition to suppressing retinal cell degeneration and mHTT aggregate formation. We also showed that the activation of e-Ado signaling enhances the effects of mHTT. Furthermore, we found that *mod(mdg4)* is a downstream target of the AdoR pathway and plays a major role in the pathogenesis of HD flies. Our work enhances our understanding of e-Ado signaling in HD pathogenesis and may open up new opportunities for HD pharmacological intervention.

Figures

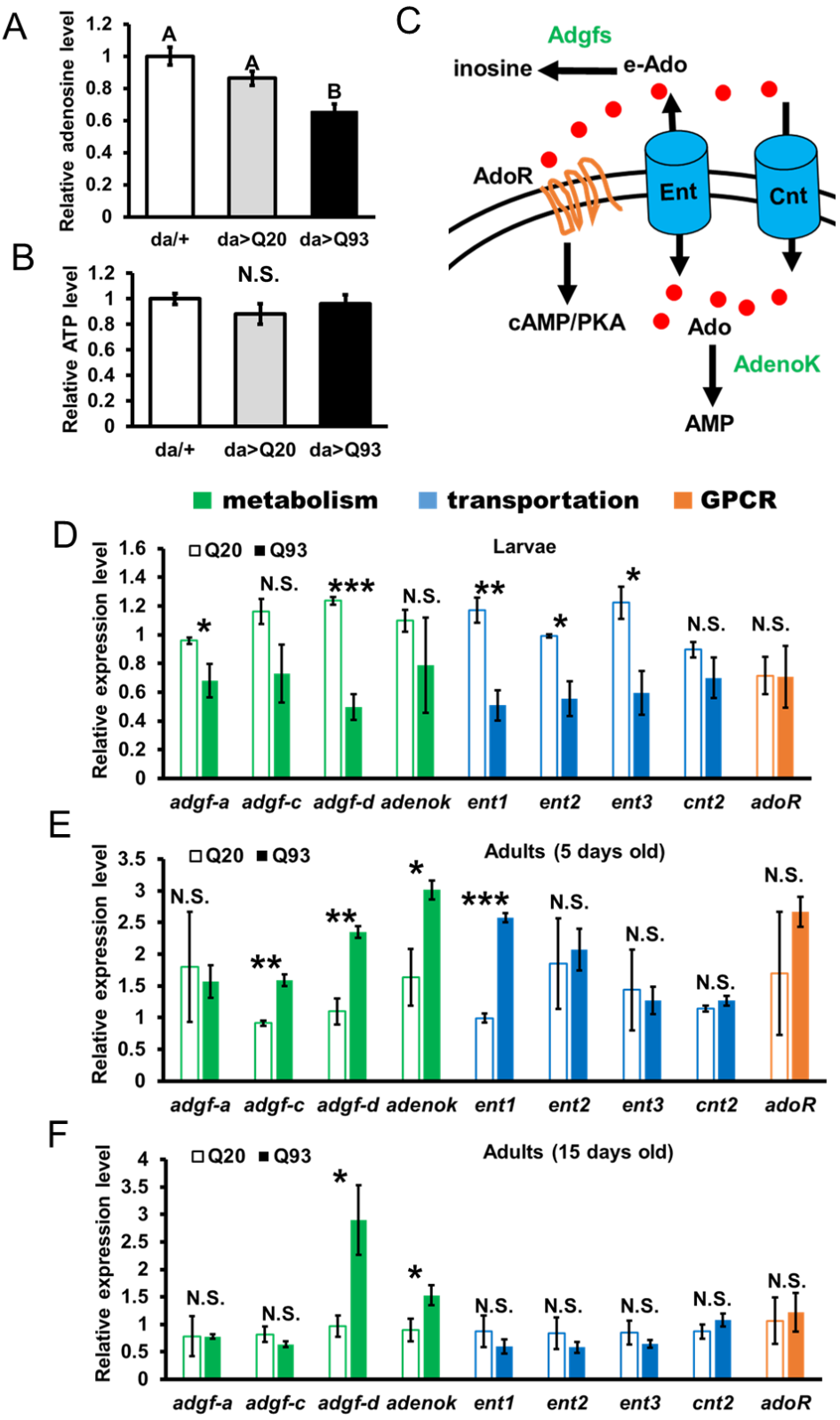

Figure 1. Alteration of adenosine homeostasis in the *Drosophila* HD model. (A-B) The measurements of extracellular adenosine levels (A) and extracellular ATP levels (B) in

Q93-expressing (da>Q93), Q20-expressing (da>Q20) and control *da*-GAL4 (da/+) larvae. Six independent replicates were measured. Significance was analyzed by ANOVA with Tukey's HSD *post-hoc* test; significant differences ($P < 0.05$) among treatment groups are marked with different letters. (C) Diagram showing the interaction of adenosine metabolic enzymes, transporters, and receptors in *Drosophila*. (D-F) Expression profiles of genes involved in adenosine metabolism (green) and adenosine transportation (blue) as well as adenosine receptors (orange) at different stages in HD *Drosophila* brains (larvae) or heads (adults). The expression of Q20 and Q93 were driven by the pan-neuronal driver (*elav*-GAL4). Three independent replicates were measured. The significances of results were examined using Student's t-test: $*P < 0.05$, $**P < 0.01$, $***P < 0.001$; N.S., not significant. All data are presented as mean ± SEM

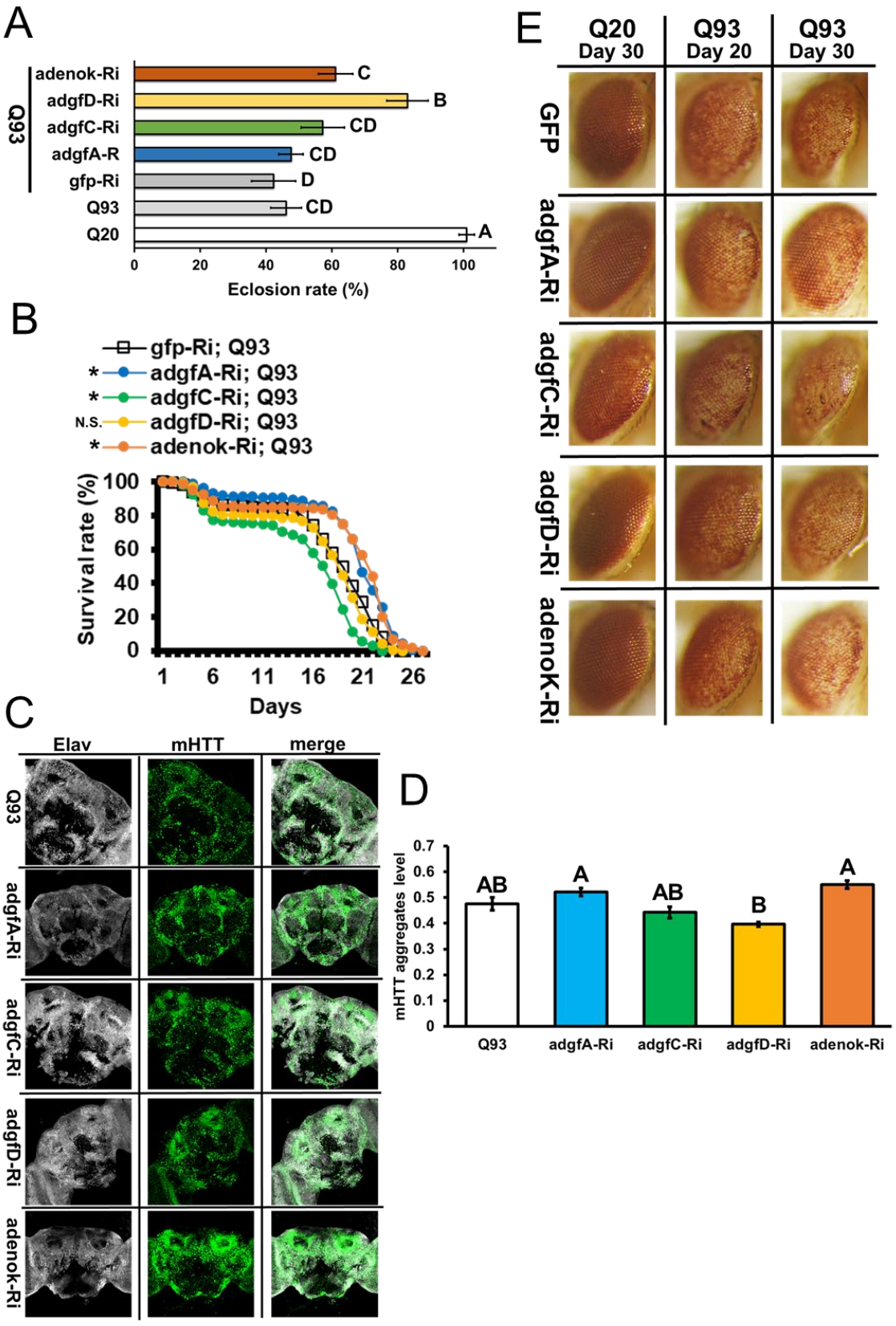

Figure 2. RNAi-mediated (Ri) downregulation of adenosine metabolic genes in HD

Drosophila. Co-expression Q93 with each RNAi transgenes were driven by the pan-neuronal driver, *elav*-GAL4 (A-D), or eye driver, *gmr-GAL4* (E). The adult eclosion rate (A), adult lifespan (B), mHTT aggregate levels (C-D), and retinal pigment cell degeneration (E) were compared. † Eye image of homozygous $adoR^{1}$ mutant without *htt* expression. At least five independent replicates were measured for eclosion rate. Detailed methodologies of the lifespan assay, eye imaging, and quantification of mHTT aggregates are described in Materials and methods. Significance values of the eclosion rate (A) and mHTT aggregates levels (D) were analyzed by ANOVA with Tukey's HSD *post-hoc* test; significant differences ($P < 0.05$) among treatment groups are marked with different letters. Significance values for the adult lifespan curve (B) were analyzed by a weighted log-rank test, and significant differences between control gfp-Ri flies with each RNAi group are labeled as follows: $*P < 0.05$; N.S., not significant. Error bars are presented as mean ± SEM

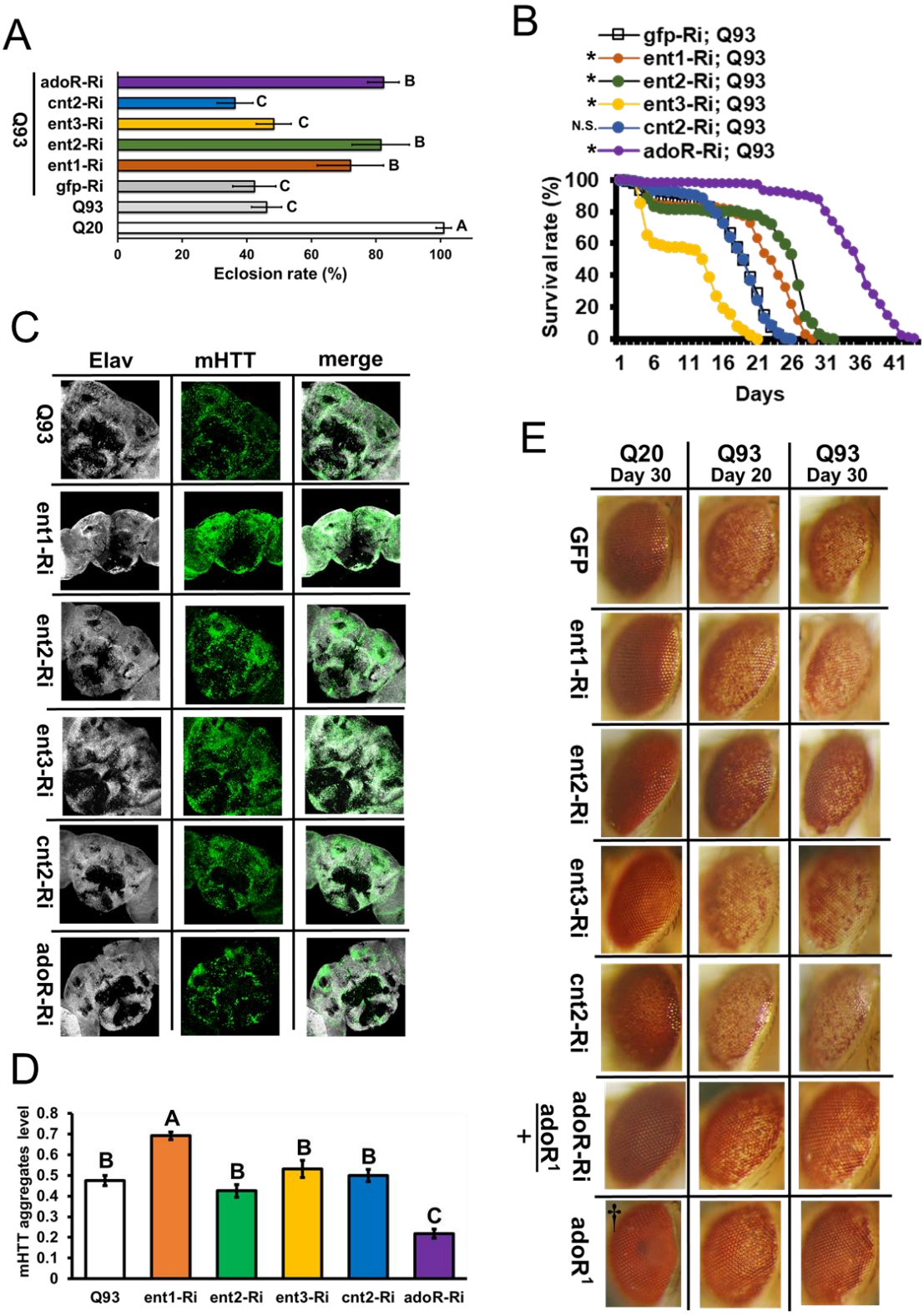

Figure 3. RNAi-mediated (Ri) downregulation of adenosine transporters and adenosine receptor (*adoR*) in HD *Drosophila*. Co-expression of Q93 with each RNAi transgene

was driven by the pan-neuronal driver, *elav*-GAL4 (A-D), or eye driver, *gmr*-GAL4 (E). The adult eclosion rate (A), adult lifespan (B), mHTT aggregate levels (C-D), and retinal pigment cell degeneration (E) were compared. At least five independent replicates were measured for eclosion rate. Detailed methodologies of the lifespan assay, eye imaging, and quantification of mHTT aggregates are described in Materials and methods. Significance values for eclosion rate (A) and mHTT aggregates levels (D) were analyzed by ANOVA with Tukey's HSD *post-hoc* test; significant differences ($P < 0.05$) among treatment groups are marked with different letters. Significance values for the adult lifespan curve (B) were analyzed by a weighted log-rank test; significant differences comparing control gfp-Ri with each RNAi group are labeled as follows: *$P < 0.05$; N.S., not significant. Error bar are presented as mean ± SEM

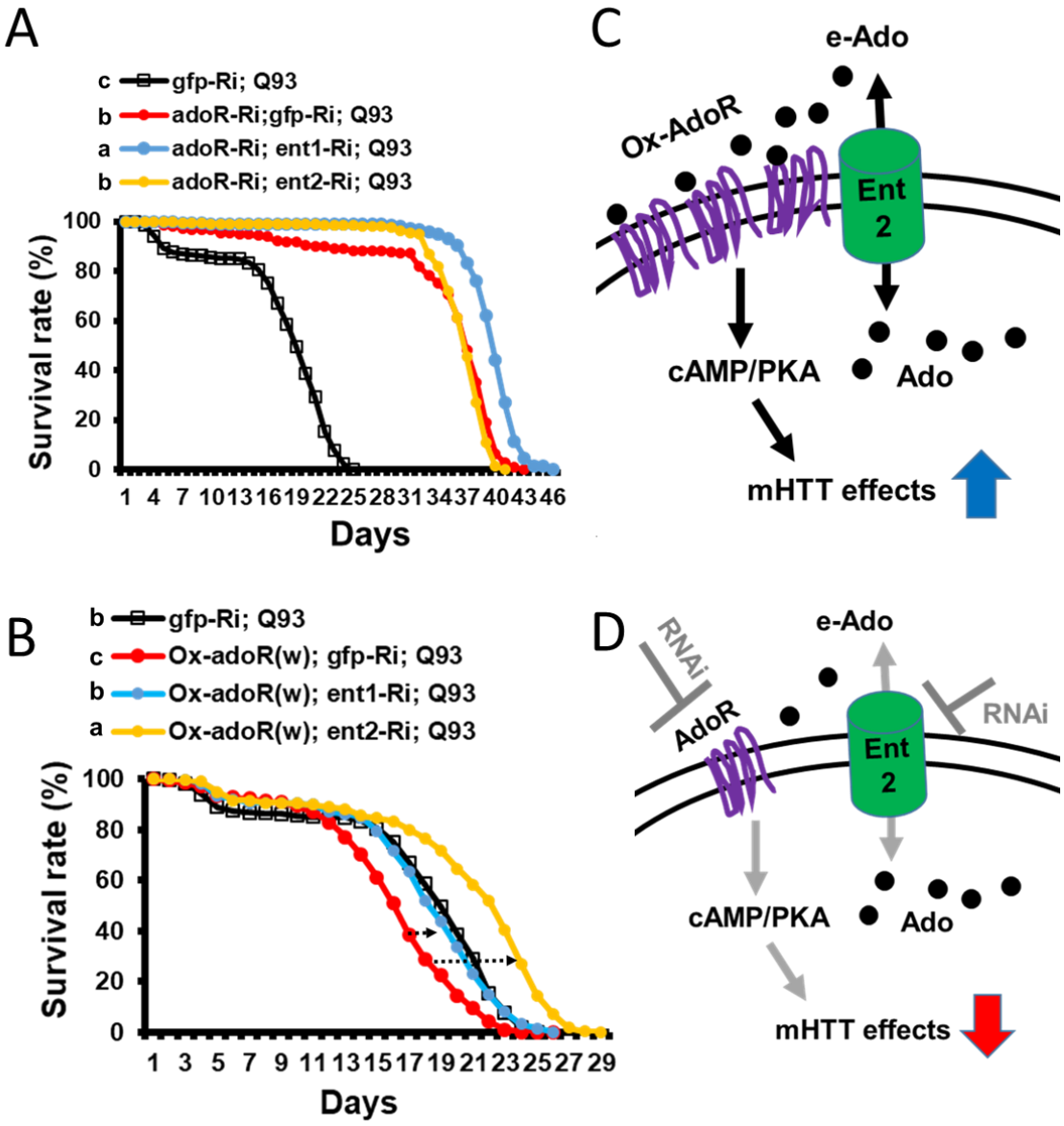

Figure 4. Interactions of AdoR and ENTs in HD *Drosophila*. (A) Co-expression of *adoR* RNAi with *ent1* or *ent2* RNAi in HD flies. (B) Co-expression of *adoR* overexpressing construct (Ox-adoR) with *ent1* or *ent2* RNAi transgenes in HD flies. Significance values of the adult lifespan curve were analyzed by a weighted log-rank test; different letters indicate significant differences ($P < 0.05$) among treatment groups. (C-D) Diagrams showing the action of Ado in mHTT pathogenesis

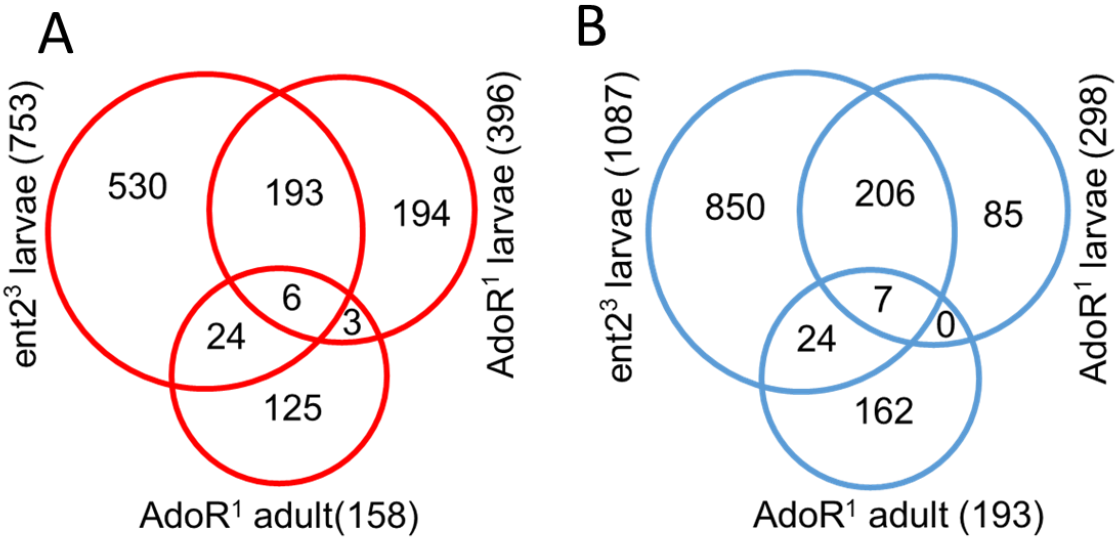

C

Probe ID	gene	CG	Log fold change			Localization
			Ent2³-L	AdoR¹-L	AdoR¹-A	
1641190_at	Jon65Aii	CG6580	2.79	2.5	3.18	MG
1627771_at		CG13075	2.58	2.91	1.93	HG, MT
1630590_at		CG18417	2.02	3.48	4.35	MG, HG
1624393_at	w	CG2759	1.77	4.97	4.5	MT
1632003_a_at	Ptp99A	CG11516	1.53	1.41	2.32	ID, NS, T
1632404_at	rtet	CG5760	1.02	0.85	2.09	MG, HG, I
1633369_s_at		CG6184	-0.23	-0.21	-0.68	NS, tes
1637389_at	Ir100a	CG11575	-0.67	-0.68	-2.61	non-spec
1635901_at		CG17197	-0.85	-0.63	-1.09	ID, tes
1624020_at	mod(mdg4)	CG32491	-1	-1.4	-0.57	NS, ID
1640850_at	cindr	CG31012	-1.11	-1.1	-1.02	NS, SS, ID, tes
1627953_at	mod(mdg4)	CG32491	-1.28	-1.08	-1.19	NS, ID
1633748_at	ND-20L	CG2014	-1.94	-2.05	-0.82	ID, tes

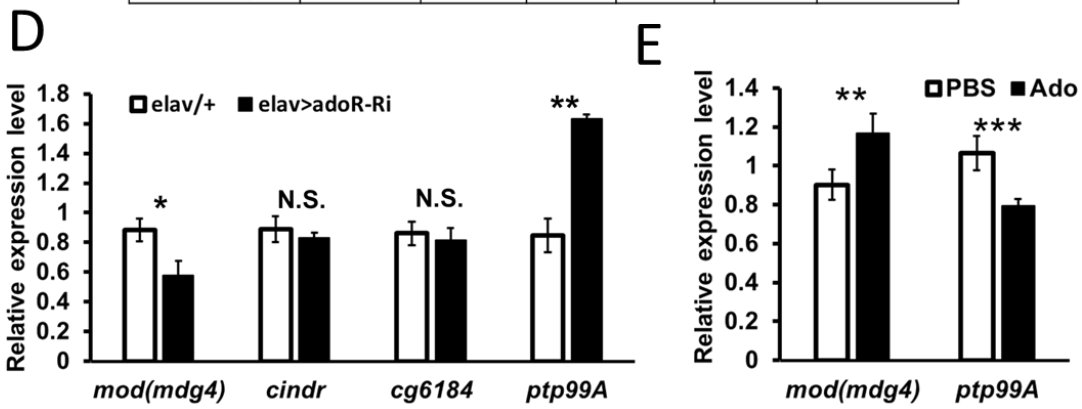

Figure 5. Identification of potential downstream targets of AdoR by microarray

analysis. (A-B) Venn diagram showing the number of common genes (in intersect region) which are upregulated (A) or downregulated (B) among the *adoR* mutant larvae vs. control (w^{1118}), *adoR* mutant adults vs. control (w^{1118}), and *ent2* mutant larvae vs. control (w^{1118}). The cutoff values for expression differences were set at $Q < 0.05$ (false discovery rate, FDR). (C) The intersection between the three datasets; tissue localization of each gene expression was obtained from Flybase (http://flybase.org/). Tissue abbreviations: midgut (MG), hindgut (HG), Malpighian tubule (MT), imaginal disc (ID), integument (I), sensory system (SS), nervous system (NS), trachea (T), testis (tes), nonspecific expression (non-spec) (D) qPCR confirmed the potential AdoR-regulated genes expressed in the nervous system. Expression of *adoR* RNAi transgenes (adoR-Ri) was driven by the pan-neuronal driver (elav>adoR-Ri), and control flies contained *elav*-GAL4 (elav/+) only. (E) Enhancing extracellular adenosine signaling by adenosine injection and qPCR examination demonstrated that *mod(mdg4)* is positively- and *ptp99A* is negatively-regulated by adenosine signaling. Three independent replicates were measured in qPCR experiments. The qPCR primers of *mod(mdg4)* were selected to target the common 5′ exon shared in all of the isoforms. Student's t-test was used to examine the significance of qPCR results: $*P < 0.05$, $**P < 0.01$, $***P < 0.001$; N.S., not significant. Error bars are presented as averages ± SEM

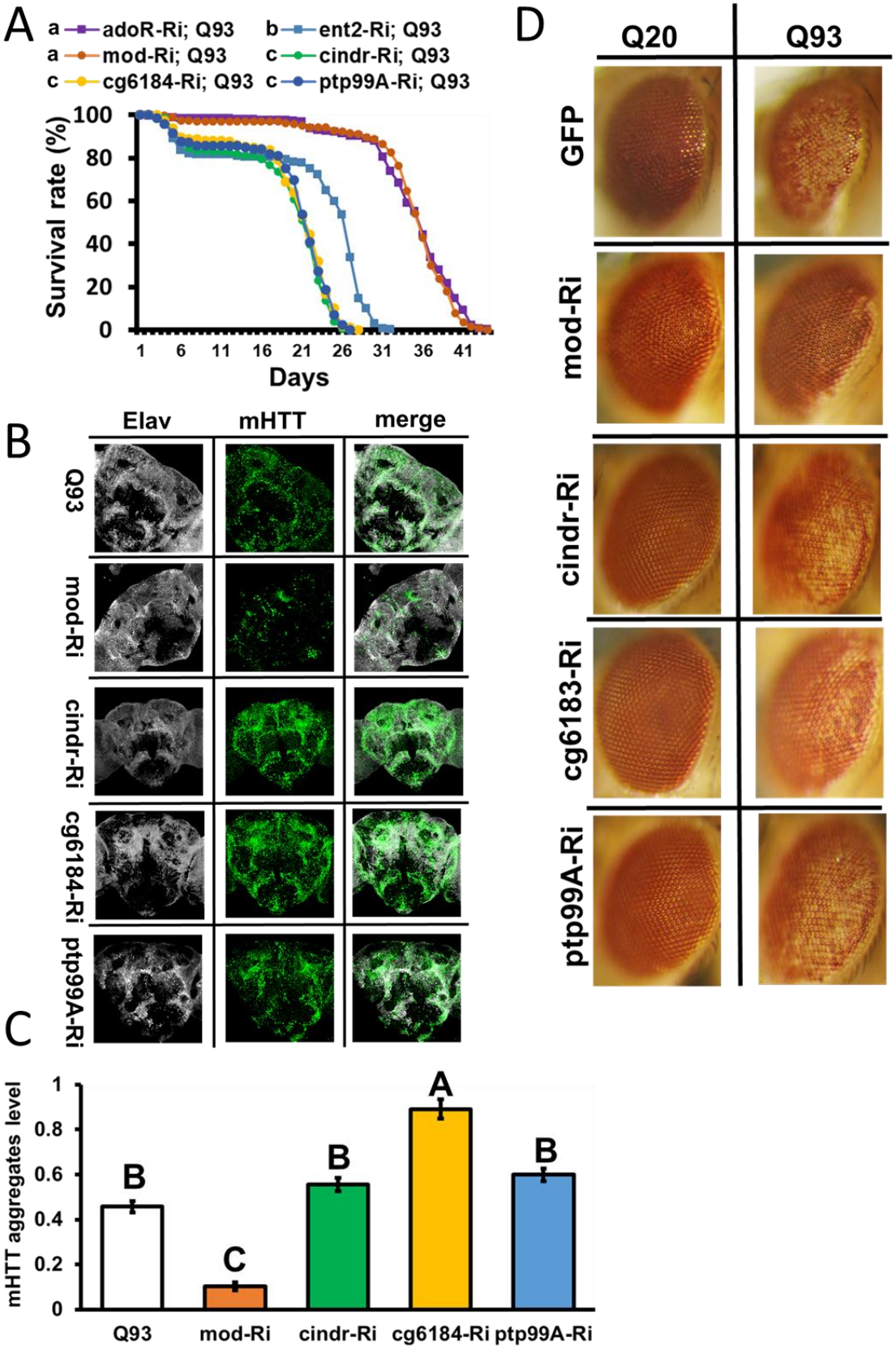

Figure 6. RNAi-mediated (Ri) downregulation of potential downstream targets of

AdoR signaling in HD *Drosophila*. Co-expression of Q93 with each RNAi transgene, including *ptp99A*, *CG6184*, *cindr*, and *mod(mdg4)*, were driven by the pan-neuronal driver, *elav*-GAL4 (A-B), or the eye driver, *gmr*-GAL4 (D). The adult lifespan (A), mHTT aggregate levels (B-C), and retinal pigment cell degeneration (D) were compared. A detailed methodology of the lifespan assay, eye imaging, and quantification of mHTT aggregates are described in Materials and methods. Significance values of the adult lifespan curve (A) were analyzed by a weighted log-rank test, and different letters indicate significant differences ($P < 0.05$) among treatment groups. Significance values of mHTT aggregate levels (C) were analyzed by ANOVA with Tukey's HSD *post-hoc* test; significant differences ($P < 0.05$) among treatment groups are marked with different letters. Error bars are presented as mean ± SEM

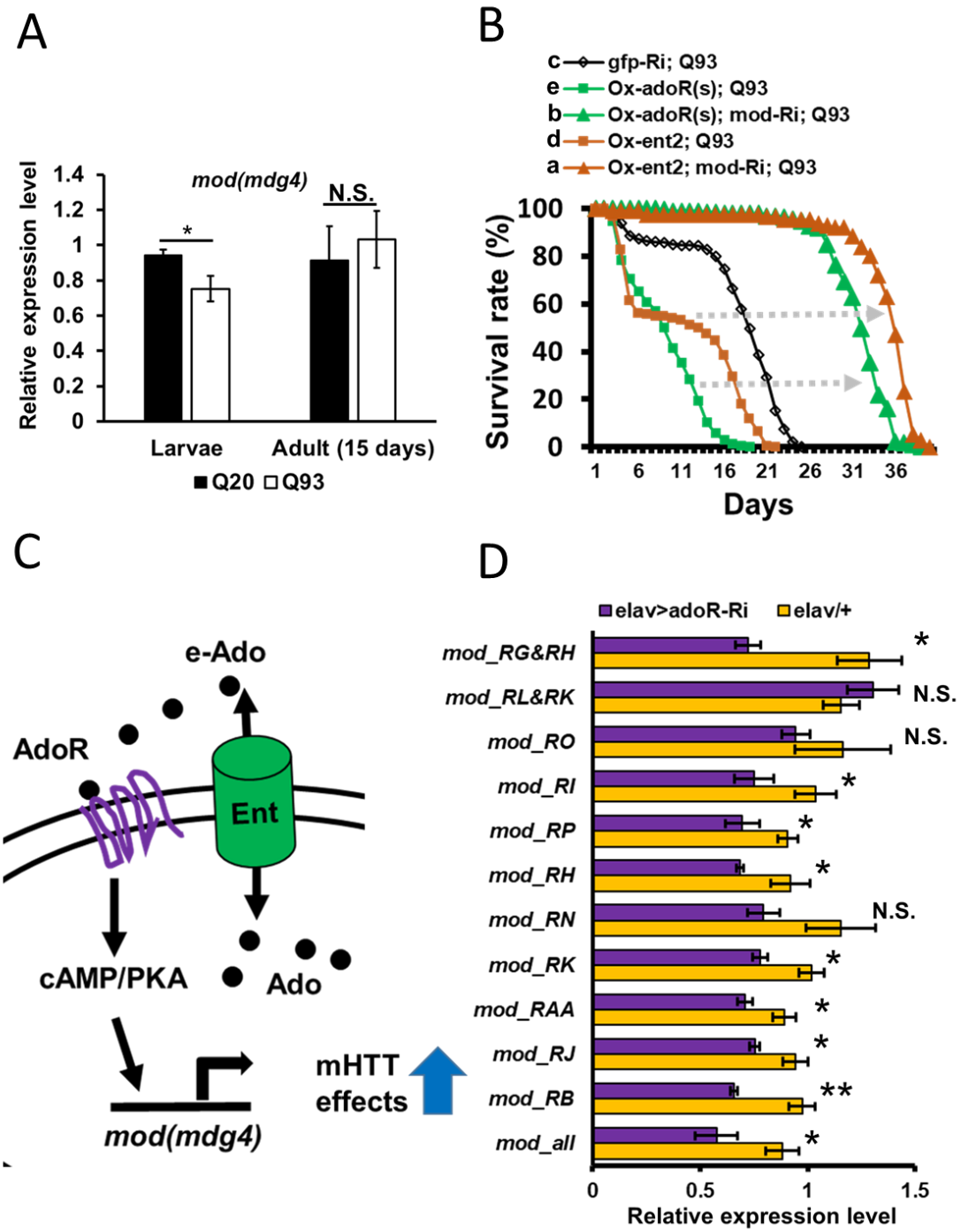

Figure 7. *mod(mdg4)* as a AdoR-regulated gene contributes to HD pathogenesis. (A) qPCR analysis of the expression of *mod(mdg4)* in the larval brain and 15-day-old adult heads of Q20- and Q93-expressing flies. The qPCR primers of *mod(mdg4)* targeted the common 5′ exon shared by all isoforms. (B) Epistasis analysis showed that *ent2* (Ox-ent2) and *adoR* overexpression (Ox-adoR) with *mod(mdg4)* RNAi transgenes in HD

flies decreased the mortality effect caused by *ent2* and *adoR* overexpression. This suggests that *mod(mdg4)* is downstream of the AdoR pathway (C). qPCR identified potential *mod(mdg4)* isoforms regulated by the AdoR pathway. *adoR* RNAi transgene (adoR-Ri) expression was driven by the pan-neuronal driver (elav>adoR-Ri); control flies contained only *elav*-GAL*4* (elav/+). Mod_all indicates that the primers targeted all *mod(mdg4)* isoforms. Isoforms L and G do not have their own unique exonal region, therefore it is possible for the qPCR primers to target two isoforms simultaneously (presented as RG&RG and RL&RK). qPCR result significance was examined using Student's t-test: $*P < 0.05$, $**P < 0.01$, $***P < 0.001$; N.S., not significant. Significance values for the adult lifespan curve (A) were analyzed by weighted log-rank test, and different letters indicate significant differences ($P < 0.05$) among treatment groups. Error bars are presented as mean ± SEM

Functional groups	*Drosophila* genes	Human orthologs
Adenosine metabolism	*adgf-a*	*ada2*
	adgf-c	
	adgf-d	
	adenoK	*adk*
Adenosine transportation	*ent1*	*ent1* (SLC29A1)
	ent2	*ent3*; *ent1* (SLC29A3; SLC29A1)
	ent3	*ent4* (SLC29A4)
	cnt2	*cnt2* (SLC28A2)
GPCR	*adoR*	*adoRA2B*

Figure S1. *Drosophila* genes involved in adenosine metabolism, transportation, and GPCR signaling and their orthologs in humans. The orthology analysis is derived from Flybase (http://flybase.org/)

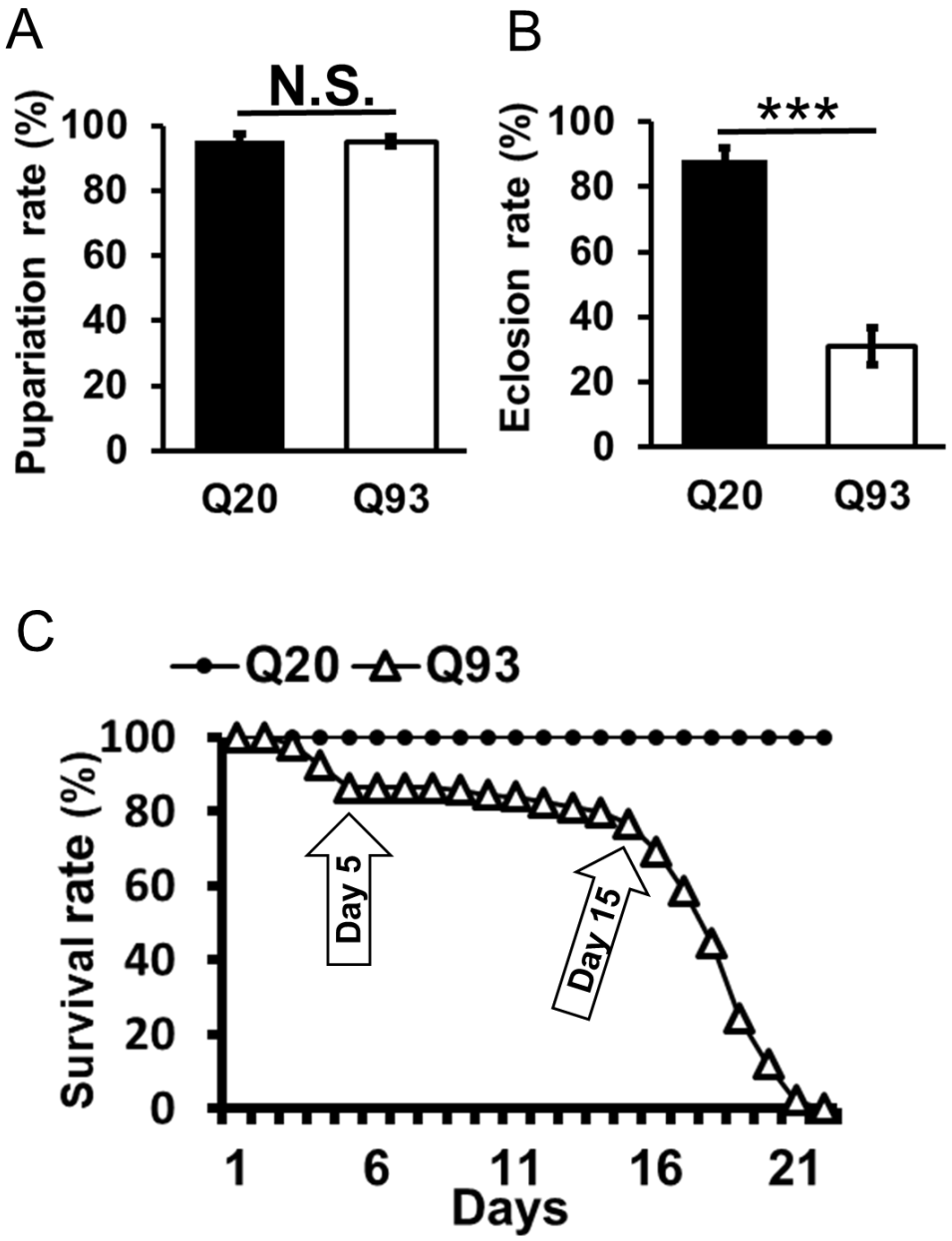

Figure S2. Assessment of the effects of mHTT in *Drosophila* development and adult lifespan. Flies expressing normal HTT (Q20) and mHTT (Q93) were driven by the pan-neuron driver (*elav*-GAL4), and the larval pupariation rate (A), adult eclosion rate (B), and adult survival (C) were recorded. At least five independent replicates were measured. The significance of results was examined using Student's t-test: ***$P <$ 0.001; N.S., not significant. Error bars are presented as mean ± SEM

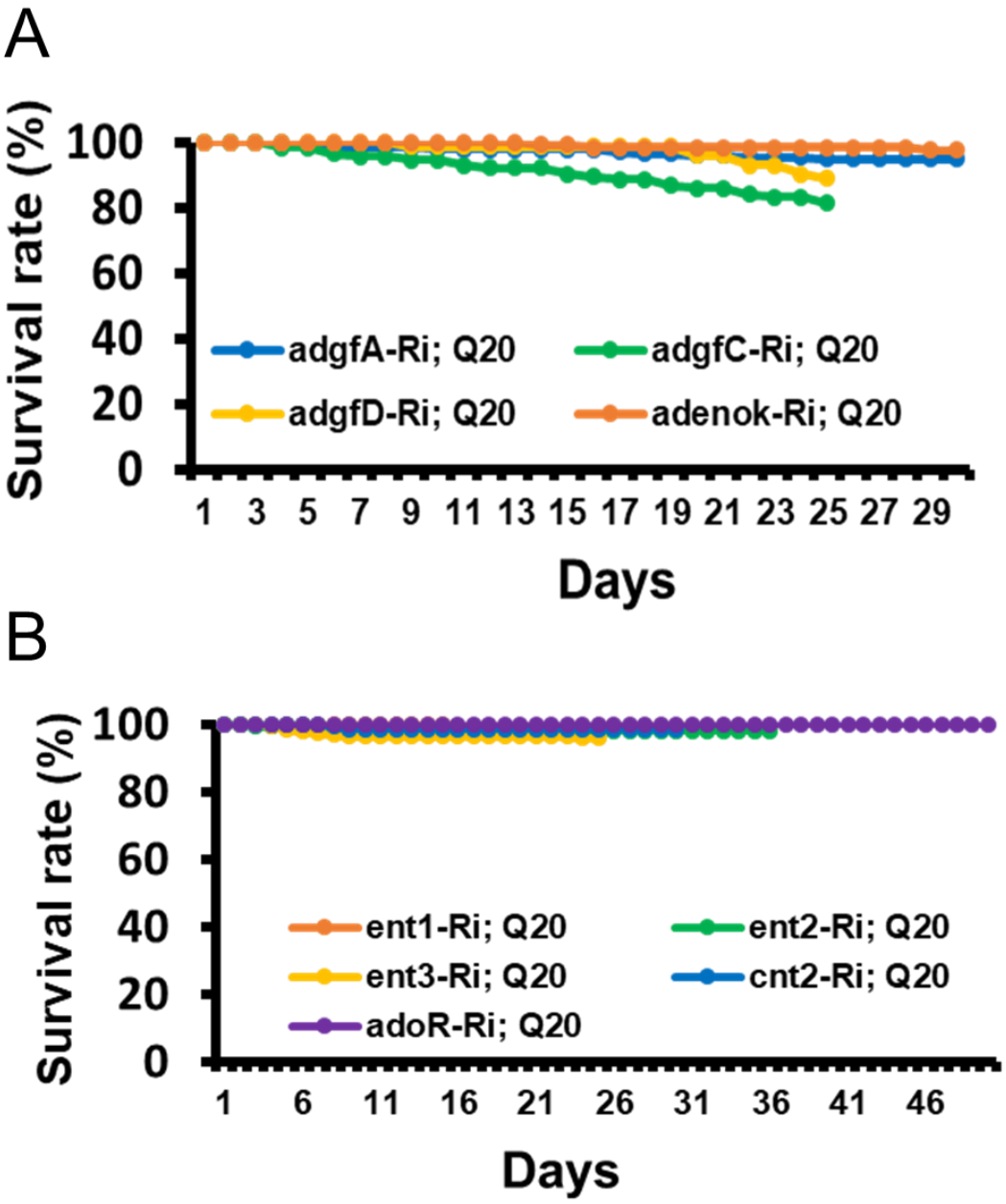

Figure S3. Co-expression of normal Q20 HTT with RNAi of *adgf-A*, *adgf-C*, *adgf-D*, *adenoK* (A) and *ent1*, *ent2*, *ent3*, *cnt2*, and *adoR* (B) driven by the pan-neuronal driver (*elav*-GAL4). The number of dead *flies was recorded* until all corresponding experimental flies (expressing Q93 together with RNAi constructs) had died

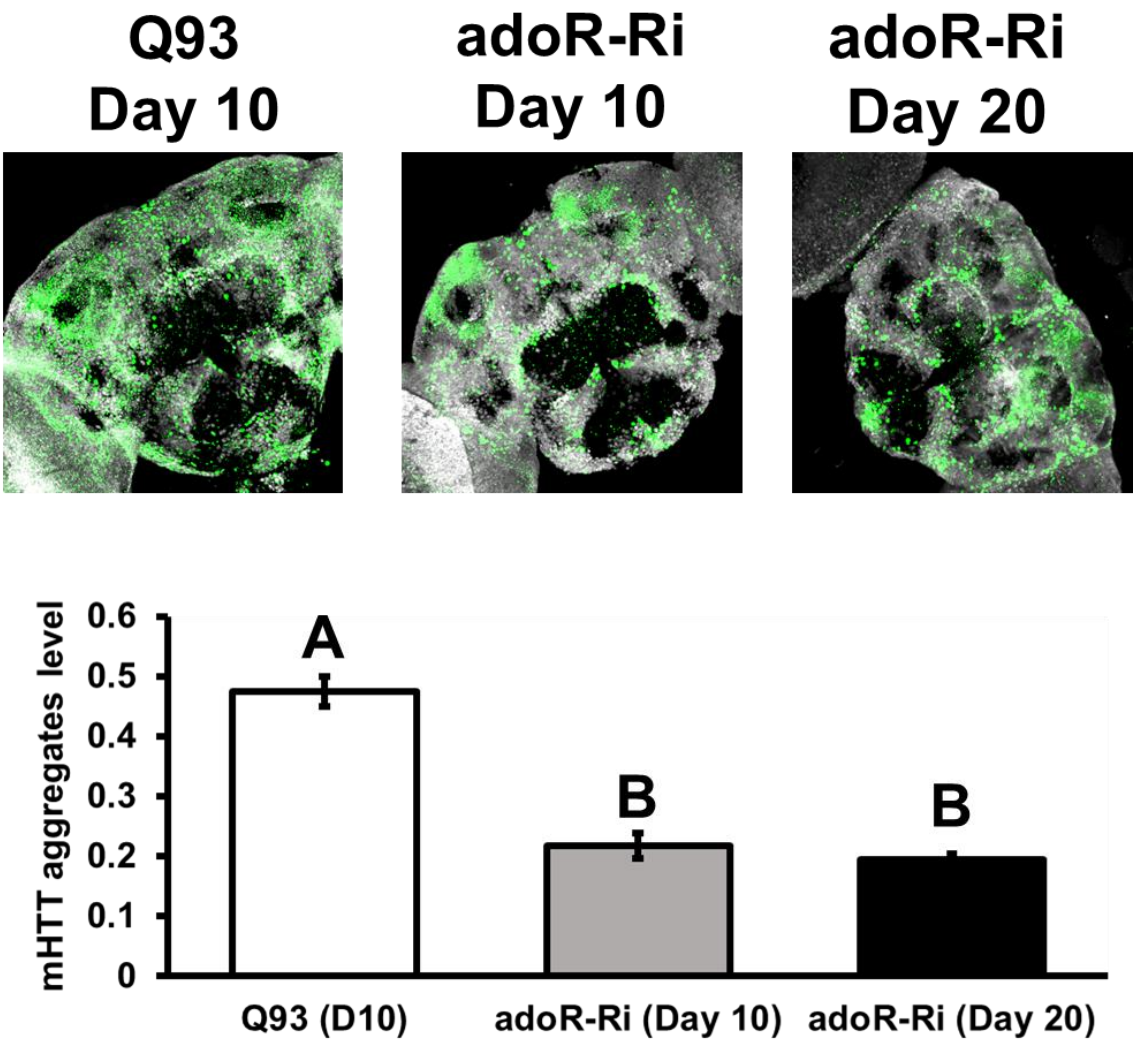

Figure S4. *AdoR* RNAi suppressed mHTT aggregates formation in the brains of 20-day-old flies

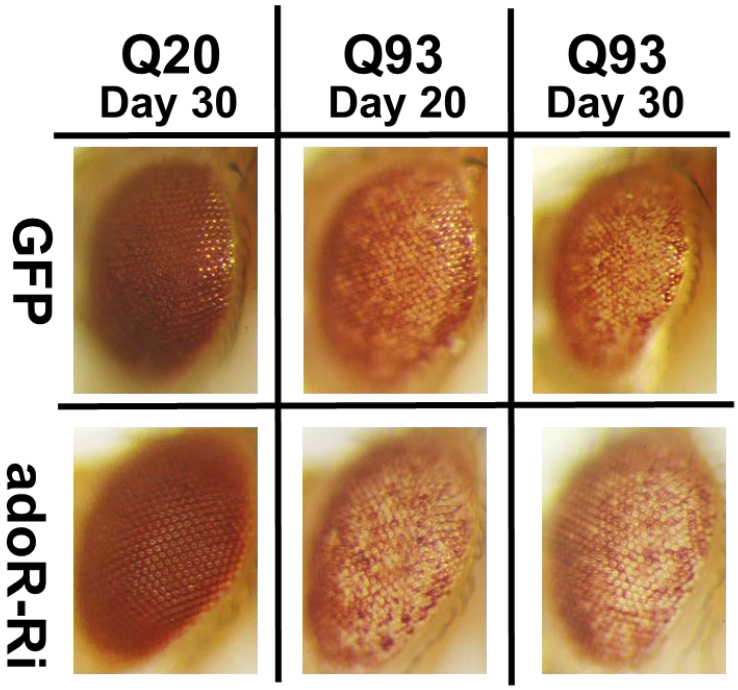

Figure S5. Co-expression of Q93 with *adoR* RNAi did not significantly rescue retinal pigment cell degeneration

A

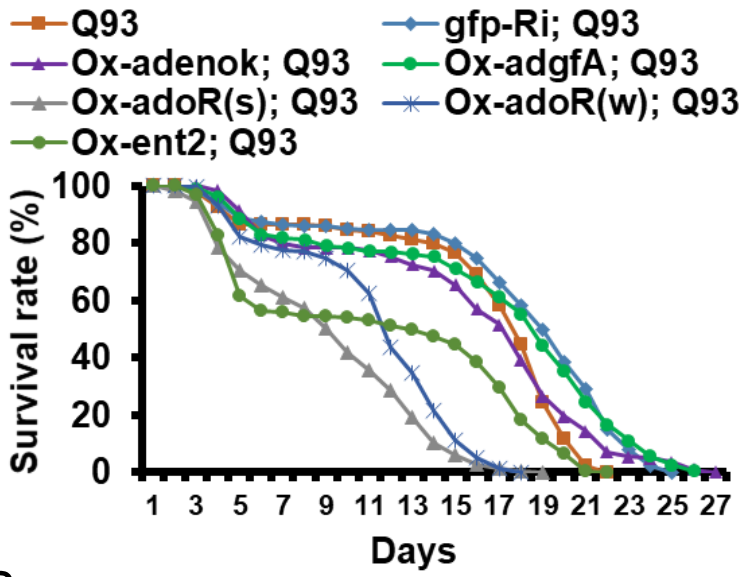

B

Paired	X^2	Bonferroni P-value
Ox-adgfA; Q93 v.s. Q93	13.96	<0.01
Ox-adgfA; Q93 v.s. gfp-Ri;Q93	1.43	1
Ox-adenoK; Q93 v.s. Q93	0.35	1
Ox-adenoK; Q93 v.s. gfp-Ri; Q03	22.32	<0.01
Ox-AdoR (w); Q93 v.s. Q93	195.28	<0.01
Ox-AdoR (w) v.s. gfp-Ri;Q93	214.87	<0.01
Ox-AdoR (s); Q93 v.s. Q93	258.09	<0.01
Ox-AdoR (s); Q93 v.s. gfp-Ri; Q93	265.06	<0.01
Ox-ent2; Q93 v.s. Q93	61.45	<0.01
Ox-ent2 ; Q93 v.s. gfp-Ri;Q93	114.98	<0.01

Figure S6. (A) Co-expression of Q93 with each overexpression (Ox) of transgenes was driven by the pan-neuronal driver (*elav-GAL4*); adult survival curves were compared. Ox-adoR(w) indicates the weak *adoR* overexpression transgene and Ox-adoR(s) indicates the strong *adoR* overexpression transgene. (B) Statistical analysis using a weighted log-rank test for (A)

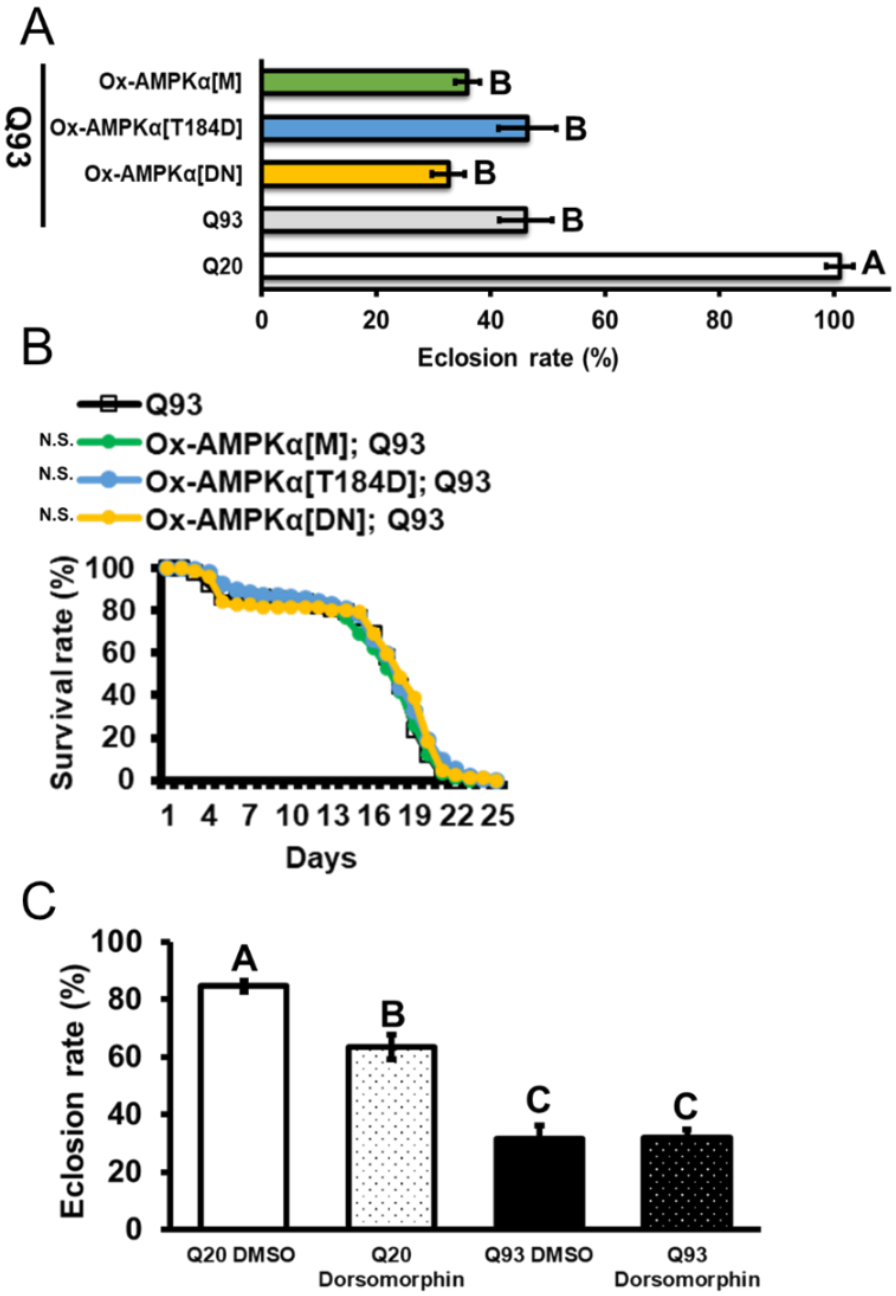

Figure S7. AMPK activity does not influence the survival of HD *Drosophila*. Co-expression of Q93 with overexpression of wild-type AMPKα [M], phosphomimetic-activated form of AMPKα [T184D], and dominant negative AMPK [DN] were driven by the pan-neuronal driver (*elav*-GAL4); the adult eclosion rate (A) and survival curve (B) were compared. (C) Q20- and Q93-expressing larvae were fed with AMPK inhibitor, dorsomorphin, or control DMSO, and the adult eclosion rates were assessed. Significance values of (A) and (C) were analyzed by ANOVA with Tukey's HSD *post-*

hoc test; significant differences ($P < 0.05$) among treatment groups are marked with different letters. Significance values of the adult lifespan curve (B) were analyzed by a weighted log-rank test; significant differences between control Q93 flies with each overexpression group are labeled as N.S., not significant. Error bars are presented as mean ± SEM

genes	left 5'-3'	right 5'-3'
adgf-a	AGGCTCATCCAGATTTCATT	CGGGTACTTTTCCTTTATTTGTT
adgf-c	TGTACACAGAGATTCGGACCAG	TAGACGGCCATAATGACTTTGA
adgf-d	CTGACCACCACCAATAATCTGTA	AGCGCTCCCAAATCTTCTT
adenoK	GAGGATCGGTACGCCAATATCT	AGGAAGAAGCCCGAAATGTAGT
ent1	TCCCTGCGCACCAAGAT	ATAAACTCGGAGGGAAATAGACG
ent2	AAGGGATCAACGTCGGTGT	AATAGGACTTGGCCGTGATG
ent3	CATCGCTCTGGGCATCAC	CCACCGTCAGACCAACATTAT
cnt2	CTTTGCCAATCCCAGTTCC	TAGTTCGCCCGCTCGTC
AdoR	TTTTGCCACCATTATCACTCC	AGGCGGGGTTCATCGTA
mod(mdg4)	CAAGATGTTCACTCAGATGC	CCGAGTGGCTGACGTTGTTC
cindr	ATGACCACAACGAACTCAAGC	CTACTGCTCCCGGTCTTCT
ptp99A	GGGAAGTGCCCGTTAAGATCG	CTGAATCCAATGTCCCCGTC
CG6184	CCCAGATCAGTGTCCAGAAGC	ATCGCCATTCAGATCAGCCG
mod(mdg4)_RO	CCACAGTCGCAAGAGCAATA	GCGGCTGGTGGTTATGTAGT
mod(mdg4)_RI	CATAAAGGAGGAGGGTGACG	TCTCGATTCATTGCAGGTTG
mod(mdg4)_RT	TTCAGTGCTGCTACCGTGAG	GCGACAGCGAGGATATGACT
mod(mdg4)_RAA	CGCTGCTCCATGTACAAAAA	CGAGCACTCTGGGAACAAAT
mod(mdg4)_RN	GACAGAAGAGGCCAAGCATC	CCTTCCGTGGTTCGAGATAA
mod(mdg4)_RH	CACAAGTGATAAGACACTCCCAAG	CGTTTTGGAAGAGCAGCAC
mod(mdg4)_RG+RH	CCGCCTCTCGTACTTATTGG	TGATGATTCGCTCCTGTGAG
mod(mdg4)_RB	CGTAAAACCCGATCAACACC	GTAACGATGCTCCCCACAGT
mod(mdg4)_RJ	CAAGACCTCGGGATTGAAAA	TAGGGCGGATGGTTATGTTG
mod(mdg4)_RL+RK	CCATTGCTTGACCAGGAACT	CGGATTCGGCCTATGACTAC
mod(mdg4)_RP	CATGCTCAAGCAACACACCT	GCTGTTCAGGATGGTGAGTG
mod(mdg4)_RK	CAAGCGTTTGAACGAGAACA	GGATGATTGTGGGCATTCTT

Table S1. List of qPCR primers used in the present study

Materials and methods

Fly stocks

Flies were reared at 25 °C on standard cornmeal medium. The following RNAi lines were acquired from the TRiP collection (Transgenic RNAi project) at Harvard Medical School: adgfA-Ri (BL67233), adgfC-Ri (BL42915), adgfD-Ri (BL56980), adenoK-Ri (BL64491), ent1-Ri (BL51055), adoR-Ri (BL27536), gfp-Ri (BL41552), mod(mdg4)-Ri (BL32995), cindr-Ri (BL38976), and ptp99A-Ri (BL57299). The following RNAi lines were acquired from the Vienna Drosophila RNAi Center (VDRC): ent2-Ri (ID100464), ent3-Ri (ID47536), cnt2-Ri (ID37161), and cg6184-Ri (ID107150). The following lines were provided by the Bloomington Drosophila Stock Center: UAS-AMPKα^{T184D} (BL32110), UAS-AMPKα^{M} (BL32108), UAS-AMPKα^{DN} (AMPKα^{K57A}, BL32112), and elav^{C155}-GAL4 (BL458).

Flies overexpressing human normal huntingtin (HTT) exon 1, Q20Httexon^{1111F1L} or mutant pathogenic fragments (mHTT), Q93Httexon^{14F132} were obtained from Prof. Lawrence Marsh (UC Irvine, USA) (Steffan et al., 2001). The UAS-overexpression lines, Ox-adenoK and Ox-adoR (s), were obtained from Dr. Ingrid Poernbacher (The Francis Crick Institute, UK) (Poernbacher and Vincent, 2018). gmr-GAL4 was obtained from Dr. Marek Jindra (Biology Centre CAS, Czechia). da-GAL4 was obtained from Dr. Ulrich Theopold (Stockholm University). The UAS overexpression strains Ox-adgfA, Ox-ent2, and Ox-adoR (w), as well as adoR^{1} and ent2^{3} mutant flies, were generated in our previous studies (Dolezal et al., 2003; Dolezal et al., 2005; Dolezelova et al., 2007; Knight et al., 2010).

Eclosion rate and adult lifespan assay

For assessing the eclosion rate, male flies containing the desired RNAi or

overexpression transgene (RiOx) in the second chromosome with genotype w^{1118}/Y; RiOx /CyO; UAS-Q93/MKRS were crossed with females of *elav-GAL4*; +/+; +/+. The ratio of eclosed adults between *elav-GAL4*/+; RiOx/+; UAS-Q93/+ and *elav-GAL4*/+; RiOx/+; +/MKRS was then calculated. If the desired RiOx transgene was in the third chromosome, female flies containing *elav-GAL4*; +/+; RiOx were crossed with male w^{1118}/Y; +/+; UAS-Q93/MKRS, and the ratio of eclosed adults between *elav-GAL4*; +/+; RiOx/UAS-Q93 and *elav-GAL4*; +/+; RiOx/MKRS was calculated.

For the adult lifespan assay, up to 30 newly emerged female adults were placed in each cornmeal vial and maintained at 25 °C. At least 200 flies of each genotype were tested, and the number of dead flies was counted every day. Flies co-expressing RiOx and Q20 were used for evaluating the effect of RNAi or overexpression of the desired transgenes (Fig. S3A&B).

Extracellular adenosine and ATP level measurements

To collect the hemolymph, six third instar larvae (96 hours post-oviposition) were torn in 150 µl of 1× PBS containing thiourea (0.1 mg/ml) to prevent melanization. The samples were then centrifuged at 5000× *g* for 5 min to separate the hemocytes and the supernatant was collected for measuring the extracellular adenosine or ATP level. For measuring the adenosine titer, 10 µl of hemolymph was mixed with reagents of an adenosine assay kit (Biovision) following the manufacturer's instructions. The fluorescent intensity was then quantified (Ex/Em = 533/ 587 nm) using a microplate reader (BioTek Synergy 4). For measuring the ATP level, 10 µl of hemolymph was incubated with 50 µl of CellTiter-Glo reagent (Promega) for 10 min. Then, the luminescent intensity was quantified using an Orion II microplate luminometer (Berthold). To calibrate the standard curve of ATP concentration, 25 µM ATP standard

solution (Epicentre) was used for preparing a concentration gradient (0, 2, 4, 6, 8, 10 μM) of ATP solution and the luminescent intensity was measured for each concentration. The protein concentration of the hemolymph sample was determined by A280 absorbance using a NanoDrop 2000 spectrophotometer (Thermo Fisher). The adenosine and ATP concentrations were first normalized to protein concentration. Then, the values of Q20 and Q93 samples were normalized to values of the *GAL4* control sample. Six independent replicates for each genotype were performed for the analysis of adenosine and ATP levels.

RNA extraction

The brains from 10 third-instar larvae (96 hours post-oviposition), heads from 30 female adults (5 days or 15 days old) or 15 whole female flies were collected. The samples were first homogenized in RiboZol (VWR) and the RNA phase was separated by chloroform. For brain or head samples, the RNA was precipitated by isopropanol, washed in 75% ethanol and dissolved in nuclease-free water. For whole fly samples, the RNA phase was purified using NucleoSpin RNA columns (Macherey-Nagel) following the manufacturer's instructions. All purified RNA samples were treated with DNase to prevent genomic DNA contamination. cDNA was synthesized from 2 μg of total RNA using a RevertAid H Minus First Strand cDNA Synthesis Kit (Thermo Fisher Scientific).

Adenosine injection

Three- to five-day-old female adults were injected with 50 nl of 10 mM adenosine using a NANOJECT II (Drummond Scientific); control flies were injected with 50 nl of 1× PBS. Two hours post-injection, 15 injected flies for each replicate were collected for

RNA extraction.

Microarray analysis

The Affymetrix GeneChip® *Drosophila* genome 2.0 array system was used for microarray analysis following the standard protocol: 100 ng of RNA was amplified with a GeneChip 3′ express kit (Affymetrix), and 10 μg of labeled cRNA was hybridized to the chip according to the manufacturer's instructions. Statistical analysis of array data was described previously in our studies (Arefin et al., 2014; Kucerova et al., 2016). Storey's q value (false discovery rate, FDR) was used to select significantly differentially transcribed genes ($q < 0.05$).

qPCR and primers

5× HOT FIREPol® EvaGreen® qPCR Mix Plus with ROX (Solis Biodyne) and an Eco Real-Time PCR System (Illumina) were used for qPCR. Each reaction contained 4 μl of EvaGreen qPCR mix, 0.5 μl each of forward and reverse primers (10 μM), 5 μl of diluted cDNA and ddH2O to adjust the total volume to 20 μl. The list of primers is shown in Table S1. The expression level was calculated using the $2^{-\Delta\Delta Ct}$ method. The ct values of target genes were normalized to reference gene, ribosomal protein 49 (*rp49*).

Imaging of retinal pigment cell degeneration

Twenty- and thirty-day-old female adults were collected and their eye depigmentation phenotypes were recorded. At least 30 individuals for each genotype were examined under a microscope, and at least five representative individuals were chosen for imaging. Pictures were taken with an EOS 550D camera (Canon) mounted on a SteREO Discovery V8 microscope (Zeiss).

Immunostaining

Brains dissected from 10- or 20-day-old adult females were used for immunostaining. The brains were fixed in 4% PFA, permeabilized with PBST (0.1% Triton X-100), blocked in PAT (PBS, 0.1% Triton X-100, 1% BSA) and stained with antibodies in PBT (PBS, 0.3% Triton X-100, 0.1% BSA). Primary antibodies used in this study were mouse anti-HTT, MW8 which specifically binds to mHTT aggregates (1:40, DSHB), and rat anti-Elav (1:40, DSHB) which is a pan-neuronal antibody. Secondary antibodies were Alexa Fluor 488 anti-mouse and Alexa Fluor 647 anti-rat (1:200, Invitrogen). The samples were mounted in Fluoromount-G (Thermo Fisher) overnight, prior to image examination.

Quantification of mHTT aggregates

Images of aggregates were taken using a Flowview 100 confocal microscope (Olympus). The intensity of mHTT aggregates detected by anti-HTT antibody (MW8) or anti-Elav were quantified using ImageJ software. The level of mHTT aggregates was quantified by normalizing the mHTT aggregates intensity to Elav intensity. At least six brain images from each genotype were analyzed.

AMPK inhibitor (dorsomorphin) feeding

Thirty first instar of Q20- or Q93-exexpressing larvae were collected for each replicate 24 hours after egg laying. Larvae were transferred to fresh vials with 0.5 g instant *Drosophila* medium (Formula 4–24, Carolina Biological Supply, Burlington, NC) supplemented with 2 mL distilled water containing either dorsomorphin (100 μM) or DMSO (1%). Total number of e*merging adults were counted*.

Statistical analysis

Error bars show standard error of the mean throughout this paper. Significance was established using Student's t-test (N.S., not significant; * $P < 0.05$, ** $P < 0.01$, *** $P < 0.001$) or one-way ANOVA analysis with Tukey's HSD *post-hoc* test. For the statistical analysis of survival curves, we used the online tool OASIS 2 to perform a weighted log-rank test (Wilcoxon-Breslow-Gehan test) for determining significance (Han et al., 2016).

Acknowledgements

We thank Dr. Ingrid Poernbacher (The Francis Crick Institute, UK), Prof. Lawrence Marsh (UC Irvine, USA), Dr. Marek Jindra (Biology Centre CAS, Czechia), Dr. Tomas Dolezal (University of South Bohemia, Czechia), Dr. Ulrich Theopold (Stockholm University), Bloomington *Drosophila* Stock Center and Vienna *Drosophila* Resource Center for providing us with fly strains. This work was supported by the grant agency of the University of South Bohemia (065/2017/P to Y-HL), junior grant project GACR (19-13784Y to LK) and European Community's Programme Interreg Östereich-Tschechische Republik (REGGEN/ATCZ207 to MZ).

Author Contributions

Y-HL performed the experiments and prepared the manuscript. HM assisted in recording the adult lifespan and eye phenotypes as well as performed the brain dissection, immunochemistry and confocal microscopy imaging. LK performed the sample preparation and analyzed the microarray data. LR assisted in recording the adult lifespan, eye phenotype and prepared fly strains. TF established the methodologies for recording the eclosion rate, survival and prepared fly strains. MZ conceived the project and supervised manuscript preparation.

References

Albagli, O., Dhordain, P., Deweindt, C., Lecocq, G., and Leprince, D. (1995). The BTB/POZ domain: a new protein-protein interaction motif common to DNA- and actin-binding proteins. *Cell Growth Differ* 6(9)**,** 1193-1198.

Anderson, C.M., and Nedergaard, M. (2006). Emerging challenges of assigning P2X7 receptor function and immunoreactivity in neurons. *Trends Neurosci* 29(5)**,** 257-262. doi: 10.1016/j.tins.2006.03.003.

Arefin, B., Kucerova, L., Dobes, P., Markus, R., Strnad, H., Wang, Z., et al. (2014). Genome-wide transcriptional analysis of Drosophila larvae infected by entomopathogenic nematodes shows involvement of complement, recognition and extracellular matrix proteins. *J Innate Immun* 6(2)**,** 192-204. doi: 10.1159/000353734.

Aymerich, I., Foufelle, F., Ferre, P., Casado, F.J., and Pastor-Anglada, M. (2006). Extracellular adenosine activates AMP-dependent protein kinase (AMPK). *J Cell Sci* 119(Pt 8)**,** 1612-1621. doi: 10.1242/jcs.02865.

Bajgar, A., and Dolezal, T. (2018). Extracellular adenosine modulates host-pathogen interactions through regulation of systemic metabolism during immune response in Drosophila. *PLoS Pathog* 14(4)**,** e1007022. doi: 10.1371/journal.ppat.1007022.

Bajgar, A., Kucerova, K., Jonatova, L., Tomcala, A., Schneedorferova, I., Okrouhlik, J., et al. (2015). Extracellular adenosine mediates a systemic metabolic switch during immune response. *PLoS Biol* 13(4)**,** e1002135. doi: 10.1371/journal.pbio.1002135.

Bardwell, V.J., and Treisman, R. (1994). The POZ domain: a conserved protein-protein interaction motif. *Genes Dev* 8(14)**,** 1664-1677. doi: 10.1101/gad.8.14.1664.

Blum, D., Chern, E.C., Domenici, M.R., Buée, L., Lin, C.Y., Ferré, S., et al. (2018a). "What Is the Role of Adenosine Tone and Adenosine Receptors in Huntington's Disease?," in *The Adenosine Receptors,* eds. P.A. Borea, K. Varani, S. Gessi, S. Merighi & F. Vincenzi. (Cham: Springer International Publishing), 281-308.

Blum, D., Chern, Y., Domenici, M.R., Buee, L., Lin, C.Y., Rea, W., et al. (2018b). The Role of Adenosine Tone and Adenosine Receptors in Huntington's Disease. *J Caffeine Adenosine Res* 8(2)**,** 43-58. doi: 10.1089/caff.2018.0006.

Blum, D., Hourez, R., Galas, M.-C., Popoli, P., and Schiffmann, S.N. (2003a). Adenosine receptors and Huntington's disease: implications for pathogenesis and therapeutics. *The Lancet Neurology* 2(6)**,** 366-374. doi: https://doi.org/10.1016/S1474-4422(03)00411-3.

Blum, D., Hourez, R., Galas, M.C., Popoli, P., and Schiffmann, S.N. (2003b). Adenosine receptors and Huntington's disease: implications for pathogenesis and therapeutics. *Lancet Neurol* 2(6)**,** 366-374. doi: 10.1016/s1474-4422(03)00411-3.

Braco, J.T., Gillespie, E.L., Alberto, G.E., Brenman, J.E., and Johnson, E.C. (2012). Energy-dependent modulation of glucagon-like signaling in Drosophila via the AMP-activated protein kinase. *Genetics* 192(2)**,** 457-466. doi: 10.1534/genetics.112.143610.

Buchner, K., Roth, P., Schotta, G., Krauss, V., Saumweber, H., Reuter, G., et al. (2000). Genetic and molecular complexity of the position effect variegation modifier mod(mdg4) in Drosophila. *Genetics* 155(1)**,** 141-157.

Chan, H.Y., Warrick, J.M., Gray-Board, G.L., Paulson, H.L., and Bonini, N.M. (2000). Mechanisms of chaperone suppression of polyglutamine disease: selectivity, synergy and modulation of protein solubility in Drosophila. *Hum Mol Genet* 9(19)**,** 2811-2820. doi: 10.1093/hmg/9.19.2811.

Cunha, R.A. (2001). Adenosine as a neuromodulator and as a homeostatic regulator in the nervous system: different roles, different sources and different receptors. *Neurochemistry International* 38(2)**,** 107-125. doi: Doi 10.1016/S0197-0186(00)00034-6.

Cunha, R.A. (2019). Signaling by adenosine receptors-Homeostatic or allostatic control? *PLoS Biol* 17(4)**,** e3000213. doi: 10.1371/journal.pbio.3000213.

Dolezal, T., Dolezelova, E., Zurovec, M., and Bryant, P.J. (2005). A role for adenosine deaminase in Drosophila larval development. *PLoS Biol* 3(7)**,** e201. doi: 10.1371/journal.pbio.0030201.

Dolezal, T., Gazi, M., Zurovec, M., and Bryant, P.J. (2003). Genetic analysis of the ADGF multigene family by homologous recombination and gene conversion in Drosophila. *Genetics* 165(2)**,** 653-666.

Dolezelova, E., Nothacker, H.P., Civelli, O., Bryant, P.J., and Zurovec, M. (2007). A Drosophila adenosine receptor activates cAMP and calcium signaling. *Insect Biochem Mol Biol* 37(4)**,** 318-329. doi: 10.1016/j.ibmb.2006.12.003.

Dolinar, K., Jan, V., Pavlin, M., Chibalin, A.V., and Pirkmajer, S. (2018). Nucleosides block AICAR-stimulated activation of AMPK in skeletal muscle and cancer cells. *Am J Physiol Cell Physiol* 315(6)**,** C803-C817. doi: 10.1152/ajpcell.00311.2017.

Domenici, M.R., Scattoni, M.L., Martire, A., Lastoria, G., Potenza, R.L., Borioni, A., et al. (2007). Behavioral and electrophysiological effects of the adenosine A2A receptor antagonist SCH 58261 in R6/2 Huntington's disease mice. *Neurobiol Dis* 28(2)**,** 197-205. doi: 10.1016/j.nbd.2007.07.009.

Dorn, R., and Krauss, V. (2003). The modifier of mdg4 locus in Drosophila: functional complexity is resolved by trans splicing. *Genetica* 117(2)**,** 165-177. doi: Doi 10.1023/A:1022983810016.

Dunwiddie, T.V., and Masino, S.A. (2001). The role and regulation of adenosine in the central nervous system. *Annu Rev Neurosci* 24**,** 31-55. doi: 10.1146/annurev.neuro.24.1.31.

Espinas, M.L., Jimenez-Garcia, E., Vaquero, A., Canudas, S., Bernues, J., and Azorin, F. (1999). The N-terminal POZ domain of GAGA mediates the formation of oligomers that bind DNA with high affinity and specificity. *J Biol Chem* 274(23)**,** 16461-16469. doi: 10.1074/jbc.274.23.16461.

Fleischmannova, J., Kucerova, L., Sandova, K., Steinbauerova, V., Broz, V., Simek, P., et al. (2012). Differential response of Drosophila cell lines to extracellular adenosine. *Insect Biochem Mol Biol* 42(5)**,** 321-331. doi: 10.1016/j.ibmb.2012.01.002.

Fountain, S.J. (2013). Primitive ATP-activated P2X receptors: discovery, function and pharmacology. *Front Cell Neurosci* 7**,** 247. doi: 10.3389/fncel.2013.00247.

Fredholm, B.B. (2007). Adenosine, an endogenous distress signal, modulates tissue damage and repair. *Cell Death Differ* 14(7)**,** 1315-1323. doi: 10.1038/sj.cdd.4402132.

Gianfriddo, M., Melani, A., Turchi, D., Giovannini, M.G., and Pedata, F. (2004). Adenosine and glutamate extracellular concentrations and mitogen-activated protein kinases in the striatum of Huntington transgenic mice. Selective antagonism of adenosine A2A receptors reduces transmitter outflow. *Neurobiol Dis* 17(1)**,** 77-88. doi: 10.1016/j.nbd.2004.05.008.

Giot, L., Bader, J.S., Brouwer, C., Chaudhuri, A., Kuang, B., Li, Y., et al. (2003). A protein interaction map of Drosophila melanogaster. *Science* 302(5651)**,** 1727-1736. doi: 10.1126/science.1090289.

Glass, M., Dragunow, M., and Faull, R.L.M. (2000). The pattern of neurodegeneration in Huntington's disease: A comparative study of cannabinoid, dopamine, adenosine and GABA(A) receptor alterations in the human basal ganglia in Huntington's disease. *Neuroscience* 97(3)**,** 505-519. doi: Doi 10.1016/S0306-4522(00)00008-7.

Gomes, C.V., Kaster, M.P., Tome, A.R., Agostinho, P.M., and Cunha, R.A. (2011). Adenosine receptors and brain diseases: Neuroprotection and neurodegeneration. *Biochimica Et Biophysica Acta-Biomembranes* 1808(5)**,** 1380-1399. doi: 10.1016/j.bbamem.2010.12.001.

Guitart, X., Bonaventura, J., Rea, W., Orru, M., Cellai, L., Dettori, I., et al. (2016). Equilibrative nucleoside transporter ENT1 as a biomarker of Huntington disease. *Neurobiol Dis* 96**,** 47-53. doi: 10.1016/j.nbd.2016.08.013.

Han, S.K., Lee, D., Lee, H., Kim, D., Son, H.G., Yang, J.S., et al. (2016). OASIS 2: online application for survival analysis 2 with features for the analysis of maximal lifespan and healthspan in aging research. *Oncotarget* 7(35)**,** 56147-56152. doi: 10.18632/oncotarget.11269.

Johnson, E.C., Kazgan, N., Bretz, C.A., Forsberg, L.J., Hector, C.E., Worthen, R.J., et al. (2010). Altered metabolism and persistent starvation behaviors caused by reduced AMPK function in Drosophila. *PLoS One* 5(9). doi: 10.1371/journal.pone.0012799.

Ju, T.C., Chen, H.M., Lin, J.T., Chang, C.P., Chang, W.C., Kang, J.J., et al. (2011). Nuclear translocation of AMPK-alpha1 potentiates striatal neurodegeneration in Huntington's disease. *J Cell Biol* 194(2)**,** 209-227. doi: 10.1083/jcb.201105010.

Kao, Y.H., Lin, M.S., Chen, C.M., Wu, Y.R., Chen, H.M., Lai, H.L., et al. (2017a). Targeting ENT1 and adenosine tone for the treatment of Huntington's disease. *Hum Mol Genet* 26(3)**,** 467-478. doi: 10.1093/hmg/ddw402.

Kao, Y.H., Lin, M.S., Chen, C.M., Wu, Y.R., Chen, H.M., Lai, H.L., et al. (2017b). Targeting ENT1 and adenosine tone for the treatment of Huntington's disease. *Human Molecular Genetics* 26(3)**,** 467-478. doi: 10.1093/hmg/ddw402.

Knight, D., Harvey, P.J., Iliadi, K.G., Klose, M.K., Iliadi, N., Dolezelova, E., et al. (2010). Equilibrative nucleoside transporter 2 regulates associative learning and synaptic function in

Drosophila. *J Neurosci* 30(14)**,** 5047-5057. doi: 10.1523/JNEUROSCI.6241-09.2010.

Krauss, V., and Dorn, R. (2004). Evolution of the trans-splicing Drosophila locus mod(mdg4) in several species of Diptera and Lepidoptera. *Gene* 331**,** 165-176. doi: 10.1016/j.gene.2004.02.019.

Kucerova, L., Broz, V., Arefin, B., Maaroufi, H.O., Hurychova, J., Strnad, H., et al. (2016). The Drosophila Chitinase-Like Protein IDGF3 Is Involved in Protection against Nematodes and in Wound Healing. *J Innate Immun* 8(2)**,** 199-210. doi: 10.1159/000442351.

Kucerova, L., Broz, V., Fleischmannova, J., Santruckova, E., Sidorov, R., Dolezal, V., et al. (2012). Characterization of the Drosophila adenosine receptor: the effect of adenosine analogs on cAMP signaling in Drosophila cells and their utility for in vivo experiments. *J Neurochem* 121(3)**,** 383-395. doi: 10.1111/j.1471-4159.2012.07701.x.

Kuo, Y., Ren, S., Lao, U., Edgar, B.A., and Wang, T. (2013). Suppression of polyglutamine protein toxicity by co-expression of a heat-shock protein 40 and a heat-shock protein 110. *Cell Death Dis* 4**,** e833. doi: 10.1038/cddis.2013.351.

Lee, C.F., and Chern, Y.J. (2014). Adenosine Receptors and Huntington's Disease. *Adenosine Receptors in Neurology and Psychiatry* 119**,** 195-232. doi: 10.1016/B978-0-12-801022-8.00010-6.

Lewis, E.A., and Smith, G.A. (2016). Using Drosophila models of Huntington's disease as a translatable tool. *J Neurosci Methods* 265**,** 89-98. doi: 10.1016/j.jneumeth.2015.07.026.

Liu, H., Adebiyi, M., Liu, R.R., Song, A., Manalo, J., Wen, Y.E., et al. (2018). Elevated ecto-5'-nucleotidase: a missing pathogenic factor and new therapeutic target for sickle cell disease. *Blood Adv* 2(15)**,** 1957-1968. doi: 10.1182/bloodadvances.2018015784.

Maier, S.A., Galellis, J.R., and McDermid, H.E. (2005). Phylogenetic analysis reveals a novel protein family closely related to adenosine deaminase. *J Mol Evol* 61(6)**,** 776-794. doi: 10.1007/s00239-005-0046-y.

Martinez-Mir, M.I., Probst, A., and Palacios, J.M. (1991). Adenosine-A2 Receptors - Selective Localization in the Human Basal Ganglia and Alterations with Disease. *Neuroscience* 42(3)**,** 697-706. doi: Doi 10.1016/0306-4522(91)90038-P.

Medina-Pulido, L., Molina-Arcas, M., Justicia, C., Soriano, E., Burgaya, F., Planas, A.M., et al. (2013). Hypoxia and P1 receptor activation regulate the high-affinity concentrative adenosine transporter CNT2 in differentiated neuronal PC12 cells. *Biochem J* 454(3)**,** 437-445. doi: 10.1042/BJ20130231.

Melnikova, L., Kostyuchenko, M., Parshikov, A., Georgiev, P., and Golovnin, A. (2018). Role of Su(Hw) zinc finger 10 and interaction with CP190 and Mod(mdg4) proteins in recruiting the Su(Hw) complex to chromatin sites in Drosophila. *PLoS One* 13(2)**,** e0193497. doi: 10.1371/journal.pone.0193497.

Mievis, S., Blum, D., and Ledent, C. (2011). A2A receptor knockout worsens survival and motor behaviour in a transgenic mouse model of Huntington's disease. *Neurobiol Dis* 41(2)**,** 570-576. doi: 10.1016/j.nbd.2010.09.021.

Mugat, B., Parmentier, M.L., Bonneaud, N., Chan, H.Y., and Maschat, F. (2008). Protective role of

Engrailed in a Drosophila model of Huntington's disease. *Hum Mol Genet* 17(22)**,** 3601-3616. doi: 10.1093/hmg/ddn255.

Mutsuddi, M., Marshall, C.M., Benzow, K.A., Koob, M.D., and Rebay, I. (2004). The spinocerebellar ataxia 8 noncoding RNA causes neurodegeneration and associates with staufen in Drosophila. *Curr Biol* 14(4)**,** 302-308. doi: 10.1016/j.cub.2004.01.034.

Oughtred, R., Stark, C., Breitkreutz, B.J., Rust, J., Boucher, L., Chang, C., et al. (2019). The BioGRID interaction database: 2019 update. *Nucleic Acids Res* 47(D1)**,** D529-D541. doi: 10.1093/nar/gky1079.

Picano, E., and Abbracchio, M.P. (2000). Adenosine, the imperfect endogenous anti-ischemic cardio-neuroprotector. *Brain Res Bull* 52(2)**,** 75-82. doi: 10.1016/s0361-9230(00)00249-5.

Poernbacher, I., and Vincent, J.P. (2018). Epithelial cells release adenosine to promote local TNF production in response to polarity disruption. *Nat Commun* 9(1)**,** 4675. doi: 10.1038/s41467-018-07114-z.

Ruan, C.C., Kong, L.R., Chen, X.H., Ma, Y., Pan, X.X., Zhang, Z.B., et al. (2018). A(2A) Receptor Activation Attenuates Hypertensive Cardiac Remodeling via Promoting Brown Adipose Tissue-Derived FGF21. *Cell Metabolism* 28(3)**,** 476-+. doi: 10.1016/j.cmet.2018.06.013.

Soltani-Bejnood, M., Thomas, S.E., Villeneuve, L., Schwartz, K., Hong, C.S., and McKee, B.D. (2007). Role of the mod(mdg4) common region in homolog segregation in Drosophila male meiosis. *Genetics* 176(1)**,** 161-180. doi: 10.1534/genetics.106.063289.

Song, W., Smith, M.R., Syed, A., Lukacsovich, T., Barbaro, B.A., Purcell, J., et al. (2013). Morphometric analysis of Huntington's disease neurodegeneration in Drosophila. *Methods Mol Biol* 1017**,** 41-57. doi: 10.1007/978-1-62703-438-8_3.

Soshnev, A.A., Baxley, R.M., Manak, J.R., Tan, K., and Geyer, P.K. (2013). The insulator protein Suppressor of Hairy-wing is an essential transcriptional repressor in the Drosophila ovary. *Development* 140(17)**,** 3613-3623. doi: 10.1242/dev.094953.

Steffan, J.S., Bodai, L., Pallos, J., Poelman, M., McCampbell, A., Apostol, B.L., et al. (2001). Histone deacetylase inhibitors arrest polyglutamine-dependent neurodegeneration in Drosophila. *Nature* 413(6857)**,** 739-743. doi: Doi 10.1038/35099568.

Stenesen, D., Suh, J.M., Seo, J., Yu, K., Lee, K.S., Kim, J.S., et al. (2013). Adenosine nucleotide biosynthesis and AMPK regulate adult life span and mediate the longevity benefit of caloric restriction in flies. *Cell Metab* 17(1)**,** 101-112. doi: 10.1016/j.cmet.2012.12.006.

Swick, L.L., Kazgan, N., Onyenwoke, R.U., and Brenman, J.E. (2013). Isolation of AMP-activated protein kinase (AMPK) alleles required for neuronal maintenance in Drosophila melanogaster. *Biol Open* 2(12)**,** 1321-1323. doi: 10.1242/bio.20136775.

Thomas, S.E., Soltani-Bejnood, M., Roth, P., Dorn, R., Logsdon, J.M., Jr., and McKee, B.D. (2005). Identification of two proteins required for conjunction and regular segregation of achiasmate homologs in Drosophila male meiosis. *Cell* 123(4)**,** 555-568. doi: 10.1016/j.cell.2005.08.043.

Toczek, M., Zielonka, D., Zukowska, P., Marcinkowski, J.T., Slominska, E., Isalan, M., et al. (2016).

An impaired metabolism of nucleotides underpins a novel mechanism of cardiac remodeling leading to Huntington's disease related cardiomyopathy. *Biochim Biophys Acta* 1862(11)**,** 2147-2157. doi: 10.1016/j.bbadis.2016.08.019.

Tyebji, S., Saavedra, A., Canas, P.M., Pliassova, A., Delgado-Garcia, J.M., Alberch, J., et al. (2015). Hyperactivation of D1 and A2A receptors contributes to cognitive dysfunction in Huntington's disease. *Neurobiol Dis* 74**,** 41-57. doi: 10.1016/j.nbd.2014.11.004.

van Eyk, C.L., O'Keefe, L.V., Lawlor, K.T., Samaraweera, S.E., McLeod, C.J., Price, G.R., et al. (2011). Perturbation of the Akt/Gsk3-beta signalling pathway is common to Drosophila expressing expanded untranslated CAG, CUG and AUUCU repeat RNAs. *Hum Mol Genet* 20(14)**,** 2783-2794. doi: 10.1093/hmg/ddr177.

Vazquez-Manrique, R.P., Farina, F., Cambon, K., Dolores Sequedo, M., Parker, A.J., Millan, J.M., et al. (2016). AMPK activation protects from neuronal dysfunction and vulnerability across nematode, cellular and mouse models of Huntington's disease. *Hum Mol Genet* 25(6)**,** 1043-1058. doi: 10.1093/hmg/ddv513.

Vonsattel, J.P., and DiFiglia, M. (1998). Huntington disease. *J Neuropathol Exp Neurol* 57(5)**,** 369-384. doi: 10.1097/00005072-199805000-00001.

Warrick, J.M., Chan, H.Y., Gray-Board, G.L., Chai, Y., Paulson, H.L., and Bonini, N.M. (1999). Suppression of polyglutamine-mediated neurodegeneration in Drosophila by the molecular chaperone HSP70. *Nat Genet* 23(4)**,** 425-428. doi: 10.1038/70532.

Xiao, C., Liu, N., Jacobson, K.A., Gavrilova, O., and Reitman, M.L. (2019). Physiology and effects of nucleosides in mice lacking all four adenosine receptors. *PLoS Biol* 17(3)**,** e3000161. doi: 10.1371/journal.pbio.3000161.

Yu, S., Waldholm, J., Bohm, S., and Visa, N. (2014). Brahma regulates a specific trans-splicing event at the mod(mdg4) locus of Drosophila melanogaster. *RNA Biol* 11(2)**,** 134-145. doi: 10.4161/rna.27866.

Zuberova, M., Fenckova, M., Simek, P., Janeckova, L., and Dolezal, T. (2010). Increased extracellular adenosine in Drosophila that are deficient in adenosine deaminase activates a release of energy stores leading to wasting and death. *Dis Model Mech* 3(11-12)**,** 773-784. doi: 10.1242/dmm.005389.

Zurovec, M., Dolezal, T., Gazi, M., Pavlova, E., and Bryant, P.J. (2002). Adenosine deaminase-related growth factors stimulate cell proliferation in Drosophila by depleting extracellular adenosine. *Proc Natl Acad Sci U S A* 99(7)**,** 4403-4408. doi: 10.1073/pnas.062059699.

7. Publication II

Yu-Hsien Lin, Houda Ouns Maaroufi, Emad Ibrahim, Lucie Kucerova, Michal Zurovec (2019). Expression of human mutant huntingtin protein in Drosophila hemocytes impairs immune responses. Frontiers in immunology. doi: 10.3389/fimmu.2019.02405

Expression of human mutant Huntingtin protein in *Drosophila* hemocytes impairs immune responses

Yu-Hsien Lin[1,2*], Houda Ouns Maaroufi[1,2], Emad Ibrahim[1,2], Lucie Kucerova[1], Michal Zurovec[1,2*]

[1]Biology Centre of the Czech Academy of Sciences, Institute of Entomology, Ceske Budejovice, Czech Republic, [2]Faculty of Science, University of South Bohemia, Ceske Budejovice, Czech Republic

*To whom correspondence should be addressed at:
Michal Zurovec, zurovec@entu.cas.cz, tel: +420-387775267 and Yu-Hsien Lin, r99632012@gmail.com, Biology Centre CAS, Institute of Entomology, Ceske Budejovice, Czech Republic

Abstract

The pathogenic effect of mutant HTT (mHTT) which causes Huntington disease (HD) are not restricted to nervous system. Such phenotypes include aberrant immune responses observed in the HD models. However, it is still unclear how this immune dysregulation influences the innate immune response against pathogenic infection. In the present study, we used transgenic *Drosophila melanogaster* expressing mutant HTT protein (mHTT) with hemocyte-specific drivers and examined the immune responses

and hemocyte function. We found that mHTT expression in the hemocytes did not affect fly viability, but the numbers of circulating hemocytes were significantly decreased. Consequently, we observed that the expression of mHTT in the hemocytes compromised the immune responses including clot formation and encapsulation which lead to the increased susceptibility to entomopathogenic nematode and parasitoid wasp infections. In addition, mHTT expression in *Drosophila* macrophage-like S2 cells *in vitro* reduced ATP levels, phagocytic activity and the induction of antimicrobial peptides. Further effects observed in mHTT-expressing cells included the altered production of cytokines and activation of JAK/STAT signaling. The present study shows that the expression of mHTT in *Drosophila* hemocytes causes deficient cellular and humoral immune responses against invading pathogens. Our findings provide the insight into the pathogenic effects of mHTT in the immune cells.

Introduction

Huntington's disease (HD) is an inherited neurodegenerative disorder caused by an abnormal expansion of CAG trinucleotide in the Huntingtin (*htt*) gene. Mutant HTT protein (mHTT) contains an extended polyglutamine tract encoded by 40 to over 150 CAG repeats, which causes cytotoxicity and leads to neurodegeneration; this results in involuntary movement, cognitive impairment and psychiatric abnormalities (Vonsattel and DiFiglia, 1998). Although many clinical symptoms of HD are related to neuronal dysfunction, emerging evidence indicates that the expression of mHTT in non-neuronal cells of the brain or in the peripheral tissues also contributes to the pathogenesis of HD (Sassone et al., 2009). Abnormal phenotypic effects caused by the dysfunction of non-neuronal cells have been described in cardiac cells, muscles, the endocrine system, adipose tissue, testes and immune cells of HD patients and also in mouse HD models

(Sathasivam et al., 1999; Sassone et al., 2009).

Abnormalities related to the immune system were observed in a number of studies of HD patients (Leblhuber et al., 1998). The expression of mHTT in both brain and peripheral immune cells (microglial and myeloid cells) induces the NF-κB signaling pathway which elevates levels of pro-inflammatory cytokines and chemokines, leading to systemic inflammation (Andre et al., 2016). In addition, macrophages isolated from HD model mice exhibited migration deficits, and microglia showed a delayed response to laser-induced injury in the brain (Kwan et al., 2012). Although several studies proposed that the immune cell response is impaired in HD, this phenomenon is still poorly characterized in relation to host responses to pathogens. One recent study reported increased proliferation of a parasite, *Toxoplasma gondii*, in HD model mice, causing premature mortality and thus suggesting that expression of mHTT in immune cells may suppress immune responses (Donley et al., 2016).

Drosophila melanogaster has been long-term established as a HD model. *In vivo* experiments have revealed that the ectopic overexpression of mutant human *htt* (exon 1 with expanded CAG repeats) in the neural tissue of transgenic flies causes neurodegeneration (Steffan et al., 2001; Song et al., 2013). The mechanisms of cellular pathology observed in the HD flies seem similar to those in human patients, including the suppression of mitochondrial function, transcriptional dysregulation and neuronal apoptosis (Taylor et al., 2003; Li et al., 2010). Genetic screening for disease modifiers in HD model flies led to the identification of the effects of sumoylation and HSP70 chaperone machinery on neurodegeneration. The subsequent confirmation that these pathways are involved in the pathology of human patients validates the *Drosophila* model for investigating HD (Warrick et al., 1999; Steffan et al., 2004). Furthermore, since the tissue-specific expression of transgenes in *Drosophila* can be easily controlled

using the UAS-Gal4 system, *Drosophila* have also been used to study the effects of HD on non-neuronal cells, including glial cells, photoreceptors, cardiac cells, and salivary glands (Marsh et al., 2000; Tamura et al., 2009; Besson et al., 2010; Weiss et al., 2012; Melkani et al., 2013).

The present study aimed to survey the physiological impact of mHTT expression in *Drosophila* hemocytes. We used the *Drosophila* UAS-Gal4 system to express mHTT with hemocyte-specific drivers and investigated the effect of mHTT on survival, hemocyte development, and susceptibility to pathogens. We also expressed mHTT in a *Drosophila* macrophage-like cell line, S2 cells, and assessed the effect of mHTT on phagocytic activity, ATP levels, antimicrobial peptides and production of cytokines. Our results suggest that the expression of mHTT in hemocytes does not directly affect survival but causes immune dysregulation, which leads to an impaired immune response against pathogenic invasion.

Results

Expression of mHTT in hemocytes did not affect larval viability but decreased the number of circulating hemocytes

In order to characterize the effects of mHTT in *Drosophila* hemocytes, we used a tissue-specific UAS-Gal4 system by expressing wild-type human HTT (Q20) or mutant HTT (Q93) under the control of a pan-neuronal driver, *elav-gal4*, or hemocyte drivers, *hml-gal4* and *he-gal4.* The flies devoid of plasmatocytes ($phago^{less}$) generated by expressing pro-apoptosis genes, *rpr* and *hid* with *hml-gal4* were used as negative control (Charroux and Royet, 2009; Defaye et al., 2009). The results showed that the ectopic expression of Q93 with the pan-neuronal driver (*elav-gal4*) decreased both the eclosion rate and the longevity of the adult flies, but not the rate of pupariation (Fig. 1).

The expression of Q20 and Q93 with both hemocyte drivers (*hml-gal4* and *he-gal4*) had no effect on pupariation and eclosion rates. Furthermore, the differences in longevity between Q20 and Q93 flies were not significant, and their survival rate was higher than *phago*^{less} flies (Fig. 1C). These results indicated that the hemocyte-specific expression of mHTT did not influence fly viability, unlike its expression in the brain.

Although the expression of mHTT did not affect fly survival, we observed a significant decrease in the number of circulating hemocytes. In first-instar larvae, the number of hemocytes differed significantly only in the *phago*^{less} flies (Fig. 2A). However, a reduced amount of circulating and sessile hemocytes was apparent in the Q93 mutants from second-instar larvae. As shown in Figure 2B, the circular hemocyte numbers in Q93 larvae were still higher than in *phago*^{less} flies, showing about 50% of the numbers observed in the Q20 control (Fig. 2B). These results showed that the expression of mHTT with two different hemocyte-specific drivers reduced the number of hemocytes.

Expression of mHTT in hemocytes impaired the immune response to parasites

To examine whether mHTT expression in *Drosophila* hemocytes affects the innate immune response and whether such larvae are still able to restrain parasite development, we tested the sensitivity of such flies to entomopathogenic nematode and parasitoid wasp infections, which are two *Drosophila* pathogenic models for examining the cellular immune response (Dobes et al., 2012; Small et al., 2012). Early third-instar larvae expressing mHTT (Q93), wild-type HTT (Q20) or *phago*^{less} were infected with nematode species, *Heterorhabditis bacteriophora* or *Steinernema carpocapsae*, which contain the bacterial symbionts *Photorhabdus luminescens* and *Xenorhabdus nematophila*, respectively. Mortality was calculated at 24 and 48 hours post-infection.

As shown in Figure 3, both *phago*^{less} and Q93 larvae displayed significantly higher mortality than Q20 controls. Previous studies revealed that the formation of hemolymph clot is an important innate immune response against entomopathogenic nematode infection in *Drosophila* (Arefin et al., 2014; Kucerova et al., 2016). To determine whether the expression of mHTT in the hemocytes caused clotting defects, we used an established bead aggregation assay (Lesch et al., 2007; Kucerova et al., 2016). Compared to the larvae expressing normal HTT (Q20), the hemolymph collected from mHTT (Q93)-expressing larvae displayed poor bead aggregation similar to *phago*^{less} larvae (Fig. 3E). This results indicated that the expression of mHTT suppresses the clotting activity and thus increases the suscepitibility to nematode infection.

Similarly, we infected *Drosophila* larvae with a parasitoid wasp, *Leptopilina boulardi* and calculated the number of emerged fly and wasp adults. The number of eclosed *Drosophila* adults was not significantly different between Q20 and Q93 driven by *hml-gal4* and *he-gal4*, while *phago*^{less} showed lower eclosion rates than both Q20 and Q93 (Fig. 4A, B). However, the number of emerged wasps were significantly higher in both Q93 and *phago*^{less} flies, thus indicating that a greater number of wasps overwhelmed the immune reaction of Q93 hosts and successfully developed to adult stage. In addition, the higher number of wasp eggs successfully hatched in both Q93 and phagoless larvae (Fig. 4C); these results indicated that Q93 and *phago*^{less} larvae have less efficient immune reaction against wasp infection. Since the encapsulation and melanization are major defense mechanisms against parasitoid wasp infection, we quantified the number of the melanized capsules to assess the immune activity after 72 hours post-infection. We found that there were more intact melanized capsules in Q20 larvae (79%) than in those expressing Q93 (51.6%) or in *phago*^{less} (17.7%) (Fig 4D & 4G left). We also observed a higher amount of melanization pieces in Q93 or *phago*^{less}

individuals than in Q20 larvae (Fig. 4E and 4G middle). The formation of such defective capsules was described previously in immune-deficient mutant flies (Mortimer et al., 2012). Moreover, 37% of the infected *phago*^{less} larvae formed no melanization capsules compared to Q20 (0%) or Q93 (4.8%) infected larvae (Fig. 4F and 4G right). These results could explain a lower proportion of *phago*^{less} adults successfully eclosed after wasp infection (Fig. 4A-B). Taken together, our results suggest, that mHTT expression impairs the innate immune reactions to nematode and parasitoid wasp infections due to the deficient cellular immune responses such as clot formation and encapsulation.

Reduced phagocytic activity and ATP levels in mHTT cells

To find out whether mHTT expression could cause a detrimental effect on hemocyte functions, we expressed mHTT or wild-type HTT in *Drosophila* S2 cells. The S2 cell line consists of macrophage-like cells with phagocytic activity and the ability to produce antimicrobial peptides (AMPs) (Ramet et al., 2002). We transfected the cells with four different recombinant constructs encoding green fluorescent protein (GFP) fused to HTT repeats under an inducible metallothionein promoter. We created stable cell lineages and confirmed that the S2 cells expressed HTT-fusion proteins by observing the GFP. As shown in Figure S1, most of the cells in all cell lineages were positive for the fluorophore. Furthermore, the cells containing the mHTT Q46, Q72, and Q97 constructs (all except wild-type Q25) showed formation of mHTT aggregates.

We further treated the HTT-expressing cells with *E. coli* particles conjugated by pH-sensitive dye (pHrodo) to examine their phagocytic activity. This causes bright fluorescence to be visible after particle engulfment in the acidic environment of phagolysosome. The results showed that after inducing mHTT expression, the fluorescence signals were significantly lower in Q46, Q72, and Q97 mHTT-expressing

cells but not in cells expressing wild-type Q25 HTT (Fig. 5A). Quantification of the cells containing fluorescent signals showed a significant reduction (20~30%) of fluorescent-positive cells in mHTT-expressing cells compared to the control cells (Q25) (Fig. 5B), thus supporting the hypothesis that expression of mHTT in immune cells impairs phagocytic activity.

The phagocytic capacity of immune cells has been associated with mitochondrial activity (West et al., 2011; Chougnet et al., 2015; Geng et al., 2015); mHTT has been shown to cause impairment of energy metabolism and mitochondrial dysfunction in human peripheral blood cells (Ehinger et al., 2016). To test whether mHTT can also impair the energy metabolism of *Drosophila* immune cells, we measured the ATP levels in S2 lineages after mHTT induction. The results showed that ATP levels significantly decreased in cells expressing Q72 and Q97 mHTT after 72 hours of induction (Fig. 6A). The ATP levels in cells expressing Q46, Q72, and Q97 mHTT were further reduced after 120 hours of induction (Fig. 6B). This indicated that the expression of mHTT reduces ATP levels, which may further limit the cellular immune responses against pathogenic infection.

The studies in human and mouse have demonstrated that the expression of Bcl-2 family proteins associated with mitochondrial dysfunction is activated by mHTT expression (Sassone et al., 2013). To assess whether the level of *Drosophila* Bcl-2 proteins is also altered by mHTT expression, we compared the transcription levels of two of *Bcl-2* genes, *buffy* and *debcl*, in Q25- and Q97- expressing S2 cells (Fig. 6C). We found that *buffy* expression is five times higher in Q97- than in Q25- expressing cells, but we did not detect any significant difference in *debcl* mRNA level. Different from pro-apoptotic function of *debcl*, *buffy* was suggested to play an anti-apoptotic role under stress conditions which is similar to mammalian Bcl-2 proteins (Quinn et al.,

2003; Monserrate et al., 2012). We conclude that the alternation of ATP synthesis and *buffy* expression indicate the abnormality of mitochondrial function in mHTT expressing cells, and the induction of *buffy* might be a protective mechanism for preventing the cell death caused by mitochondrial dysfunction.

Upregulation of cytokines expression and downstream JAK/STAT signaling in mHTT expression cells

It has been reported that the level of cytokines and chemokines are abnormally increased in the plasma of HD patients (Bjorkqvist et al., 2008). Consistently, the production of cytokines from monocytes and macrophages of HD patients have shown hyper-activation after lipopolysaccharide stimulation (Trager et al., 2014). To test whether mHTT has a similar effect in *Drosophila*, we used Schneider 2 (S2) cells and measured the the effect of mHTT expression on three *Drosophila* cytokines, *upd1*, *upd2*, and *upd3*, as well as *dome*, *jak* (*hop*) and downstream targets of JAK-STAT signaling (Fig. 7A). The results showed that the expression of cytokine *upd3* is significantly increased in Q97 mHTT-expressing cells compared to Q25 controls (Fig. 7B). In addition, the expression of *dome* receptor and four downstream targets, *tep1*, *totA*, *totB* and *totC* were also significantly increased in Q97-expressing cells. These results indicated that the expression of mHTT induced the production of cytokines and activates JAK/STAT signaling.

Decreased antimicrobial peptide (AMP) production in response to bacteria

Drosophila Toll and Imd pathways control the humoral immune response against invasive microorganisms by regulating the induction of downstream AMP genes in both hemocytes and the fat body (Lemaitre and Hoffmann, 2007). To examine whether AMP

induction was affected by mHTT expression in *Drosophila* S2 cells, we treated mHTT-expressing cells with a mixture of heat-inactivated Gram-negative bacteria, *Escherichia coli*, and Gram-positive bacteria, *Micrococcus luteus*. The induction of AMPs was assessed using qPCR. As shown in Figure 8, there was no difference in the expression of AMPs between Q25 and Q97 in the absence of bacterial treatment. In contrast, all AMP genes were significantly induced in both Q25- and Q97-expressing cells at 8 hours after bacterial treatment. However, AMP induction levels were significantly lower in cells expressing Q97 (Fig. 8A). We further assessed the AMP expression levels under *in vivo* condition after infecting larvae with phytopathogenic bacteria, *Erwinia carotovora carotovora 15* (Ecc15). We examined the expression levels of *dpt*, *dptB*, *attA* and *cecA* which were known as being highly induced after Ecc15 infection (Basset et al., 2000). Our results of larval infections showed that except for *attA*, the induction levels of *dpt*, *dptB* and *cecA* in Q93 or $phago^{less}$ larvae were significantly lower than in Q20 controls (Fig. 8B). These results confirm that the induction of AMPs in response to bacteria was significantly suppressed in mHTT-expressing cells or larvae.

Discussion

Peripheral immune dysregulation is considered as one of the clinical features of HD pathogenesis (Wild et al., 2011). Previous studies in mice and HD patients have suggested that mHTT expression in immune cells accelerates the neurodegenerative process. The activation of pro-inflammatory products in mHTT-expressing microglial cells elevate the reactive oxygen species (ROS) and cause neuroinflammation, which contributes to neurodegeneration (Chen et al., 2007; Andre et al., 2016). Genetic ablation or pharmacologically-blocked cannabinoid receptor 2 (interleukin-6 regulator), as well as drug suppression of the cytokine-responsive kynurenine pathway, can both

slow neurodegeneration and improve the phenotype of R6/2 HD mice (Zwilling et al., 2011; Bouchard et al., 2012). Since the expression of mHTT in HD mice and human patients is ubiquitous, it is still unclear whether mHTT expression in blood cells directly contributes to the lethal effect of HD. The present study examined mHTT expressed specifically in *Drosophila* blood cells and assessed its impacts on development and longevity (Fig. 1). We found that the expression of mHTT in hemocytes did not cause mortality or a shortening in life span, which is in contrast to expression in the brain. Our results, therefore, suggest that expression of mHTT in immune cells does not directly contribute to mortality.

A reduced proliferation of immune cells has been observed in *T. gondii*-infected HD mice, in which the expansion of CD8+ T-cells in the spleen and brain was significantly suppressed during infection (Donley et al., 2016). Our results showed that the expression of mHTT in flies with hemocyte-specific drivers causes a significant reduction in the number of circulating hemocytes (Fig. 2), and this decrease might be caused by dysfunction of mitochondria (Fig. 7). The mitochondrial abnormalities resulting in metabolic dysregulation in peripheral blood cells of HD patients increase oxidative damage and suppress their anti-oxidant capacity (Chen et al., 2007). The activation of caspase-3 and caspase-9 in lymphoblasts of HD patients increases apoptosis under stress conditions (Sawa et al., 1999).

The mHTT-expressing larvae revealed a higher susceptibility to wasp and nematode infections and this phenotype was caused by defects of clot formation and encapsulation (Figs. 3 and 4). It has been shown that wasp egg recognition by circulating plasmatocytes and their differentiation to lamellocytes for further encapsulation are important processes of the immune response against wasp invasion in *Drosophila* (Anderl et al., 2016). The production of clotting components from

hemocytes also contributes to wound healing and melanization, which are important against nematode or wasp infections (Keebaugh and Schlenke, 2014; Kucerova et al., 2016). mHTT-expressing macrophages and monocytes from HD mice and patients also showed migration defects toward an inflammatory stimulus (Kwan et al., 2012). Hemocyte migration and adhesion are important factors for the development of embryonic macrophages, as well as successful wound healing and encapsulation during wasp infection (Fauvarque and Williams, 2011). Furthermore, decreased phagocytic activity toward bacterial particles (Fig. 5) and a suppressed induction of antimicrobial peptides (Fig. 8) can also contribute to immune deficiency against the bacterial symbionts of nematodes (Castillo et al., 2013; Arefin et al., 2014).

A previous study showed that macrophages isolated from HD patients and R6/2 mice displayed increased phagocytosis when incubated with fluorescent polystyrene beads (Trager et al., 2015). Our results seemingly differ because we observed reduced phagocytic activity of the *Drosophila* macrophage-like cells expressing different mHTT fragments (Fig. 5). Unlike their approach, we tested phagocytic activity using *E. coli* particles with a pH-sensitive fluorescent dye that can accurately confirm phagosome formation and initiation of the phagolysosome acidification. However, similar to their results, we found that S2 cells expressing mHTT were able to initiate phagocytosis. We tested this by treating the S2 cells with heat-inactivated *E. coli* labeled with DNA-specific fluorescent dye (without pH-sensor); the results showed that mHTT-expressing cells were indeed able to engulf *E. coli* (Fig. S2). Thus, our results suggest that mHTT-expressing cells were unable to complete the process of phagocytosis to final phagolysosome acidification. In addition, a defective actin function has been reported in HD mouse immune cells leading to failure of membrane ruffling (Kwan et al., 2012), which supports our results since actin assembly is required to trigger engulfment and

phagolysosome maturation for successful phagocytosis (Swanson, 2008).

Consistent with previous observations in HD mice and patients, we also found that *Drosophila* hemocyte cytokine *udp3* was upregulated in mHTT-expressing cells (Fig. 8). *Udp3* binds to the JAK/STAT signaling receptor, Dome, and initiates phosphorylation cascades which translocate the transcription factor, Stat92E, into the nucleus and activates downstream target genes (Fig. 7A) (Morin-Poulard et al., 2013). Two selected downstream target genes, *tep1* and *totA*, were highly expressed in mHTT-expressing cells (Fig. 7B). Notably, we found that the induction of antimicrobial peptides was significantly suppressed in mHTT-expressing cells after bacterial treatments, which has not yet been observed in other HD models. It is known that several human antimicrobial peptides are expressed in blood cells including neutrophils and macrophages (Wang, 2014). Since the transcriptomic analysis in HD blood cells has shown dysregulation of transcription in large genomic regions (Anderson et al., 2008), further studies will be needed to understand whether the production of antimicrobial peptides is impaired in the blood cells of patients or HD mice during infection.

In summary, the present study demonstrates immune dysregulation in flies expressing mHTT in hemocytes (Fig. 9). This expression does not directly cause a lethal effect, although it does reduce the number of circulating hemocytes and decrease ATP levels. Cytokine expression and downstream JAK/STAT signaling are activated upon mHTT expression, which has also been observed in HD patients and mice. In addition, the induction of antimicrobial peptides as well as the immune response against different pathogenic infections are impaired in mHTT-expressing *Drosophila* cells. The present study introduces a system for studying the tissue-specific effects of mHTT in *Drosophila* immune cells. Further studies can be applied to clarify the molecular

interaction between mHTT and antimicrobial peptide pathways (Toll and IMD signaling) as well as the mechanisms of phagocytosis suppression.

Figures

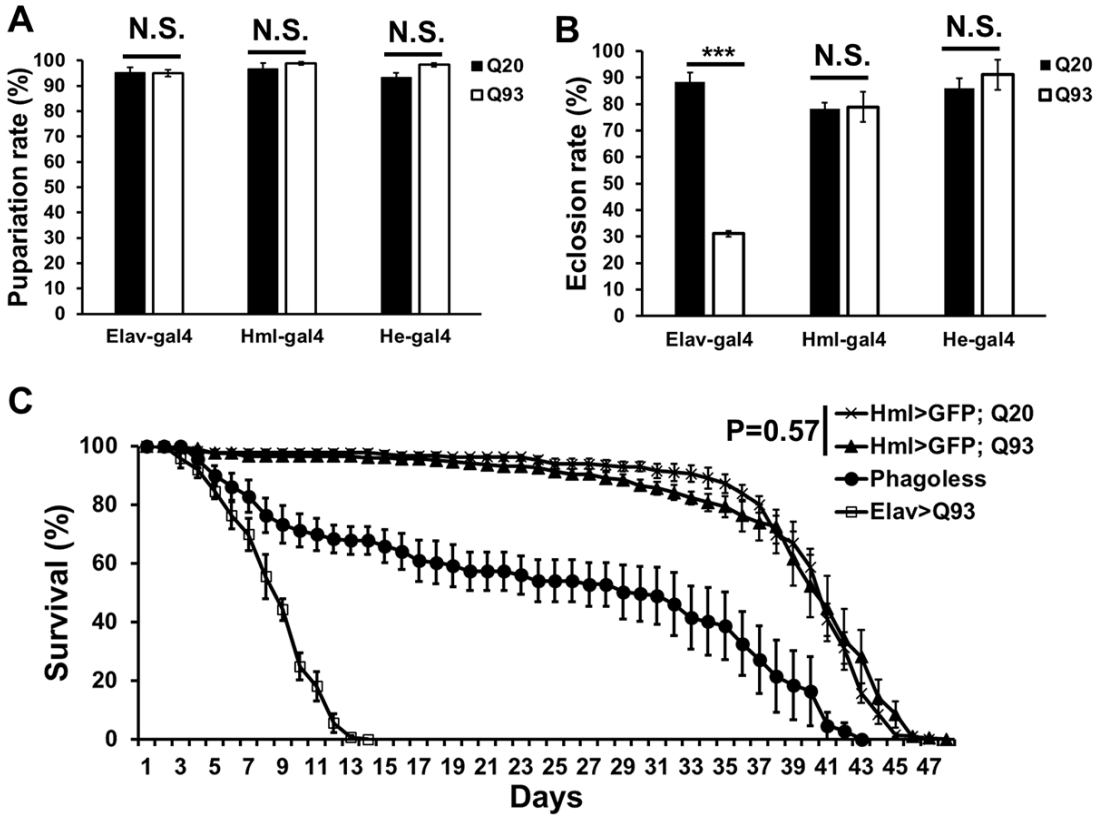

Figure 1. The viability assays of mHTT-expressing flies under the control of the pan-neuronal driver (*elav-gal4*) and hemocyte drivers (*hml-gal4* and *he-gal4*). (A) The effect of mHTT expression on pupariation (survival to pupal stage). (B) Eclosion (survival to adulthood) and (C) adult longevities were measured in control Q20 and mHTT Q93. All the experiments performed in at least six independent replicates. Data are presented as averages ± SEM. *P*-values for pupariation and eclosion rate using Student's t-test, *** $P < 0.001$, N.S., not significant. Significance analysis for longevity curve using weighted log-rank test.

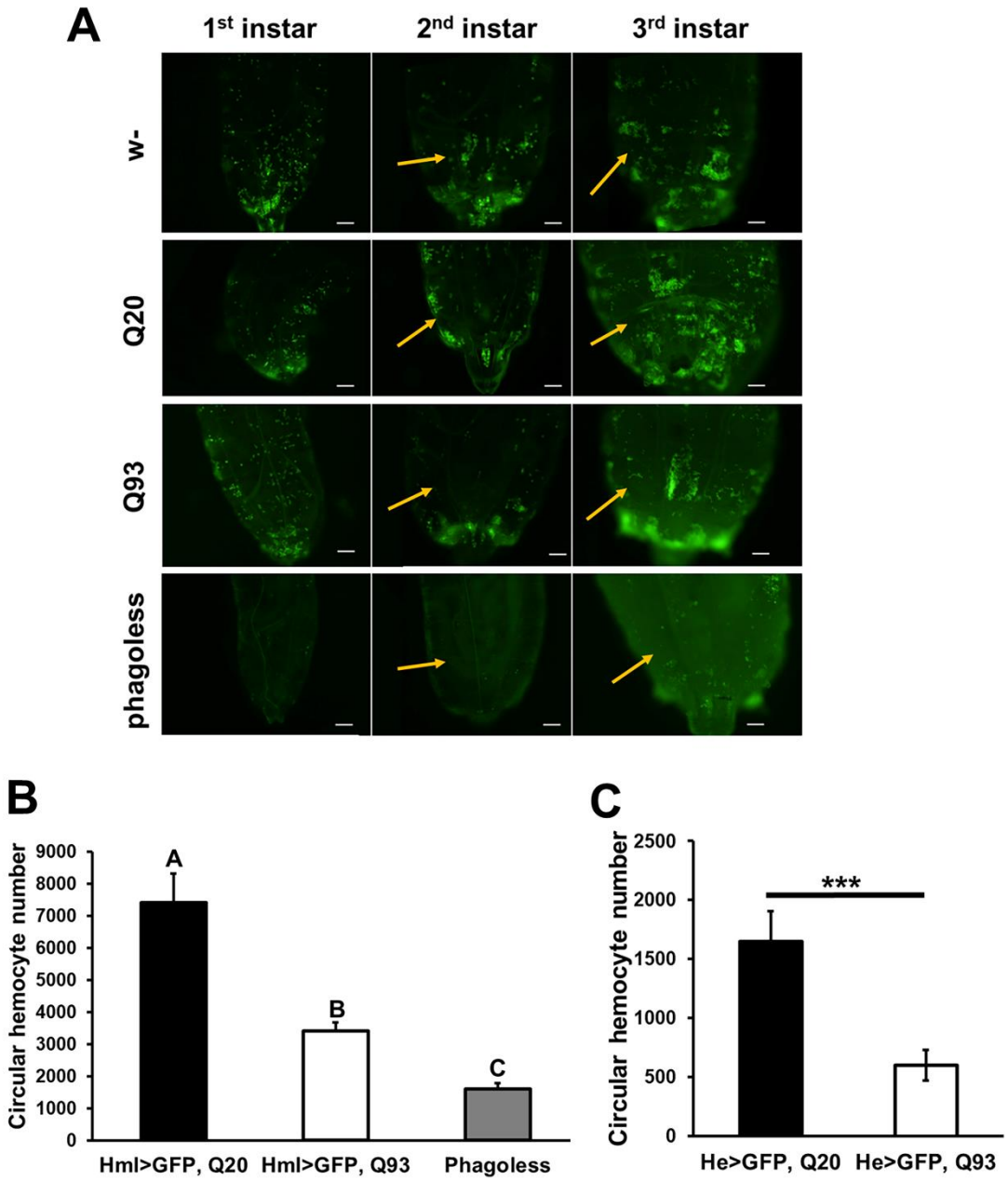

Figure 2. Ectopic expression of mHTT decreased hemocyte numbers. (A) Microscope images indicated the decreased number of circulating and sessile hemocytes in mHTT-expressing second-instar larvae. Quantification of hemocytes by ectopic co-expression of HTT with GFP using *hml-gal4* (B) or *he-gal4* (C). *Phago*^{less} flies with hemocyte ablation (*hml>UAS-rpr, hid*) were used as a negative control. The number of the circular hemocyte corresponded to the total number of GFP positive cells in 25 μL of collected sample. At least five independent replicates were analyzed. Data are presented as

averages ± SEM. Significances were analyzed by ANOVA with Fisher LSD *post-hoc* test (B), and the significant differences among treatment groups are marked with different letters ($P < 0.05$). Student's t-test was used for (C), *** $P < 0.001$.

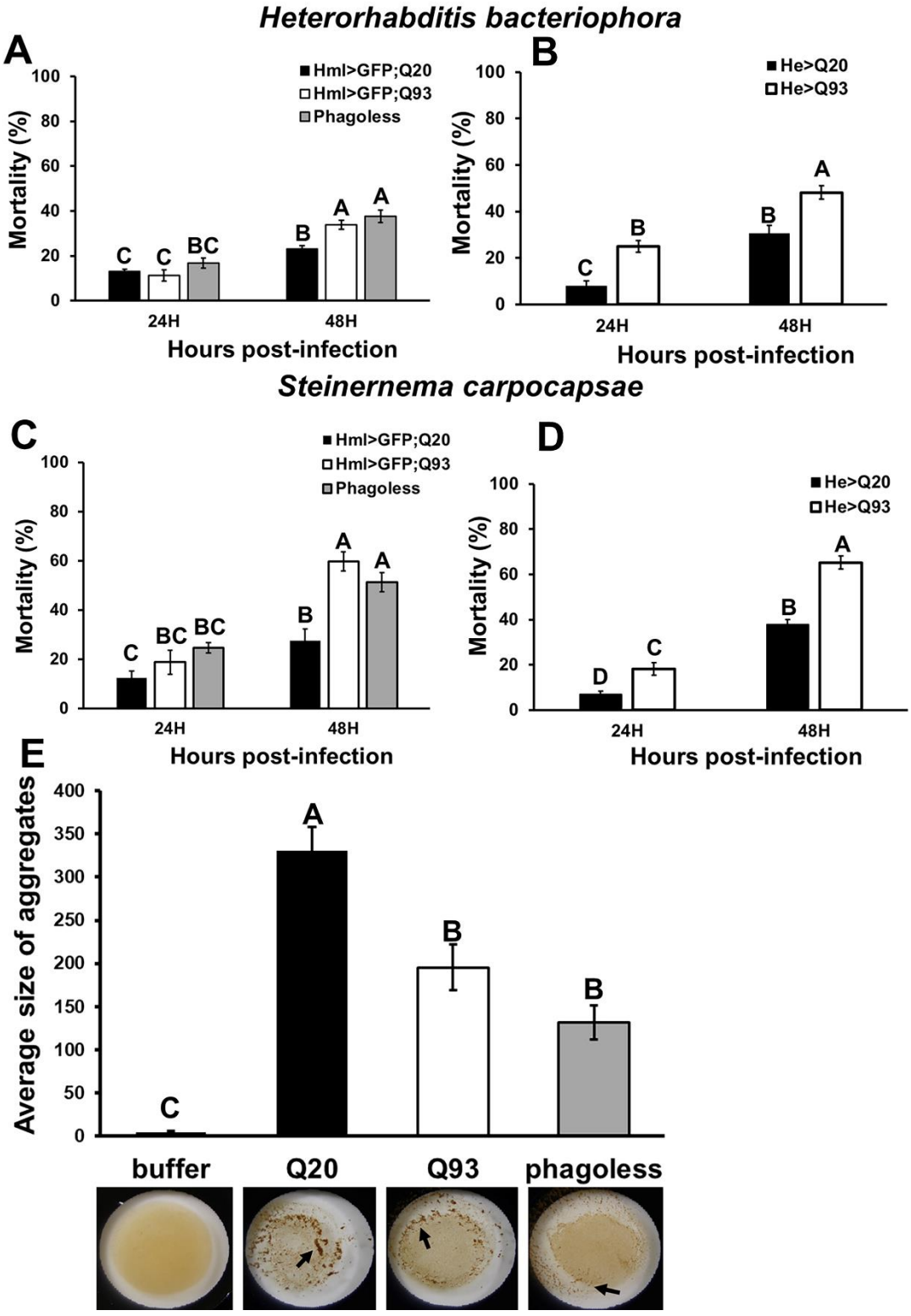

Figure 3. Immune challenge with entomopathogenic nematode infection and clotting assay. Larvae expressing mHTT Q93 or HTT Q20 with *hml-gal4* or *he-gal4* hemocyte

drivers were infected with *H. bacteriophora* (A, B), or *S. carpocapsae* (C, D). Mortality was calculated 24 and 48 hours after infection. *Phago*^{less} flies with hemocyte ablation (*hml>UAS-rpr, hid*) were used as negative control. Bead aggregation assay was used for assessing the clotting activity (E). Hemolymph was collected from Q93, Q20 and *Phago*^{less} (*hml-gal4*) larvae, mixed with a bead suspension, and the aggregates were quantified by ImageJ software. All the experiments were performed in five to six independent replicates. Data are presented as averages ± SEM. Significances were analyzed by ANOVA with Fisher LSD *post-hoc* test; significant differences among treatment groups are marked with different letters ($P < 0.05$).

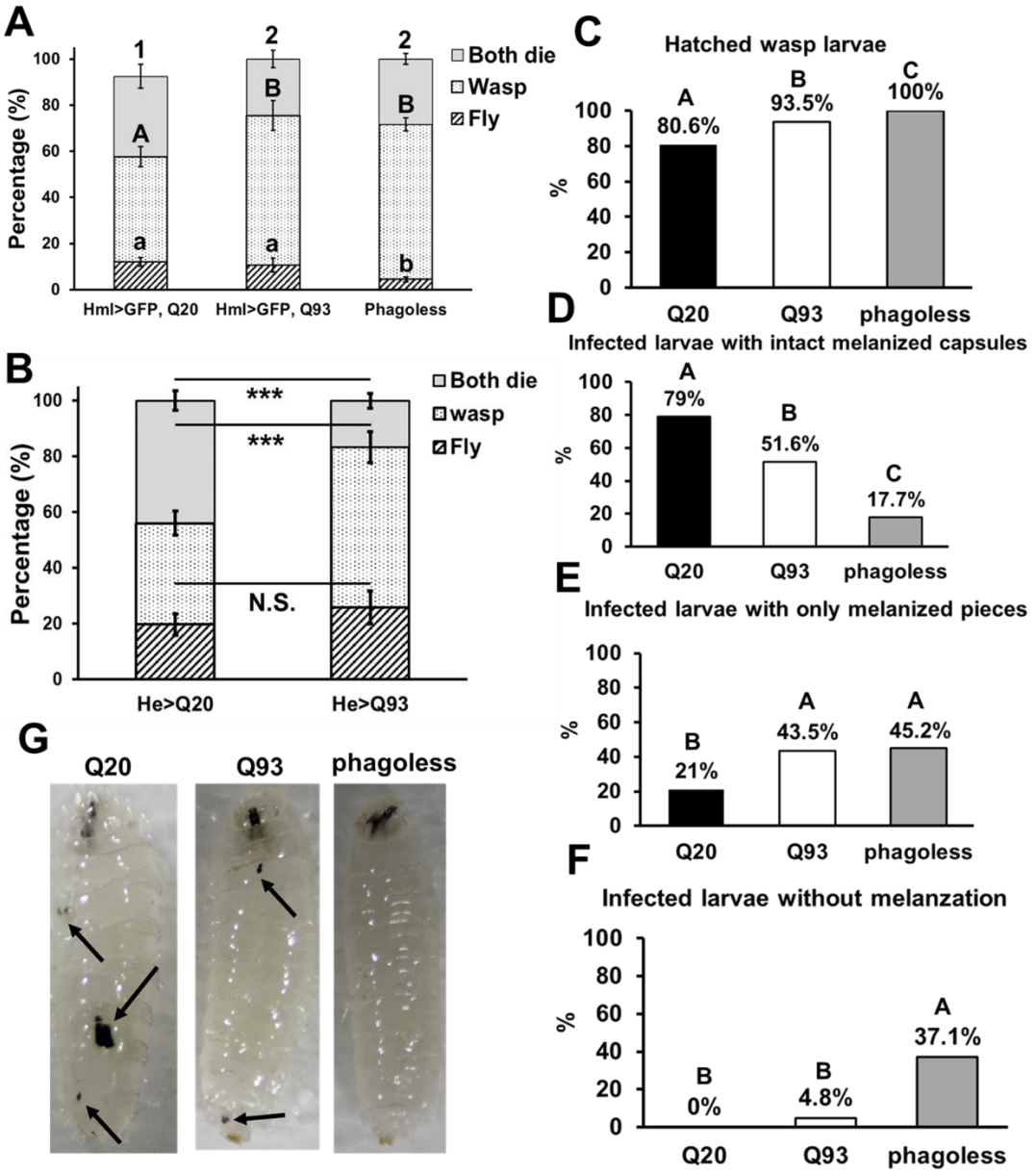

Figure 4. Immune challenge with parasitoid wasp infection and encapsulation activity assay. Larvae expressing mHTT Q93 and HTT Q20 with *hml-gal4* (A) or *he-gal4* (B) hemocyte driver were infected with parasitoid wasp, *L. boulardi*. *Phago*^{less} flies (which underwent hemocyte ablation) were used as negative control. Thirty infected larvae were collected and the numbers of eclosed flies and wasps were calculated, indicating the number of flies overcoming the wasp infection and the number of wasps successfully escaping the fly's immune reaction, respectively. Data are presented as

average ± SEM with more than 10 biological replicates. The significances of results for (A) were analyzed by ANOVA with a Fisher LSD *post-hoc* test; different letters on the treatment group indicate significant differences at $P < 0.05$. The significances of results for (B) were examined using Student's t-test, *** $P < 0.001$, N.S., not significant. For assessing the encapsulation activity, the numbers of fly larvae containing larvae of parasitic wasps (C), intact melanized capsules (D), melanized pieces (E) as well the numbers of the infected larvae without melanization (F) were recorded. The significances of the results were analyzed by Mann–Whitney U-test (paired); significant differences among treatment groups are marked with different letters ($P < 0.05$). The photos show examples of intact melanized capsule in Q20 larvae, melanized pieces in Q20 and Q93 larvae and infected phagoless without melanization reaction (G).

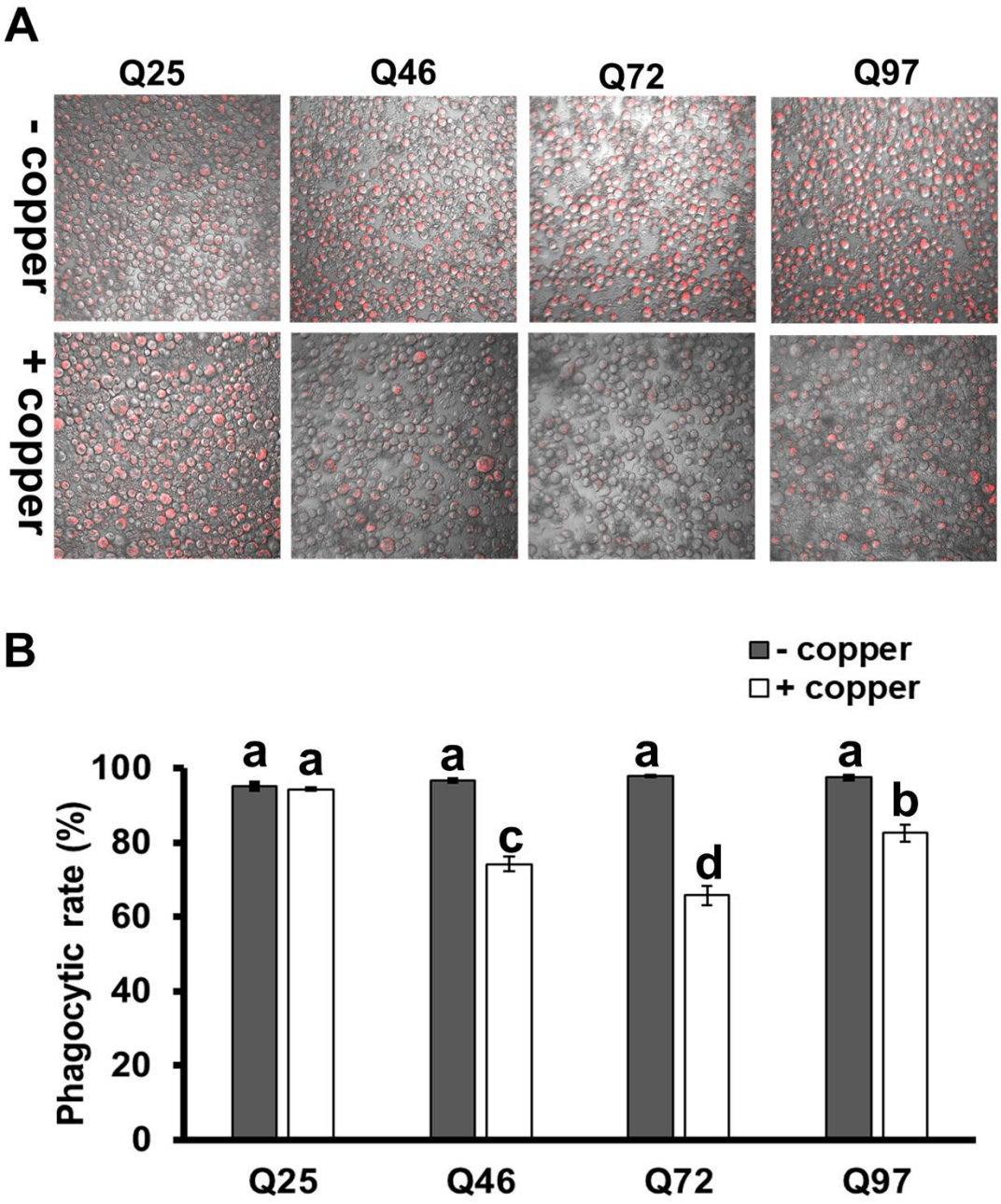

Figure 5. Impairment of phagocytic activities in mHTT-expressing S2 cells. S2 cell lineages expressing wild-type HTT (Q25) and mHTT (Q46, Q72, and Q97) were treated with pHrodo Red *E. coli* for 8 hours. (A) Fluorescence microscope images show the decreased intensity of red fluorescence signals in mHTT-expressing cells. (B) The phagocytic rate was calculated as the percentage of cells showing a red fluorescence signal to the total number of cells in each image. Each treatment was performed in three

independent replicates with (+copper) or without (-copper) $CuSO_4$ induction. Data are presented as average ± SEM. Significances were analyzed by ANOVA with Tukey HSD *post-hoc* test; different letters on the treatment group indicate significant differences at $P < 0.05$.

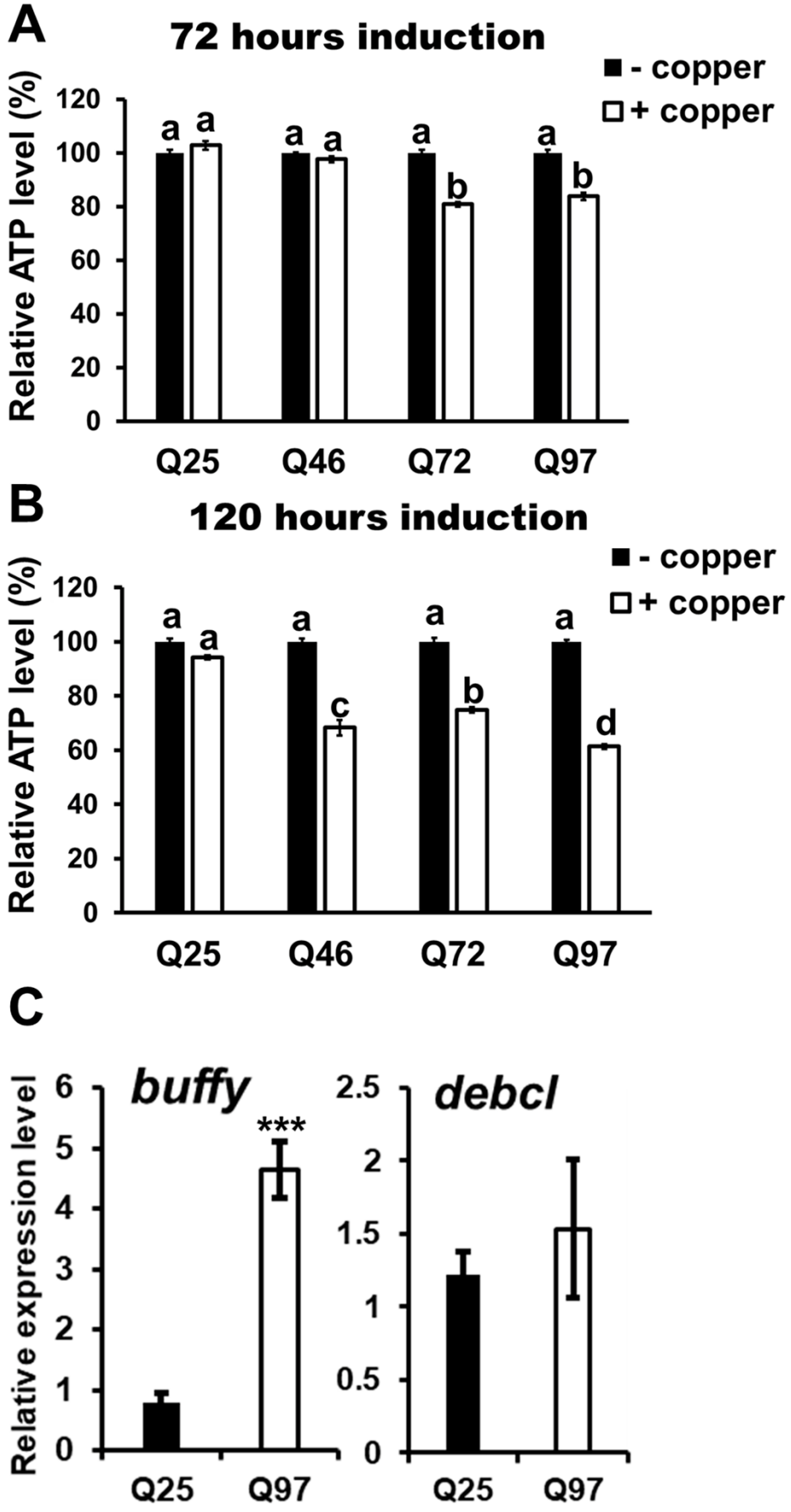
A
72 hours induction
- copper
+ copper
Relative ATP level (%)
120
100
80
60
40
20
0
a a a a a b a b
Q25 Q46 Q72 Q97
B
120 hours induction
- copper
+ copper
Relative ATP level (%)
120
100
80
60
40
20
0
a a a c a b a d
Q25 Q46 Q72 Q97
C
buffy
***
debcl
Relative expression level
6
5
4
3
2
1
0
2.5
2
1.5
1
0.5
0
Q25 Q97
Q25 Q97

Figure 6. Decrease of ATP level and alternation of Bcl-2 protein expression in mHTT-expressing S2 cells. ATP levels of HTT- and mHTT-expressing S2 cells (5×10^4 cells) were measured after 72 (A) and 120 hours (B) of copper induction. Each treatment was performed in five independent replicates with (+copper) or without (-copper) copper induction. Data are presented as average ± SEM. Significances were analyzed by ANOVA with Tukey HSD *post-hoc* test; different letters on the treatment group indicate significant differences at $P < 0.05$. The mRNA levels of *Drosophila* Bcl-2 proteins, *buffy* and *debcl* were measured in Q25 HTT and Q97 mHTT-expressing S2 cells after 120 hours of induction (C). All the expressions were normalized to *rp49* transcript and Q25 control (△△CT). Data are presented as average ± SEM from three independent replicates. *P*-values were determined using Student's t-test, *** $P < 0.001$.

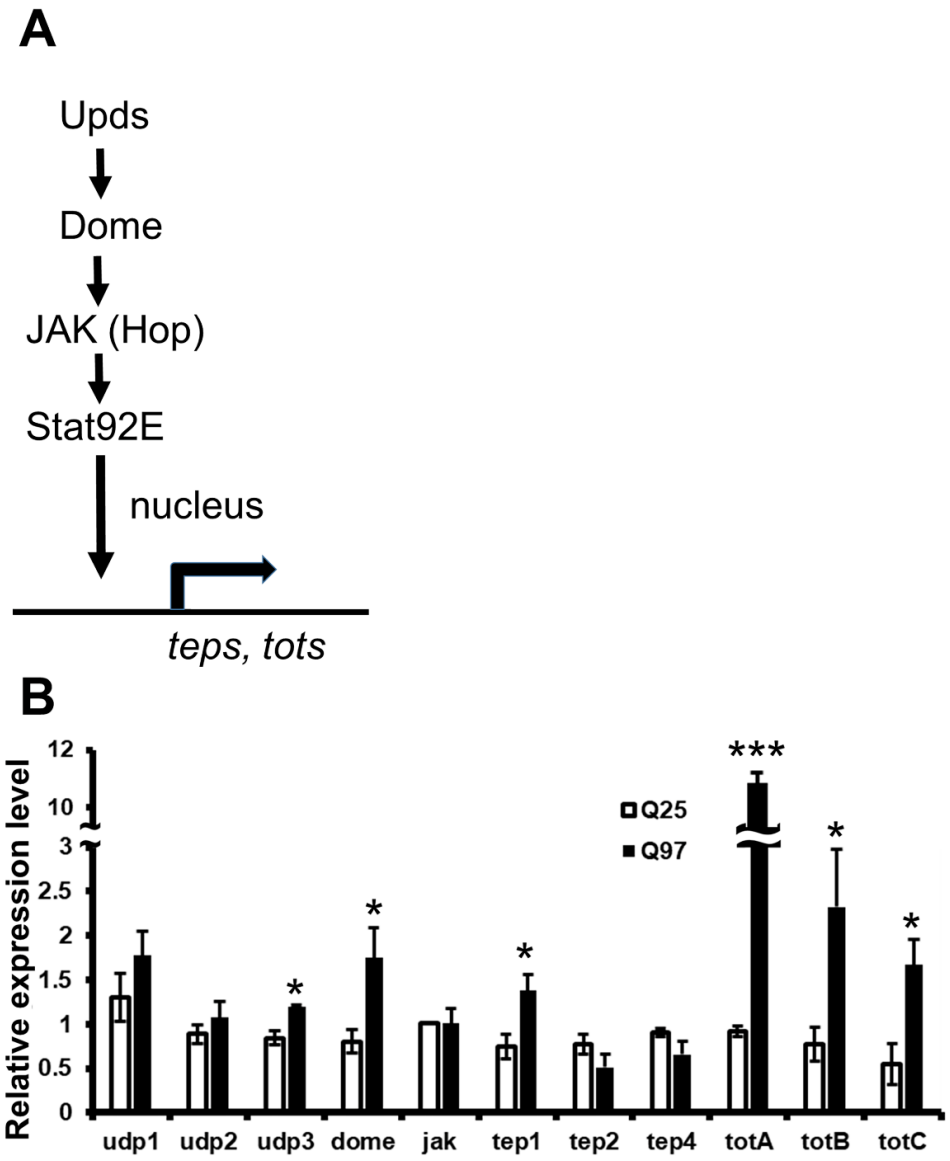

Figure 7. Activation of cytokine expression and JAK/STAT signaling in the mHTT-expressing S2 cells. (A) Schematic representation of the interaction between Upds and JAK/STAT pathway. (B) The gene expression of cytokines (*udp1-3*), *dome*, *jak*(*hop*) and JAK/STAT downstream target genes (*teps* and *tots*) were measured in Q25 HTT and Q97 mHTT-expressing S2 cells after 120 hours of copper induction. All the expressions were normalized to *rp49* expression and Q25 control (△△CT). Data are presented as average ± SEM from three independent replicates. *P*-values using Student's t-test, * $P < 0.05$, *** $P < 0.001$.

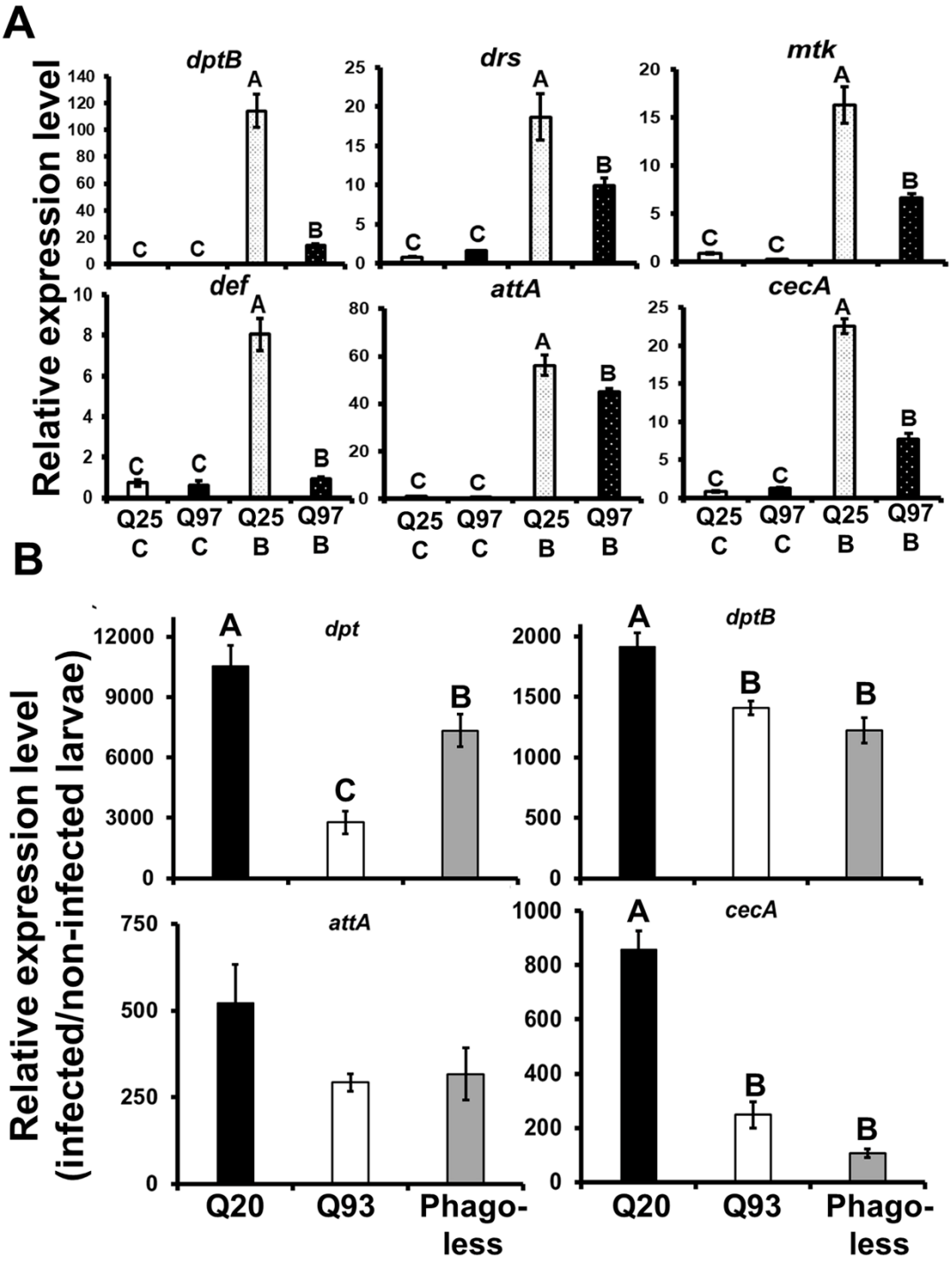

Figure 8. Suppression of antimicrobial peptides (AMPs) induction after bacterial treatment in the mHTT-expressing S2 cells and larvae. (A) Q25 and Q97-expressing S2 cells were incubated with *E. coli* and *M. luteus* (Q25_B and Q97_B) or without bacteria (Q25_C and Q97_C) for 8 hours, and the expression levels of AMPs was measured. The AMPs expressions were normalized to *rp49* expression and Q25 control. (B)

Larvae expressing mHTT Q93 or HTT Q20 under *hml-gal4* hemocyte drivers as well as *Phago*^{less} mutants were infected with ECC15-GFP and their expression of AMPs was determined after 8 hours. The expressions were normalized to *rp49* transcripts and non-infected controls. The AMPs expression levels of non-infected controls for each genotype were set to one. All the data are presented as average ± SEM from three independent replicates. The significances were analyzed by ANOVA with Fisher LSD *post-hoc* test; different letters on the treatment group indicate significant differences at $P < 0.05$.

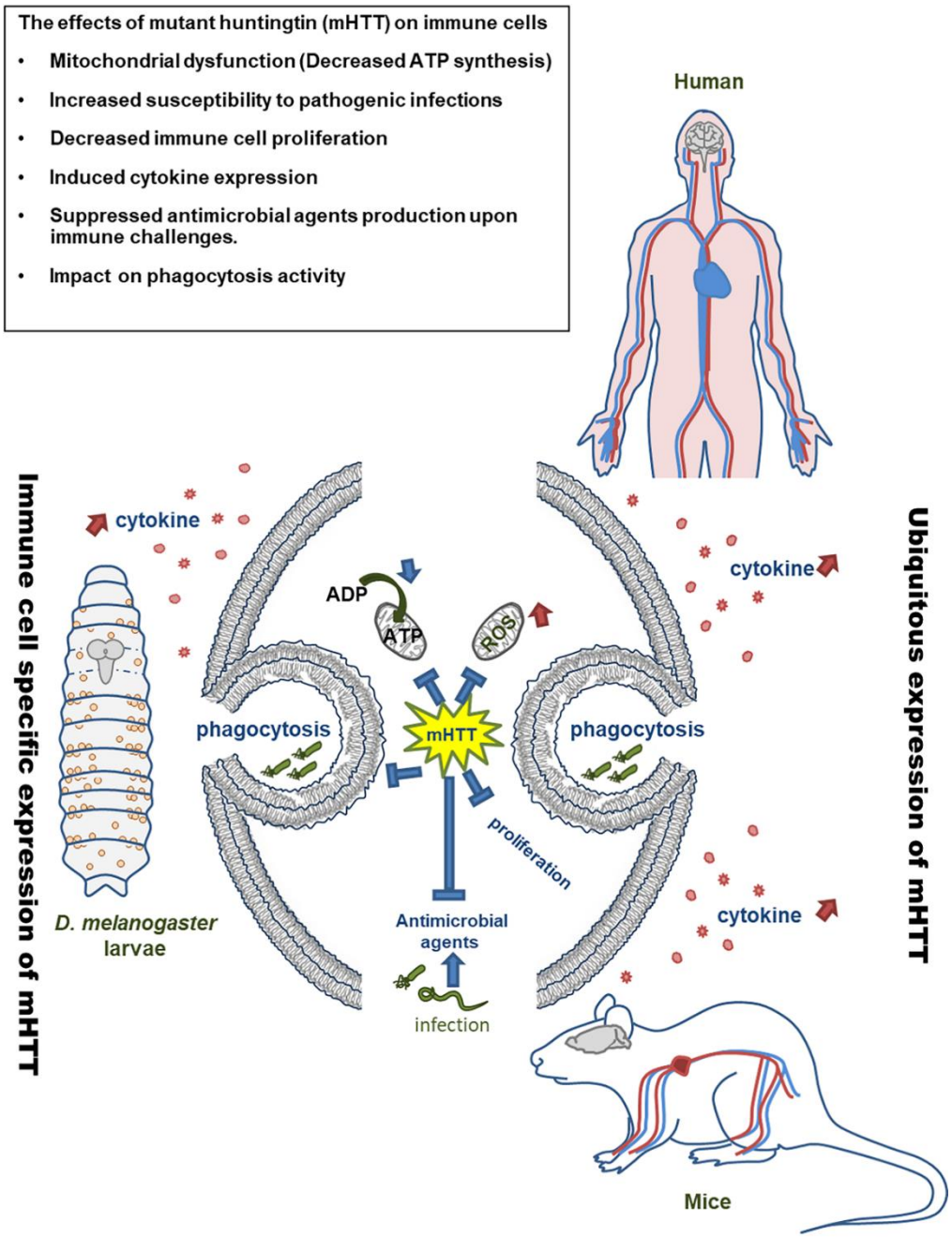

Figure 9. Model of mHTT effects on *Drosophila* and mammalian immune cells. The expression of mHTT in hemocytes of *Drosophila* displays similar effects on the immune cells of HD patients and mice.

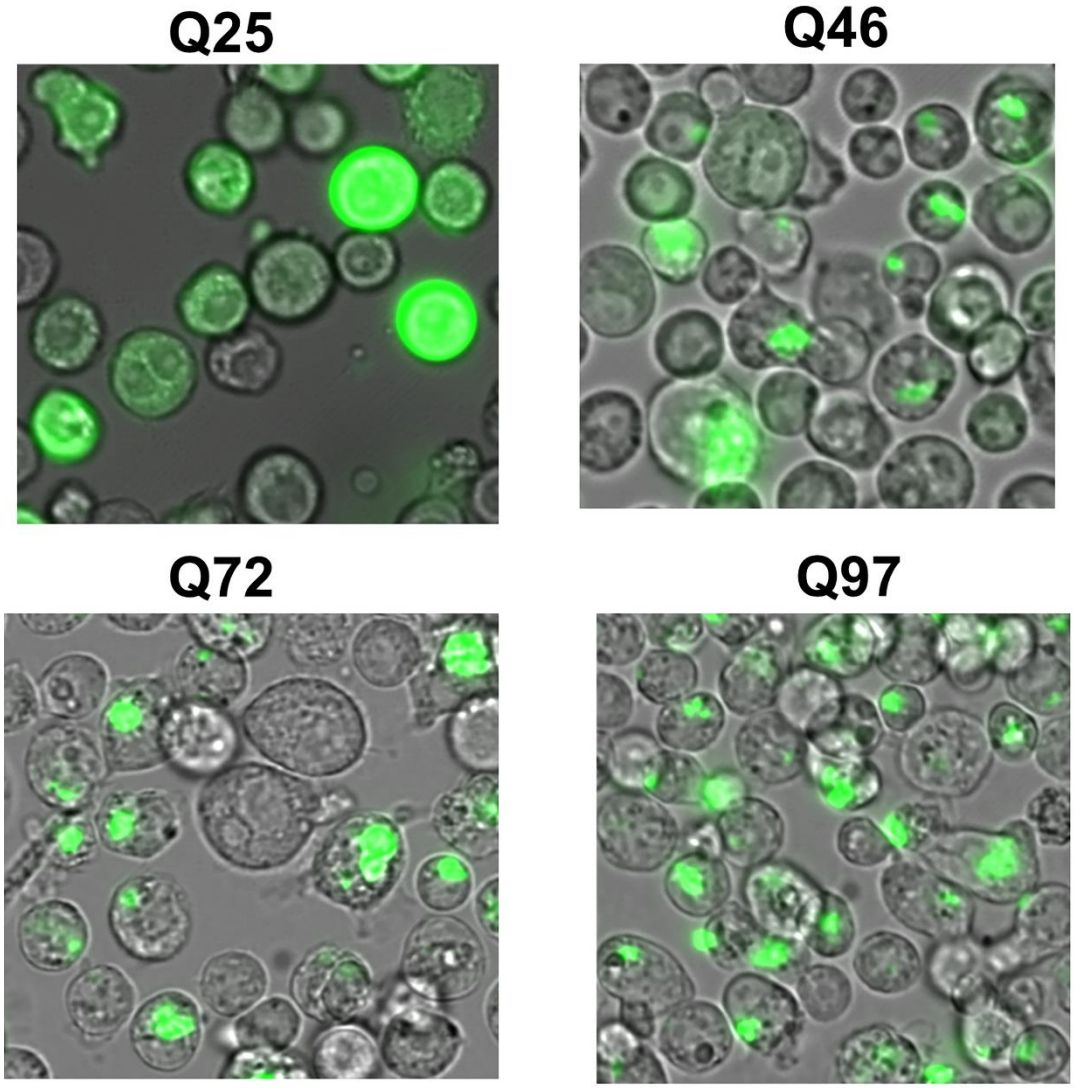

Supplemental Fig. 1. Expression of four different lengths of HTT-GFP fusion proteins under a fluorescence microscope. mHTT-expressing cells (Q46, Q72, and Q97) showed significant mHTT aggregates after copper induction, while there was no aggregate formation in normal HTT-expressing cells (Q25).

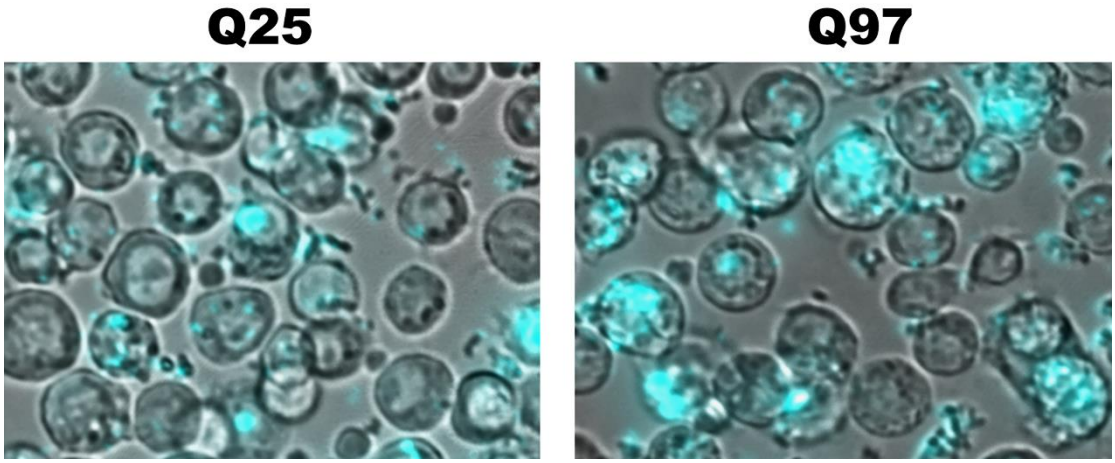

Supplemental Fig. 2. Phagocytosis assay in Q25- and Q97-expressing S2 cells with *E. coli* labeled by DNA-specific dye (Hoechst 33342). Cells expressing mHTT were able to initiate phagocytosis.

genes	left 5'-3'	right 5'-3'
upd1	AATCAGCTGAAGCGCCACG	GGAATTGGGCTTGAGCTTGG
upd2	AAGACTTGGTACCGCCACAT	GGCTCTTCTGCTGATCCTTG
upd3	ATCGCGACCTGCAGATTTAC	TGTACAGCAGGTTGGTCAGG
totA	ATTCTTCAACTGCTCTTATGTGCT	ATCGTCCTGGGCGTTTTT
tep1	GTCCTGCTCGCCCTTCTC	TCAAATGCCAAAACTCTATGTCA
tep2	CGTTCTGCTGGCTTTCTTC	ATACTGGTCGTCCGTCTTGTC
dptB	CTATTCATTGGACTGGCTTGTG	GTCCATTGGGGCTCTGC
drs	CCCTCTTCGCTGTCCTGA	TTAGCATCCTTCGCACCAG
mtk	TGGCCACGGCTACATCA	CCCGGTCTTGGTTGGTTA
def	CGTGGCTATCGCTTTTGCTC	GAGTAGGTCGCATGTGGCTC
attA	TGGTCATGGTGCCTCTTTG	GATTGTGTCTGCCATTGTTGA
cecA	CTTCGTTTTCGTCGCTCTC	TTTTCTTGCCAATTTTCTTCAG
rp49	CTTCATCCGCCACCAGTC	GGCGACGCACTCTGTTGT

Supplemental Tab. 1. List of qPCR primers used in this study.

Materials and methods

Fly stocks

Flies were reared at 25 °C on standard cornmeal medium. The fly strains used were UAS-Q20Httexon1^{111F1L} and UAS-Q93Httexon1^{4F132} obtained from Prof. Lawrence Marsh (UC Irvine, USA) (Steffan et al., 2001), which contain 20 (wild-type) and 93 (mutant HTT) polyglutamine repeats, respectively. The pan-neuronal driver, *elav-gal4*[C155], and hemocyte drivers, *he-gal4* and *hml-gal4*, were obtained from Bloomington *Drosophila* Stock Center and Dr. Tomas Dolezal (University of South Bohemia), respectively (Lin and Goodman, 1994; Sinenko and Mathey-Prevot, 2004; Zettervall et al., 2004). Hemocyte-ablated flies (*phago^{less}*) were used as negative controls and were generated by overexpressing pro-apoptotic proteins (*UAS-rpr*, *-hid*) with *hml-gal4* (Zhou et al., 1997; Charroux and Royet, 2009; Defaye et al., 2009).

Developmental and longevity assay

Thirty first-instar larvae collected from a juice plate were transferred into vials to measure the number of pupae and adults for each replicate. For the longevity assay, about 20 to 30 newly emerged male adults were collected for each replicate and maintained at 29 ℃. Q93 expression driven by pan-neuronal driver, elav-gal4 and *phago^{less}* flies were used as positive controls for longevity assay. Since expression of Q93 driven by elav-gal4 (X chromosome insertion) results in high mortality of male progeny (dosage compensation) (Warrick et al., 1998), female progeny were used for recording the longevity. The number of dead flies was counted every day. All the experiments were performed in at least six independent replicates.

Circulating hemocyte counting

Circulating hemocytes were obtained from larvae by cuticle tearing in Ringer's buffer

with thiourea to prevent melanization (25 µl of buffer per 6 larvae). The number of hemocytes expressing GFP (*hml-gal4* or *he-gal4 > UAS-gfp*) were counted using a hemocytometer. At least five independent replicates were analyzed for each genotype.

Parasitoid wasp infection, eclosion and encapsulation assay

Leptopilina boulardi parasitoid wasps were obtained from Dr. Jan Hrček (Biology Centre CAS) and maintained by infecting wild-type *Drosophila* larvae. For the wasp infection assay, forty larvae (second-instar) were transferred onto a dish containing cornmeal food, and three female wasps were then placed onto the dish and allowed to attack for 72 hours. After infection, 30 infected larvae were collected from the dish and transferred into a vial containing cornmeal for each replicate. Each genotype was tested in at least 10 independent replicates. The total number of eclosed flies and wasps were calculated (Mortimer et al., 2012). For the encapsulation assay, the infected larvae were dissected 72 hours post-infection and the number of larvae containing intact melanized capsules, broken melanized pieces as well as wasp larvae was recorded.

Nematode infection

Two nematode species, *Steinernema carpocapsae* and *Heterorhabditis bacteriophora*, were used in this study, under previously described maintainance conditions (Ibrahim et al., 2018). For the infection assay, nematodes were combined with autoclaved water to achieve a concentration of 25 infective juveniles per 10 µl. Then, 10 µl of nematode suspension was applied to paper and placed in each wells of a 96-well plate. Individual larvae were transferred to each well where they stayed in contact with the nematodes, and the plate was covered with Parafilm. The infection was conducted at 25 °C in the dark. Each experimental replicate consisted of 32 early third-instar larvae (72 hours

after egg hatching), and all experiments were done at least in five replicates. The number of dead larvae were counted after 24 and 48 hours of infection (Arefin et al., 2014; Kucerova et al., 2016).

Bead aggregation assay

The bead aggregation assay was described in our previous study (Kucerova et al., 2016). Briefly, 2.5 µl of hemolymph was collected from six late third-instar larvae, mixed with BSA-blocked bead suspension (tosylactivated Dynabeads M-280, Invitrogen), diluted in *Drosophila* Ringer (pH 6.0) in a well of cavity diagnostic slide (Thermo Scientific) and covered with round cover glass. Pictures were taken with a Nikon SMZ-745T stereomicroscope associated with a CANON EOS 550D. The images were analyzed and quantified with the ImageJ graphics software with the "Analyze Particles" module.

Cell culture

Drosophila Schneider 2 (S2) cells were grown at 25 ℃ in Shields and Sang medium (Sigma) with 0.1% yeast extract, 0.25% peptone, and 10% heat inactivated fetal bovine serum. To generate stable lines expressing polyglutamine repeats, the S2 cells were transfected with four different Httex1-eGFP pMK33 plasmids (Q25, Q46, Q72, and Q97) containing copper-inducible metallothionein promoter (obtained from Dr. Sheng Zhang) (Zhang et al., 2010).

Phagocytosis assay

After induction for 5 days (120 hours) with 1 mM copper ($CuSO_4$; Sigma), 100 µl of cell suspension (1×10^6 cells/ml) was transferred to each well of a 96-well plate. Then, 100 µl of pHrodo Red *E. coli* (1 mg/ml; Thermo Fisher Scientific) was applied to each

well for phagocytosis testing. After 8 hours of treatment, the supernatant was removed, the cells were washed two times with 1× PBS, and 100 µl of fresh medium was applied. Cells were observed and photographed with a confocal microscope. From the images, the total number of cells and the number of cells displaying red fluorescence were counted. Three experimental repeats for each treatment were done for statistical analysis.

ATP measurement

Cells were treated with 1 mM copper for 3 days (72 hours) and 5 days (120 hours) to induce mHTT expression. 50 µl of a 1×10^6 cells/ml solution (5×10^4 cells) was transferred to each well of a 96-well plate. After removing the supernatant, 60 µl of CellTiter-Glo solution (Promega) was applied to each well for 10 minutes. Then, 50 µl of the mixture was transferred to each well of 96-well white plates and the intensity of luminescence was then measured. Five independent replicates for each treatment were performed for analysis.

Bacterial infection *in vitro* and *in vivo*

5 ml of S2 cells (1×10^6 cells/ml) carrying copper-inducible Q25 HTT or Q97 mHTT transgenes were incubated in media containing 1 mM $CuSO_4$ for 120 hours in 60 mm tissue culture plates. After the induction, the cells were treated for 8 hours with 1 ml of bacterial mixture containing *Escherichia coli* and *Micrococcus luteus* at an optical density (600 nm) of 1 ($OD_{600} = 1$) (Lemaitre and Hoffmann, 2007). The cells were then harvested for RNA extraction.

For the *in vivo* infection, late third instar larvae (96 hours after egg hatching) were

collected and transferred into a vial with 0.5 g instant *Drosophila* medium (Formula 4-24, Carolina Biological Supply, Burlington, NC) supplemented with 200 µl of bacterial suspension (OD_{600}= 50) *Erwinia carotovora carotovora 15*-GFP (ECC15-GFP) and 1300 µl of distilled water. The larvae were collected for RNA extraction eight hours after the infection (Basset et al., 2000; Charroux and Royet, 2009).

RNA extraction

For *in vitro* experiments, S2 cells were washed with 1× PBS three times and harvested with 800 µl of RiboZol (VWR). Samples were preserved at -80 °C until RNA purification. For *in vivo* experiments, ten larvae were washed by distilled water and homogenized by the pestle motor (Kimble) in 200 µl of RiboZol (VWR Life Science, Radnor, PA). The sample were then preserved at -80°C for further RNA purification. RNA was isolated using NucleoSpin RNA columns (Macherey-Nagel) following the manufacturer's instructions and cDNA was synthesized from 2 µg of total RNA using a RevertAid H Minus First Strand cDNA Synthesis Kit (Thermo Fisher Scientific).

qPCR and primers

5× HOT FIREPol® EvaGreen® qPCR Mix Plus with ROX (Solis Biodyne) and an Eco Real-Time PCR System (Illumina®) were used for qPCR. The cDNA was diluted 50 times before use. Each reaction contained 4 µl of EvaGreen qPCR mix, 0.5 µl of forward and reverse primer (10 µM), 5 µl of diluted cDNA and ddH2O to adjust the total volume to 20 µl. The list of primers is shown in supplementary table 1. The expression level was calculated by using the (2-ΔΔCt) method. The ct value of target genes were normalized to reference gene, ribosomal protein 49 (*rp49*).

Statistical analysis

Error bars show standard error of the mean throughout this paper. Significance was established using Student's t-test (N.S.: not significant, * $P < 0.05$, ** $P < 0.01$, *** $P < 0.001$) or one- way ANOVA analysis with Fisher LSD or Tukey HSD *post-hoc* test. The Mann-Whitney U test was used for examing the significance of the data on wasp larval hatching and the host encapsulation activites (Fig. 4C-F). For the statistical analysis of longevity curve, we used online tool OASIS 2 to perform the weighted log-rank test for determining significance (Han et al., 2016).

Acknowledgements

We thank Dr. Sheng Zhang (UThealth) for the Httex1-eGFP pMK33 plasmids, Prof L. Marsh (UC Irvine, USA) for Q20 and Q93 flies, Dr. Tomas Dolezal (University of South Bohemia) for the hemocyte driver line, Dr. Pavel Hyrsl, Pavel Dobes (Masaryk University) for the nematodes, and Dr. Hrcek Jan, Dr. Chia-Hua Lue (Biology Centre CAS) and Dr. Adam Bajgar (University of South Bohemia) for the parasitoid wasps, Dr. Julien Royet (IBDM, Frence) for bacteria ECC-15. This work was supported by the grant agency of the University of South Bohemia (065/2017 / P to YHL), junior grant project GACR (19-13784Y to LK). MZ is a member of the COST action "Maximizing impact of research in neurodevelopmental disorders" (CA16210).

References

Anderl, I., Vesala, L., Ihalainen, T.O., Vanha-Aho, L.M., Ando, I., Ramet, M., et al. (2016). Transdifferentiation and Proliferation in Two Distinct Hemocyte Lineages in Drosophila melanogaster Larvae after Wasp Infection. PLoS Pathog 12(7), e1005746. doi: 10.1371/journal.ppat.1005746.

Anderson, A.N., Roncaroli, F., Hodges, A., Deprez, M., and Turkheimer, F.E. (2008). Chromosomal profiles of gene expression in Huntington's disease. Brain 131(Pt 2), 381-388. doi: 10.1093/brain/awm312.

Andre, R., Carty, L., and Tabrizi, S.J. (2016). Disruption of immune cell function by mutant huntingtin in Huntington's disease pathogenesis. Curr Opin Pharmacol 26, 33-38. doi: 10.1016/j.coph.2015.09.008.

Arefin, B., Kucerova, L., Dobes, P., Markus, R., Strnad, H., Wang, Z., et al. (2014). Genome-wide transcriptional analysis of Drosophila larvae infected by entomopathogenic nematodes shows involvement of complement, recognition and extracellular matrix proteins. J Innate Immun 6(2), 192-204. doi: 10.1159/000353734.

Basset, A., Khush, R.S., Braun, A., Gardan, L., Boccard, F., Hoffmann, J.A., et al. (2000). The phytopathogenic bacteria Erwinia carotovora infects Drosophila and activates an immune response. Proc Natl Acad Sci U S A 97(7), 3376-3381. doi: 10.1073/pnas.070357597.

Besson, M.T., Dupont, P., Fridell, Y.W., and Lievens, J.C. (2010). Increased energy metabolism rescues glia-induced pathology in a Drosophila model of Huntington's disease. Hum Mol Genet 19(17), 3372-3382. doi: 10.1093/hmg/ddq249.

Bjorkqvist, M., Wild, E.J., Thiele, J., Silvestroni, A., Andre, R., Lahiri, N., et al. (2008). A novel pathogenic pathway of immune activation detectable before clinical onset in Huntington's disease. J Exp Med 205(8), 1869-1877. doi: 10.1084/jem.20080178.

Bouchard, J., Truong, J., Bouchard, K., Dunkelberger, D., Desrayaud, S., Moussaoui, S., et al. (2012). Cannabinoid receptor 2 signaling in peripheral immune cells modulates disease onset and severity in mouse models of Huntington's disease. J Neurosci 32(50), 18259-18268. doi: 10.1523/JNEUROSCI.4008-12.2012.

Castillo, J.C., Shokal, U., and Eleftherianos, I. (2013). Immune gene transcription in Drosophila adult flies infected by entomopathogenic nematodes and their mutualistic bacteria. J Insect Physiol 59(2), 179-185. doi: 10.1016/j.jinsphys.2012.08.003.

Charroux, B., and Royet, J. (2009). Elimination of plasmatocytes by targeted apoptosis reveals their role in multiple aspects of the Drosophila immune response. Proc Natl Acad Sci U S A 106(24), 9797-9802. doi: 10.1073/pnas.0903971106.

Chen, C.M., Wu, Y.R., Cheng, M.L., Liu, J.L., Lee, Y.M., Lee, P.W., et al. (2007). Increased oxidative damage and mitochondrial abnormalities in the peripheral blood of Huntington's disease patients. Biochem Biophys Res Commun 359(2), 335-340. doi: 10.1016/j.bbrc.2007.05.093.

Chougnet, C.A., Thacker, R.I., Shehata, H.M., Hennies, C.M., Lehn, M.A., Lages, C.S., et al. (2015). Loss of Phagocytic and Antigen Cross-Presenting Capacity in Aging Dendritic Cells Is Associated with Mitochondrial Dysfunction. J Immunol 195(6), 2624-2632. doi: 10.4049/jimmunol.1501006.

Defaye, A., Evans, I., Crozatier, M., Wood, W., Lemaitre, B., and Leulier, F. (2009). Genetic ablation of Drosophila phagocytes reveals their contribution to both development and resistance to bacterial infection. J Innate Immun 1(4), 322-334. doi: 10.1159/000210264.

Dobes, P., Wang, Z., Markus, R., Theopold, U., and Hyrsl, P. (2012). An improved method for nematode infection assays in Drosophila larvae. Fly (Austin) 6(2), 75-79. doi: 10.4161/fly.19553.

Donley, D.W., Olson, A.R., Raisbeck, M.F., Fox, J.H., and Gigley, J.P. (2016). Huntingtons Disease Mice

Infected with Toxoplasma gondii Demonstrate Early Kynurenine Pathway Activation, Altered CD8+ T-Cell Responses, and Premature Mortality. PLoS One 11(9), e0162404. doi: 10.1371/journal.pone.0162404.

Ehinger, J.K., Morota, S., Hansson, M.J., Paul, G., and Elmer, E. (2016). Mitochondrial Respiratory Function in Peripheral Blood Cells from Huntington's Disease Patients. Mov Disord Clin Pract 3(5), 472-482. doi: 10.1002/mdc3.12308.

Fauvarque, M.O., and Williams, M.J. (2011). Drosophila cellular immunity: a story of migration and adhesion. J Cell Sci 124(Pt 9), 1373-1382. doi: 10.1242/jcs.064592.

Geng, J., Sun, X., Wang, P., Zhang, S., Wang, X., Wu, H., et al. (2015). Kinases Mst1 and Mst2 positively regulate phagocytic induction of reactive oxygen species and bactericidal activity. Nat Immunol 16(11), 1142-1152. doi: 10.1038/ni.3268.

Han, S.K., Lee, D., Lee, H., Kim, D., Son, H.G., Yang, J.S., et al. (2016). OASIS 2: online application for survival analysis 2 with features for the analysis of maximal lifespan and healthspan in aging research. Oncotarget 7(35), 56147-56152. doi: 10.18632/oncotarget.11269.

Ibrahim, E., Dobes, P., Kunc, M., Hyrsl, P., and Kodrik, D. (2018). Adipokinetic hormone and adenosine interfere with nematobacterial infection and locomotion in Drosophila melanogaster. J Insect Physiol 107, 167-174. doi: 10.1016/j.jinsphys.2018.04.002.

Keebaugh, E.S., and Schlenke, T.A. (2014). Insights from natural host-parasite interactions: the Drosophila model. Dev Comp Immunol 42(1), 111-123. doi: 10.1016/j.dci.2013.06.001.

Kucerova, L., Broz, V., Arefin, B., Maaroufi, H.O., Hurychova, J., Strnad, H., et al. (2016). The Drosophila Chitinase-Like Protein IDGF3 Is Involved in Protection against Nematodes and in Wound Healing. J Innate Immun 8(2), 199-210. doi: 10.1159/000442351.

Kwan, W., Trager, U., Davalos, D., Chou, A., Bouchard, J., Andre, R., et al. (2012). Mutant huntingtin impairs immune cell migration in Huntington disease. J Clin Invest 122(12), 4737-4747. doi: 10.1172/JCI64484.

Leblhuber, F., Walli, J., Jellinger, K., Tilz, G.P., Widner, B., Laccone, F., et al. (1998). Activated immune system in patients with Huntington's disease. Clin Chem Lab Med 36(10), 747-750. doi: 10.1515/CCLM.1998.132.

Lemaitre, B., and Hoffmann, J. (2007). The host defense of Drosophila melanogaster. Annu Rev Immunol 25, 697-743. doi: 10.1146/annurev.immunol.25.022106.141615.

Lesch, C., Goto, A., Lindgren, M., Bidla, G., Dushay, M.S., and Theopold, U. (2007). A role for Hemolectin in coagulation and immunity in Drosophila melanogaster. Dev Comp Immunol 31(12), 1255-1263. doi: 10.1016/j.dci.2007.03.012.

Li, X.J., Orr, A.L., and Li, S. (2010). Impaired mitochondrial trafficking in Huntington's disease. Biochim Biophys Acta 1802(1), 62-65. doi: 10.1016/j.bbadis.2009.06.008.

Lin, D.M., and Goodman, C.S. (1994). Ectopic and increased expression of Fasciclin II alters motoneuron growth cone guidance. Neuron 13(3), 507-523.

Marsh, J.L., Walker, H., Theisen, H., Zhu, Y.Z., Fielder, T., Purcell, J., et al. (2000). Expanded

polyglutamine peptides alone are intrinsically cytotoxic and cause neurodegeneration in Drosophila. Hum Mol Genet 9(1), 13-25.

Melkani, G.C., Trujillo, A.S., Ramos, R., Bodmer, R., Bernstein, S.I., and Ocorr, K. (2013). Huntington's disease induced cardiac amyloidosis is reversed by modulating protein folding and oxidative stress pathways in the Drosophila heart. PLoS Genet 9(12), e1004024. doi: 10.1371/journal.pgen.1004024.

Monserrate, J.P., Chen, M.Y., and Brachmann, C.B. (2012). Drosophila larvae lacking the bcl-2 gene, buffy, are sensitive to nutrient stress, maintain increased basal target of rapamycin (Tor) signaling and exhibit characteristics of altered basal energy metabolism. BMC Biol 10, 63. doi: 10.1186/1741-7007-10-63.

Morin-Poulard, I., Vincent, A., and Crozatier, M. (2013). The Drosophila JAK-STAT pathway in blood cell formation and immunity. JAKSTAT 2(3), e25700. doi: 10.4161/jkst.25700.

Mortimer, N.T., Kacsoh, B.Z., Keebaugh, E.S., and Schlenke, T.A. (2012). Mgat1-dependent N-glycosylation of membrane components primes Drosophila melanogaster blood cells for the cellular encapsulation response. PLoS Pathog 8(7), e1002819. doi: 10.1371/journal.ppat.1002819.

Quinn, L., Coombe, M., Mills, K., Daish, T., Colussi, P., Kumar, S., et al. (2003). Buffy, a Drosophila Bcl-2 protein, has anti-apoptotic and cell cycle inhibitory functions. EMBO J 22(14), 3568-3579. doi: 10.1093/emboj/cdg355.

Ramet, M., Manfruelli, P., Pearson, A., Mathey-Prevot, B., and Ezekowitz, R.A. (2002). Functional genomic analysis of phagocytosis and identification of a Drosophila receptor for E. coli. Nature 416(6881), 644-648. doi: 10.1038/nature735.

Sassone, J., Colciago, C., Cislaghi, G., Silani, V., and Ciammola, A. (2009). Huntington's disease: the current state of research with peripheral tissues. Exp Neurol 219(2), 385-397. doi: 10.1016/j.expneurol.2009.05.012.

Sassone, J., Maraschi, A., Sassone, F., Silani, V., and Ciammola, A. (2013). Defining the role of the Bcl-2 family proteins in Huntington's disease. Cell Death Dis 4, e772. doi: 10.1038/cddis.2013.300.

Sathasivam, K., Hobbs, C., Turmaine, M., Mangiarini, L., Mahal, A., Bertaux, F., et al. (1999). Formation of polyglutamine inclusions in non-CNS tissue. Hum Mol Genet 8(5), 813-822.

Sawa, A., Wiegand, G.W., Cooper, J., Margolis, R.L., Sharp, A.H., Lawler, J.F., Jr., et al. (1999). Increased apoptosis of Huntington disease lymphoblasts associated with repeat length-dependent mitochondrial depolarization. Nat Med 5(10), 1194-1198. doi: 10.1038/13518.

Sinenko, S.A., and Mathey-Prevot, B. (2004). Increased expression of Drosophila tetraspanin, Tsp68C, suppresses the abnormal proliferation of ytr-deficient and Ras/Raf-activated hemocytes. Oncogene 23(56), 9120-9128. doi: 10.1038/sj.onc.1208156.

Small, C., Paddibhatla, I., Rajwani, R., and Govind, S. (2012). An introduction to parasitic wasps of Drosophila and the antiparasite immune response. J Vis Exp (63), e3347. doi: 10.3791/3347.

Song, W., Smith, M.R., Syed, A., Lukacsovich, T., Barbaro, B.A., Purcell, J., et al. (2013). Morphometric analysis of Huntington's disease neurodegeneration in Drosophila. Methods Mol Biol 1017, 41-57.

doi: 10.1007/978-1-62703-438-8_3.

Steffan, J.S., Agrawal, N., Pallos, J., Rockabrand, E., Trotman, L.C., Slepko, N., et al. (2004). SUMO modification of Huntingtin and Huntington's disease pathology. Science 304(5667), 100-104. doi: 10.1126/science.1092194.

Steffan, J.S., Bodai, L., Pallos, J., Poelman, M., McCampbell, A., Apostol, B.L., et al. (2001). Histone deacetylase inhibitors arrest polyglutamine-dependent neurodegeneration in Drosophila. Nature 413(6857), 739-743. doi: 10.1038/35099568.

Swanson, J.A. (2008). Shaping cups into phagosomes and macropinosomes. Nat Rev Mol Cell Biol 9(8), 639-649. doi: 10.1038/nrm2447.

Tamura, T., Sone, M., Yamashita, M., Wanker, E.E., and Okazawa, H. (2009). Glial cell lineage expression of mutant ataxin-1 and huntingtin induces developmental and late-onset neuronal pathologies in Drosophila models. PLoS One 4(1), e4262. doi: 10.1371/journal.pone.0004262.

Taylor, J.P., Taye, A.A., Campbell, C., Kazemi-Esfarjani, P., Fischbeck, K.H., and Min, K.T. (2003). Aberrant histone acetylation, altered transcription, and retinal degeneration in a Drosophila model of polyglutamine disease are rescued by CREB-binding protein. Genes Dev 17(12), 1463-1468. doi: 10.1101/gad.1087503.

Trager, U., Andre, R., Lahiri, N., Magnusson-Lind, A., Weiss, A., Grueninger, S., et al. (2014). HTT-lowering reverses Huntington's disease immune dysfunction caused by NFkappaB pathway dysregulation. Brain 137(Pt 3), 819-833. doi: 10.1093/brain/awt355.

Trager, U., Andre, R., Magnusson-Lind, A., Miller, J.R., Connolly, C., Weiss, A., et al. (2015). Characterisation of immune cell function in fragment and full-length Huntington's disease mouse models. Neurobiol Dis 73, 388-398. doi: 10.1016/j.nbd.2014.10.012.

Vonsattel, J.P., and DiFiglia, M. (1998). Huntington disease. J Neuropathol Exp Neurol 57(5), 369-384.

Wang, G. (2014). Human antimicrobial peptides and proteins. Pharmaceuticals (Basel) 7(5), 545-594. doi: 10.3390/ph7050545.

Warrick, J.M., Chan, H.Y., Gray-Board, G.L., Chai, Y., Paulson, H.L., and Bonini, N.M. (1999). Suppression of polyglutamine-mediated neurodegeneration in Drosophila by the molecular chaperone HSP70. Nat Genet 23(4), 425-428. doi: 10.1038/70532.

Warrick, J.M., Paulson, H.L., Gray-Board, G.L., Bui, Q.T., Fischbeck, K.H., Pittman, R.N., et al. (1998). Expanded polyglutamine protein forms nuclear inclusions and causes neural degeneration in Drosophila. Cell 93(6), 939-949.

Weiss, K.R., Kimura, Y., Lee, W.C., and Littleton, J.T. (2012). Huntingtin aggregation kinetics and their pathological role in a Drosophila Huntington's disease model. Genetics 190(2), 581-600. doi: 10.1534/genetics.111.133710.

West, A.P., Brodsky, I.E., Rahner, C., Woo, D.K., Erdjument-Bromage, H., Tempst, P., et al. (2011). TLR signalling augments macrophage bactericidal activity through mitochondrial ROS. Nature 472(7344), 476-480. doi: 10.1038/nature09973.

Wild, E., Magnusson, A., Lahiri, N., Krus, U., Orth, M., Tabrizi, S.J., et al. (2011). Abnormal peripheral

chemokine profile in Huntington's disease. PLoS Curr 3, Rrn1231. doi: 10.1371/currents.RRN1231.

Zettervall, C.J., Anderl, I., Williams, M.J., Palmer, R., Kurucz, E., Ando, I., et al. (2004). A directed screen for genes involved in Drosophila blood cell activation. Proc Natl Acad Sci U S A 101(39), 14192-14197. doi: 10.1073/pnas.0403789101.

Zhang, S., Binari, R., Zhou, R., and Perrimon, N. (2010). A genomewide RNA interference screen for modifiers of aggregates formation by mutant Huntingtin in Drosophila. Genetics 184(4), 1165-1179. doi: 10.1534/genetics.109.112516.

Zhou, L., Schnitzler, A., Agapite, J., Schwartz, L.M., Steller, H., and Nambu, J.R. (1997). Cooperative functions of the reaper and head involution defective genes in the programmed cell death of Drosophila central nervous system midline cells. Proc Natl Acad Sci U S A 94(10), 5131-5136.

Zwilling, D., Huang, S.Y., Sathyasaikumar, K.V., Notarangelo, F.M., Guidetti, P., Wu, H.Q., et al. (2011). Kynurenine 3-monooxygenase inhibition in blood ameliorates neurodegeneration. Cell 145(6), 863-874. doi: 10.1016/j.cell.2011.05.020.

8. Curriculum Vitae

Yu-Hsien Lin

Laboratory of Molecular Genetics, Institute of Entomology, Biology Centre, Czech Academic of Science
Faculty of Science, University of South Bohemia, Czechia
Phone: +420-774803150 (Czech Republic)
e-Mail: r99632012@gmail.com
Nationality: Taiwan

Education

- *Doctor, Sep 2014 – Now*

Animal Physiology program, Department of Zoology, Faculty of Science, University of South Bohemia & Institute of Entomology, Biology Center, Czech Academy of Sciences (CAS)

- *Master, Sep 2010 – Aug 2012*

Department of Entomology, College of Bioresources and Agriculture, National Taiwan University, Taiwan

- *Bachelor, Sep 2006 – July 2010*

Department of Life Science (present name: Department of Biological Science and Technology), College of Agriculture, National Pingtung University of Science and Technology, Taiwan

Research Experience

- *Doctor project, Sep 2014 – Now*

Laboratory of Molecular Genetics, Institute of Entomology, Biology Center, CAS (supervisor: Prof. Michal Zurovec)

Czech Lab Projects:

1. The regulation of adenosine signaling in Huntington's disease using *Drosophila* model
2. Function characterization of adenosine deaminase-like protein by CRISPR/Cas9 mutagenesis
3. Insect silk and glue proteomic study

Collaborative project:

1. Studying the mechanisms of insect antivirus responses regulated by adenosine signaling (International cooperation with Dr. Yueh-Lung Wu, Department of Entomology, National Taiwan University)

- *Research assistant, Aug 2013 – Sep 2014*

Department of Entomology, National Taiwan University. (supervisor: Dr. How-Jing Lee)

1. Architecture of ancestral insect clock – combination of mammalian and *Drosophila* genetic components **(**International cooperation project with Dr. David Doležel lab, Institute of Entomology, Biology Centre ASCR, Czech Republic. Supporting by NSC, Taiwan)
2. Insect pest control with RNAi (International cooperation project with Prof. Xavier Bellés lab, CSIC, Spain, Supporting by NSC, Taiwan)

- *Master project, Sep 2010 – Aug 2012*

Glutathione S-Transferase underlying the rhythmic resistance against permethrin in the German cockroach (*Blattella germanica*) (supervisor: Dr. How-Jing Lee)

- *Undergraduate intern, Sep 2008 – July 2009*

Undergraduate internship at Ecology and Evolution laboratory (supervisor: Dr. Ming-Lin Tsai)

Studying in comparative physiology of Osmotic regulation between sea water and fresh water crabs

Publications

Chang Y, Tang CK, **Lin YH**, Tsai CH, Lu YH, Wu YL. 2020. *Snellenius manilae* bracovirus suppresses the host immune system by regulating extracellular adenosine levels in *Spodoptera litura*. Scientific Report. (Accepted)

Lin YH, Maaroufi HO, Ibrahim E, Kucerova L, Zurovec M. 2019. Expression of human mutant Huntingtin protein in Drosophila hemocytes impairs immune responses. Frontiers in Immunology. DOI: 10.3389/fimmu.2019.02405

Wu PC, **Lin YH**, Wu TC, Lee ST, Wu CP, Chang Y, Wu YL. 2018. MicroRNAs derived from the insect virus HzNV-1 promote lytic infection by suppressing histone methylation. Scientific Reports. DOI: 10.1038/s41598-018-35782-w

Huang JH, Liu Y, **Lin YH**, Belles X and Lee HJ. 2018. Practical Use of RNA Interference: Oral Delivery of Double-Stranded RNA in Liposome Carriers for Cockroaches. Journal of Visualized Experiments. DOI: 10.3791/57385

Lin YH, Huang JH, Liu Y, Belles X, Lee HJ. 2017. Oral delivery of dsRNA lipoplexes to German cockroach protects dsRNA from degradation and induces RNAi response. Pest Management Science. DOI: 10.1002/ps.4407

Lin YH, Lee CM, Huang JH, Lee HJ. 2014. Circadian regulation of permethrin susceptibility by Glutathione S-Transferase (BgGSTD1) in the German cockroach (*Blattella germanica*). Journal of Insect Physiology. DOI: 10.1016/j.jinsphys.2014.05.001

Conference Presentation

- **Oral presentation**

Lin YH, Maaroufi HO, Ibrahim E, Zurovec M: Expression of human mutant Huntingtin protein (mHTT) in Drosophila hemocytes impairs immune responses, Eighth

International Symposium on Molecular Insect Science, Sitges, Spain, 07/2019.

Lin YH, Zurovec M: Immune dysfunction caused by the expression of polyglutamine expansion in hemocytes of *Drosophila melanogaster*, 39th Annual Meeting of Taiwan Entomological Society, Tainan, Taiwan, 10/2018

Lin YH, Filip T, Zurovec M: *Functional study of two adenosine metabolic genes, adgf-d and ada, in Drosophila melanogaster*. XXV International Congress of Entomology, Orlando, USA; 09/2016

Lin YH, Filip T, Zurovec M: *The effect of adenosine/ adenosine receptor signaling on Drosophila larval development*. 5th International Symposium on Insect Physiology, Biochemistry and Molecular Biology, Guangzhou, China; 06/2015

Lin YH, Zurovec M: *Regulation of larval development by extracellular adenosine*. Molecular Method in Insect Physiology, Ceske Budejovice, Czech Republic; 06/2015

Lin YH, Lee HJ: *Rhythmic regulation of the insecticide susceptibility by glutathione S-transferase in the German cockroach (Blattella germanica)*. Congress of Animal Behavior & Ecology, Taichung, Taiwan; 01/2014

- **Poster presentation**

Lin YH, Zurovec M: *Functional characterization of Drosophila adenosine deaminase-like protein (ADAL) in embryogenesis*. 25th European Drosophila Research Conference, London, UK; 09/2017

Lin YH, Huang JH, Liu Y, Belles X, Lee HJ: *Oral delivery of dsRNA lipoplexes to German cockroach, Blattella germanica, protects dsRNA from degradation*. XXV International Congress of Entomology, Orlando, USA; 09/2016

Lin YH, Filip T, Broz V, Zurovec M: *Adenosine, a growth regulator of Drosophila*

melanogaster. 24th European Drosophila Research Conference, Heidelberg, Germany; 09/2015

Huang JH, **Lin YH**, Liu Y, Lee HJ: *Molecular characterization of the circadian clock genes, timeless and cryptochromes, in the German cockroach Blattella germanica*. Seventh International Symposium on Molecular Insect Science, Amsterdam, Netherlands; 07/2014

Lin YH, Huang JH, Liu Y, Lee HJ: *GST underlying the rhythmic resistance against permethrin in the German cockroach (Blattella germanica)*. XXIV International Congress of Entomology, Daegu, Korea; 08/2012

Awards

- Award for the Best PhD Student Publications in 2019, Institute of Entomology, Biology Centre CAS, Jan 2020
- First Place Winner of oral presentation competition, doctoral conference in Department of Zoology, Faculty of Science, University of South Bohemia, May 2018
- Award of oral presentation competition, 39th Annual Meeting of Taiwan Entomological Society, Tainan, Taiwan, Oct 2018
- First Place Winner of oral presentation competition, doctoral conference in Department of Zoology, Faculty of Science, University of South Bohemia, 2017
- Student Travel Award in the 5th International Symposium of Insect Physiology, Biochemistry and Molecular Biology, Guangzhou, China, Jun 2015
- The award of academic research thesis in master, National Taiwan University, Jun 2014
- First Place Winner of Oral Presentation Competition, Congress of Animal

Behavior & Ecology, Taichung, Taiwan, Jan 2014

- Excellent Teaching Assistant Award, Center for Teaching and Learning Development, National Taiwan University, Mar 2012

Approved Grants and Fellowships application

- Travel grant from IBERA Grant program of the Biology Centre CAS, 2020
- Erasmus+ traineeship fellowship, 2019
- Mobility grant from Bavarian-Czech Academic Agency, 2019
- Travel grant from IBERA Grant program of the Biology Centre CAS, 2019
- Proposals for cooperation activity with leading research institutions in Taiwan in 2018, supporting by Czech Academic of Science, 2018 (Applied two proposals and both were approved)
- Student research grant competition from Grant Agency of University of South Bohemia, 2017 (support 200000 CZK, about 7700 EUR)
- Bilateral Mobility Project Proposal (PPP) between Taiwan MOST and Czech Academic of Science, 2016-2017 (two-year project)
- Graduate Travel Grant from National Science Council (Ministry of Science and Technology, Taiwan), 2013

Visiting Scientist

- Traineeship: Learning honeybee behavior assay in Dr. Markus Thamm lab, Biocenter, University of Würzburg, Germany, June-July 2019
- Visiting and Traineeship: Learning *Drosophila* ovary immunostaining in Dr. Hwei-Jan Hsu's lab, and giving a lecture for students, lecture topic: CRISPR/Cas9 application in *Drosophila.* Institute of Cellular and Organismic Biology, Academia

Sinica, Taiwan, Oct 2018

- Visiting: Wu YL's lab and giving a lecture for undergraduates, lecture topic: Four modern approaches of insect reverse genetics study: RNA interference (RNAi), Zinc-Finger Nuclease (ZFN), TALENs and CRISPR, Department of Entomology, Nation Taiwan University, July 2017
- Visiting: Dr. Tsai CW's lab, supporting by Czech-Taiwan Bilateral Mobility Project, Department of Entomology, Nation Taiwan University, March 2016

Instruction Experience

- Teaching assistant in National University

Mar 2012 - Jun 2012, Medical Ethics of Life and Death in the Movie (Philosophy)

Sep 2011 – Jan 2012, Clinic Thanatology (Philosophy)

Mar 2011 – Jun 201, Biological Clock and Introductory Sleep Medicine (Biology)

- Lecturer

Jan 2012, Invited to give a lecture on Teaching Assistant (TA) Training Seminar. Lecture topic: The management and application of instruction website system

- ISW training

Mar 2012, Invited to participate Instruction Skill Workshop at Center for Teaching and Learning Development

Other working experience

- Military service

Aug 2012- July 2013, Navy Academy and Navy Recruit Training Center